STIMULI-RESPONSIVE POLYMERS AND THEIR APPLICATIONS IN GENE DELIVERY

by

Hee Sook Hwang

A dissertation submitted to the faculty of
The University of Utah
in partial fulfillment of the requirements for the degree of

Doctor of Philosophy

Department of Pharmaceutics and Pharmaceutical Chemistry

The University of Utah

December 2015

The University of Utah Graduate School

STATEMENT OF DISSERTATION APPROVAL

The dissertation of **Hee Sook Hwang**

has been approved by the following supervisory committee members:

You Han Bae	, Chair	**06/11/15** Date Approved
Margit M. Janat-Amsbury	, Member	**06/11/15** Date Approved
Mingnan Chen	, Member	**06/11/15** Date Approved
James N. Herron	, Member	Date Approved
Shawn Owen	, Member	**06/12/15** Date Approved

and by **David W. Grainger** , Chair/Dean of

the Department/College/School of **Pharmaceutics and Pharmaceutical Chemistry**

and by David B. Kieda, Dean of The Graduate School.

ABSTRACT

Polymeric gene delivery is introducing specific genes to enhance or silence gene expression using synthesized polymers which have low immunogenicity and good biocompatibility. This dissertations specifically focused on the synthesis and characterization of stimuli-responsive polymers for gene delivery. The polymers are designed to respond to specific biological stimuli such as redox potential and pH changes.

In the first stimuli-responsive polymer, a reducible poly($_L$-lysine) (RPLL) was constructed and mediated gene delivery. Polyplex, polymer/gene complex, biocompatibility can be improved by using amino acids as nontoxic building blocks. To synthesize an amino-acid-based reducible polymer, a decapeptide composed of lysine and cysteine (Cys-Lys8-Cys) has been selected due to primary amines and sulfhydryl functional groups, respectively. A reducible polymer introduced with disulfide bonds enables control of the rate of biodegradation and decomplexation of polyplex which will impact plasmid DNA (pDNA) release.

In the second stimuli-responsive polymer, a pH-dependent polymeric-mediated gene delivery was conducted via PLL grafted with either mono-$_L$-histidine (PLL-*g*-mHis) or poly($_L$-histidine) (PLL-*g*-PHis). The pH-sensitive ionizable groups in histidine were used as an endosomolytic agent to construct a pH-sensitive polymeric gene carrier. Two types of histidine grafted PLL, PLL-*g*-mHis and PLL-*g*-PHis, were synthesized with the same number of imidazole groups to compare the effective arrangement of histidine in terms of

endosomolytic activity and transfection efficiency.

A wide range of observations have been made to conclude that a stimuli-sensitive property in polymer imparts a rapid response to specific stimulus compared to a non-sensitive polymer and the improved gene transfer activity shows much promise for gene delivery. Since gene carriers have been applied in cancer gene therapy to safely and efficiently deliver a therapeutic gene into the target site, these stimuli-sensitive polymers will bring efficient translation levels of the therapeutic protein to treat cancer. Therefore, it is essential to further investigate the gene expression *in vivo* applications in an engaging and accessible way.

TABLE OF CONTENTS

LIST OF FIGURES

LIST OF TABLES

LIST OF ABBREVIATIONS

BSA: Bovine Serum Albumin

DMSO: Dimethylsulfoxide

DMEM: Dulbecco's Modified Eagle's Medium

EtBr: Ethidium Bromide

FBS: Fetal Bovine Serum

GPC: Gel Permeation Chromatography

GSH: Glutathione

HEK293: Human Embryonic Kidney cell line

HEPES: 4-(2-hydroxy-ethyl)-1-piperazine ethanesulfonic acid

HepG2 : Hepatoma cell lines

Hela: Human cervical carcinoma

MCF7: Human breast denocarcinoma cell line

MTT: 3-(4,5-di-methylthiazol-2-yl)-2,5-diphenyltetrazolium bromide

pDNA: Plasmid DNA

PLL: Poly($_L$-lysine)

PRLx: $PLL_{100-x}RPLL_x$

PHis: Poly($_L$-histidine)

RBC: Red Blood Cell

RPLL: Reducible poly($_L$-lysine)

CHAPTER 1

INTRODUCTION

1.1. Cancer

Cancer is the second leading cause of death in the USA.[1] The 5-year relative cancer survival rate from 2001 to 2007 is 67 % and the survival rate of many other cancers, excepting cancers of the lung and pancreas, has improved dramatically due to an increase of early diagnosis and better treatments; however, it has been estimated that 25% of all deaths will still occur as a result of cancer.[1]

Cancer occurs when normal cells undergo abnormal cell division without the regulation of cell growth, and thereby allow cancerous cells to proliferate and grow uncontrollably, forming tumors. Development of malignant tumors with the ability to metastasize may lead to death if tumor cells travel through the bloodstream and lymph system through which they invade other tissues and spread to other sites.[2]

It is important to study the cell of origin and initiation of cancer in order to better understand and develop more effective cancer therapies. The cancer stem cell hypothesis and the clonal evolution model are two current models that follow a stem cell model, but each model has distinctive characteristics. In the cancer stem cells (CSCs) model, the origin of a tumor starts with CSCs where a small population of tumor cells that has self-

renewal capacity and proliferative potential recapitulates the tumors. The CSC hypothesis follows a hierarchical organization with CSCs located on the apex of the hierarchy, and CSCs generate a tumor.[3] Since CSCs are responsible for tumor development, tumor recurrence, progression, and metastasis, several cell-surface markers that can identify and isolate CSCs from the mixture of tumorigenic and nontumorigenic cancer cells have been developed. For examples, $CD44^{+}CD24^{-/low}$ was used as a marker for breast cancer, and CD 133 appeared to be a marker for glioblastomar, medulloblastoma, and ependymomas.[4]

However, some of the solid tumors appear to be caused by genomic instability, a theory supported by the clonal evolution model, in which most proliferating cells have a tumorigenic ability that drives tumorigenesis.[5] In the clonal evolution model, tumorigenic cells and heterogeneity are explained through genetic mutation and epigenetic changes. Brocks *et al.* demonstrated the genetic and epigenetic heterogeneity of multiregions on the same tumor by analyzing methylation patterns in prostate cancer, suggesting that the aberrant methylation in tumors is associated with the clonal genetic origins of the tumor.[6] Thus far, it is still unclear whether tumors are derived from the CSCs model, the clonal evolution model, or a mixture of the two models based on available evidence.

1.2. Tumor Microenvironmental Physiology

The tumor microenvironment is different than that of normal tissues in terms of pH, oxygen levels, tumor cells energy metabolism, blood vessel formation, interstitial fluid flow, and extracellular matrix components. It is important to understand the physiological environment of a tumor in order to better understand current treatments and overcome the

limitations of targeting the tumor.

The cellular pH is represented by an Na+/H+ exchanger, and normal tissue maintains a higher extracellular pH (pH_e) of 7.4, and a lower intracellular pH (pH_i) of 7.2.[7, 8] However, abnormal hydrogen ion regulation in tumor cells make a tumor an acidic environment, leading to a reverse pH gradient as compared to normal tissue. Thus, tumor pH_e is lower than pH_i. In addition, inadequate lymphatic drainage in tumor builds up lactic acid which is produced after glycolysis and makes the tumor environment even more acidic. The pH_e of tumors is below 7, usually hovering around 6.6 – 6.98.[8]

Hypoxia, or low oxygen level, is another well-known characteristics of tumor. The oxygen partial pressure (pO_2) of a solid tumor is below 20 mmHg which is lower than the surrounding normal tissue, where pO_2 is around 24 – 66 mmHg. This number decreases further as the tumor grows in size.[9, 10] The reason for the poor oxygenation of tumors is due to abnormal, leaky blood vessels with increased distance from the tumor region to vessel that limit enough oxygen supply. It has been reported that poor oxygen levels in tumors is also related to tumor aggressiveness and metastasis, leading to poor results after chemo and radiotherapy treatments.[9] Therefore, many researchers have studied the relationship between hypoxia and chemo/radiotherapy, focusing on targeting hypoxia to improve the cancer treatment outcomes.

Normal tissue obtains a small portion of cellular energy ATP from glycolysis which converts glucose to pyruvate, and derives the rest of its energy from mitochondria. However, cancer cells' energy metabolism is different than that of normal tissue. Cancer cells maintain a high rate of aerobic glycolysis to generate ATP, also known as the Warburg effect.[11] This high aerobic glycolysis is associated with the function of hypoxia

inducible factor 1 (HIF-1). HIF-1 is the main regulator consisting of α and β subunits and controlling oxygen delivery. The transcription factor HIF-1 regulates energy production by increasing glycolysis and decreasing mitochondria-mediated energy production. Thus, the HIF-1 level is activated or overexpressed in cancer cells due to the intratumoral hypoxia condition. Furthermore, HIF-1 expression is related to activated oncogenes and mutant tumor suppressor. After the expression of activated oncogenes such as Ras, or the loss of tumor suppressor genes like PTEN, HIF-1 accumulation in tumor cells was observed.[12]

Tumor angiogenesis is one of the hallmarks of cancer.[13] As tumor size increases, new blood vessel formation is necessary to supply oxygen and nutrients for tumor expansion. Vascular structure in tumors is very different than that of normal vessels. Tumor vessels are disorganized with lots of branching, and vessel diameter is uneven and dilated. Formation of new tumor vessels is influenced by environmental stress on the tumor, caused by low oxygen, low pH, and pressure around proliferating cells.[13] Tumor cells also secrete cytokines and growth factors, especially hypoxic areas release angiogenic growth factors such as fibroblast growth factor (FGF) and vascular endothelial growth factor (VEGF) to supply oxygen and nutrition to the tumor cells.[14] It has been observed that VEGF is the dominant angiogenic factor that plays a critical role in regulation during blood vessel formation often resulting in dilated, leaky, and more permeable vessels.[14] Thus, anti-angiogenic therapies that suppress angiogenesis by targeting VEGF have been studied as a potential approach for cancer treatment.

Increased interstitial fluid pressure (IFP) is also observed in many solid tumors. While IFP measures about 5-10 mmHg in normal tissues, IFP up to 50 mmHg has been

reported in solid tumors.[15] Such a high IFP is due to the formation of abnormal leaky vessels and lymphatic function which in turn create an irregular and bulk flow of fluid. As a consequence, increased fluid accumulation in tumor areas with poor drains through the lymphatic vasculature causes the interstitial pressure to rise. It eventually causes a steep pressure gradient between the tumor and its surrounding tissue, resulting in high interstitial fluid flow into the tissue.[16, 17] Since high IFP in tumor has been recognized as a barrier for effective drug delivery, much research regarding IFP lowering treatments has been conducted.

Extracellular matrix (ECM) components between tumor and normal tissue are also shown to be different. The ECM is composed of proteins, glycoproteins, proteoglycans, and polysaccharides.[18] It forms the basement membrane which is generally rich in fibronectin, laminins, collagen, elastin, and linker proteins that creates a more compact structure than that of an interstitial matrix.[19] The normal ECM is highly organized and controlled by multiple regulatory mechanisms. It plays an important role in cell migration, growth factor signaling, and cell-cell communication.[18] However, in the case of a tumor microenvironment, the ECM is commonly deregulated and highly disorganized. The ECM in tumors has a dense cell population and an increased collagen deposition that makes the collagen fiber network more complicated.[19] As a result, ECM stiffness in tumors is stronger than that of the surrounding tissue which affects the cell migration and proliferation rate, differentiation, and tumorigenesis.[16, 20]

1.3. Cancer Treatments

Chemotherapy, radiation therapy, immunotherapy, and surgery have been widely used for cancer treatments.[21] Chemotherapy uses a wide range of anticancer drugs such as DNA fragmenting/cross-linking agents, intercalating agents, protein synthesis inhibitors, topoisomerase poisons, kinase inhibitors, and hormones.[22] These anticancer drugs induce apoptosis by attacking fast-growing and dividing cancer cells. Chemotherapy is often combined with radiation therapy to shrink tumors before the surgery.

Radiation therapy destroys localized cancer cells by using high-energy radiation that can be subdivided into photon and particle radiation. Photon radiation includes x-rays and gamma rays, whereas particle radiation includes electron, proton, neutron, carbon, alpha, and beta particles.[23] Such different types of radiation damage cancer cells DNA with their respective beam energies. Radiation therapy can be also applied along with chemotherapy, surgery, and immunotherapy.

The strategy of immunotherapy is to make the host's immune system attack cancer cells via monoclonal antibodies (mAbs) and cancer vaccines already known to be major immunotherapy treatments used for treating cancer.[24] mAbs as therapeutic agents can activate or suppress immune response against cancer cells by mediating T lymphocytes, dendritic cells, and natural killer cells.[24, 25] Cancer vaccines also elicit immune response as a defense mechanism from diseases and protect the body by recognizing and fighting against cancer cells. There are several types of cancer vaccines that are used in clinical trials for treating patients: virus, DNA, peptide, heat shock proteins, dendritic cell, and tumor cell-based vaccines.[26]

Despite the advantages of chemotherapy, radiation therapy, and immunotherapy,

these treatments face some challenges. Chemotherapy shows toxic effect to normal cells and also kills fast-proliferating healthy cells including those in bone marrow, the digestive system, and hair follicles.[27] In addition, many anticancer drugs used in chemotherapy develop drug resistance which may contribute to a low therapeutic index and lead to administration of the maximum tolerated dose, often resulting in a non-specific toxic effect in the body due to the drug insensitivity development. Although radiation therapy targets the localized cancer cells, the reactive free radical ions formed during radiation can affect and destroy normal cells.[21] Common initial side effects of radiation therapy include nausea, diarrhea, mucous membrane inflammation, and skin redness, and late side effects involve fibrosis, neural and vascular damage, endocrine and growth-related effects.[28] In the case of immunotherapy, cancer-targeted treatments by monoclonal antibodies may also induce autoimmunity, and systemic inflammation.[24]

1.4. Gene Therapy in Cancer

Gene therapy is an attractive approach to treat cancer, in that it introduces specific genes to enhance gene expression, and silences or replaces mutated genes to correct genetic defects in cancer. Thus, transgenes, an artificial gene, can be effectively delivered to target sites to be activated and express the therapeutic genes necessary to slow cancer cell growth or lead to cancer cell death. Tumor suppressor genes, stability genes, and oncogenes are three types of genes that have been used in cancer gene therapy.[29] Table 1.1. summarizes the therapeutic genes that belong to tumor suppressor genes, stability genes, and oncogenes, and their therapeutic function with regard to target tumors.

Tumor suppressor genes are involved in cell growth, arrest, and cell death. These

Table 1.1. Cancer gene therapy

Gene category	Target genes	Function	Tumor types
Tumor suppressor genes	p53	Cell growth arrest, apoptosis	Breast, ovary, bladder [30, 31]
	p21	Cell cycle arrest	Breast, colon [32]
	Rb	Cell cycle entry regulation, apoptosis	Liver [33]
	PTEN	PI3K pathway negative regulator (inhibit cell proliferation, growth, and cell survival)	Prostate, bladder [34, 35, 36]
Stability genes	BRCA1/2	DNA repair	Breast, ovary [37, 38]
Oncogenes	MDM2	p53 inhibition	Prostate [39]
	HER2	Cell cycle progression, survival, proliferation	Breast , ovary, gastric [40, 41, 42]
	c-kit	Cell growth, proliferation, survival	Gastrointestinal stromal tumors [43, 44]
	MET	Cell proliferation, motility	Lung, breast, colorectal, prostate [45-47]
	Ras	Cell proliferation, survival, differentiation	Colorectal, pancrease lung, thyroid, melanoma, liver, kidney [48, 2]

Rb: retinoblastoma
PTEN: phosphatase, tensin homologue, deleted on chromosome 10
PI3K: phosphatidylinositol 3-kinases
BRCA1: breast cancer 1
MDM2: murine double minute 2
HER2: human epidermal growth factor receptor 2, tyrosine kinase receptor
c-kit: tyrosine kinase receptor
MET: tyrosine kinase receptor encoded for hepatocyte growth factor
Ras: gene involved in kinase signaling pathways

genes are mutated in many cancers, and this mutation reduces their normal activity. The inactivation of tumor suppressor genes affects the cell number and rate of cell growth which can cause cancer.[29] p53 is one of the most well-known tumor suppressor proteins, playing an important role in cell cycle arrest, DNA repair, and apoptosis, and it has been reported to be mutated in many types of human cancer.[49] Thus, p53 has been delivered via several virus and nonviral vectors, and demonstrated efficient p53 expression, apoptosis, and tumor regression.[50, 51]

Stability genes are related to genomic stability, and DNA damage without an appropriate response can result in genomic instability and an accumulation of mutations. Specifically, BRCA1 is one of the stability genes involved in repairing double strand DNA breaks in the presence of BRCA2 and the BARD1 (BRCA1-binding protein). It has been demonstrated that chromosome instability and no repairing of damaged DNA were observed in the BRCA1 deficient cells.[52] Because many cancers have been found to be defective with these stability genes, therapies using genes targeting DNA repair have been conducted to treat cancer.[53, 54]

Oncogenes are genes with the ability to induce cancer. If proto-oncogenes are mutated or too many oncogenes are expressed, it can cause cell growth without control and contribute to cancer development. HER2 is a well-known oncogene that is overexpressed in aggressive breast cancer and encodes a tyrosine kinase growth factor receptor which is involved in cell growth, motility, and differentiation.[40, 41] Therefore, changes in HER2 levels activate the downstream signaling pathway, PI3K, MAPK, and PLCγ, and induce cell proliferation while preventing apoptosis.[42] HER2 gene targeting therapy has been widely used with chemotherapy, and HER2-specific siRNA has been

delivered to treat cancers.[55, 56]

In order to achieve a successful cancer gene therapy, gene vectors are often utilized. These are helpful tools for transferring sufficient copies of the necessary therapeutic genes to cancer cells to reach the most effective therapeutic gene expression levels. Therefore, gene vectors play an important role in gene transfer and gene expression to treat cancer. Two main gene vectors for cancer gene therapy, viral and nonviral vectors, will be covered in depth in section 1.4.1.

1.4.1. Viral and Nonviral Gene Vectors

Viral vectors can efficiently deliver genes to target cells since transferred DNA integrates into the host chromosomal DNA. Viruses are composed of viral genes, proteins, and in some cases, membrane lipids for enveloped viruses.[57] The capsid proteins protect viral genomes, and the lipid bilayer membrane protects the capsid. In order to integrate into the host genome, viruses must across the cell membrane. Viruses enter the host cell via endocytic pathways.[58] An enveloped virus penetrates the membrane via fusion; on the other hand, a nonenveloped virus enters the cell via nuclear pore formation or membrane lysis. The virus, such as influenza virus, is delivered into the endosome, lysosomes, and endoplasmic reticulum after penetration, and later moved to the perinuclear regions via microtubules. Then the virus binds to the nuclear pore complex, and the viral genome is released into the nucleus for replication. Therefore, viruses exhibit highly efficient gene delivery and gene expression of the therapeutic gene.

Viruses can also carry foreign genes and provide efficient gene delivery and expression. However, viral gene therapy has several disadvantages including

mutagenicity, cytotoxicity, immunogenicity, and limited loading space. Viral vectors also have difficulties in manufacturing and storage.

Naked/plasmid DNA is one of the most popular nonviral vector-mediated approaches that has been applied in the gene therapy clinical trials. However, the large size of the naked genes is susceptible to rapid clearance and nuclease degradation. Moreover, its hydrophilicity hampers the crossing of the hydrophobic cell membrane. Thus, naked DNA is delivered into target tissues by injection and results in gene expression with therapeutic protein production. Specifically, jet injection, electroporation, and gene gun methods were applied to deliver naked DNA to improve the gene transfer efficiency. These methods deliver DNA directly inside the cell, thus, DNA can avoid membrane penetration, intracellular trafficking, and enzymatic degradation. In this way, more DNA is delivered to the nucleus and transcribed by transcriptional machinery.

Nonviral vectors have been studied and applied to gene therapy due to their overall nonimmunogenicity and nontoxicity as compared to viral vectors, and nonviral vectors have been divided into two major categories: cationic lipids and polycations. The most commonly used cationic lipids include 1,2-dioleoyloxy-3-(trimethylammonio)-propane (DOTAP), N[1-(2,3-dioleyloxy) propyl]-N,N,N-trimethylammonium chloride (DOTMA), 1,2-Dioleyl-3-phosphatidylethanolamine (DOPE), and Dioctadecylamidoglycylspermine (DOGS).[59] Cationic lipid is composed of charged polar head group and hydrophobic carbon chains that form stable complexes with pDNA, called lipoplexes. It has been reported that DOTAP is the most popular liposomal transfection reagent that used for DNA and siRNA delivery, and DOPE is known as a helper lipid, often mixed with other lipids to facilitate cellular uptake, and endosomal escaping of lipoplexes, and to enhance

the liposome-mediated gene transfection.[60, 61]

Cationic polymers include poly ($_L$-lysine) (PLL), branched polyethylenimine (bPEI), and polyamidoamine dendrimers (PAMAM). PLL was the first polycation used as a gene carrier, and bPEI has been considered as the gold standard for the gene delivery system. Cationic PAMAM has been also investigated as a gene carrier due to the facile regulation of number of functional groups, as well as size and surface charge by producing different generation of dendrimers.[62] In addition, chitosan, gelatin, dextran, pullulan, and pronectin are typical examples of natural polymers which are widely used in gene delivery due to their outstanding biocompatibility and degradability.[63, 64]

Cationic lipids and polymers bind to negatively-charged DNA via electrostatic interactions to form lipoplexes and polyplexes. Both lipids and polymers can enhance the cellular uptake of genes via an endocytosis-mediated uptake. After the gene containing nonviral vectors are internalized, the complexes will undergo intracellular trafficking pathways. Consequently, endosomal acidification causes membrane fusion, and genes are released to the cytosol and delivered to the nucleus in order to be transcribed.

Nonviral vectors are easy to prepare and have the ability to carry a large cargo size. These vectors are viable for large-scale manufacturing. They show lower immunogenicity than viral vectors, thus making them suitable for repeated use. That being said, the main disadvantages to their use include their low transfection efficiency and transient gene expression. Table 1.2. lists types of viral and nonviral vectors, delivered genes, and major drawbacks of each vector type.

Table. 1.2. Gene delivery vectors, delivered genes, and disadvantages of vectors

Vector types	Sub vectors	Genes	Drawbacks
Viral	Adenovirus	HSV-tk, p53, IL-6, E2F-1 [57]	Transient gene expression [66]
	Adeno-associated virus	HSV-TK, IL-2, p53 [59]	Gene packing capacity is limited [68] Risk of mutagenesis [69]
	Herpes virus	IL-2, Cx43, CYP2B1, CPA, CD, IL-4, 10, 12 [70, 71, 72]	Transient gene expression, inflammatory response [57]
	Retrovirus	HSV-tk, GCV [62]	Only works in replicating cells [65]
	Lentivirus	IFN-α, hIFN-β [63,64]	Possibility of oncogenesis during integration [57], poor production capability [76]
Nonviral	Naked DNA	IL-12, TNF- α [66, 67]	Low transfection efficiency, degradation of plasmid [68]
	Cationic liposomes	IL-12, p53, HLA-B7, β-2 microglobulin, IL-2 [66, 69-71]	Poor transfection rate [68], activate innate immune response [54]
	Cationic polymers	VEGF, p53, IL-4, IL-10 [71]	Transient transfection efficiency

HSV-tk: herpes simplex virus thymidine kinase, IL6: Interleukin-6, E2F-1: transcription factor, Cx43: Connexin 43
CYP2B1: rat cytochrome P450, CD: yeast cytosine deaminase, CPA: cyclophosphamide, hIFN-β: transferred human interferon beta, TNF- α: human tumor necrosis factor alpha, HLA-B7: Human histocompatibility surface antigen: VEGF: Vascular endothelial growth factor

1.4.2. Clinical Trials

Gene carriers used in clinical trials are dominated primarily by viral vectors, with only small fractions of nonviral vectors used in gene therapy clinical trials. More specifically, viral vector-mediated gene therapy currently occupies almost 70% of the clinical trials to treat cancer, inherited monogenic disorders such as cystic fibrosis, and infectious disease like HIV.[78]

The first clinical trial was performed and reported in 1990, using a retrovirus to treat metastatic melanoma.[79] In 1999, adenovirus vector mediated gene therapy resulted in the death of a patient with ornithine transcarbamylase (OTC), and in 2000, three patients with X-linked severe combined immunodeficiency (SCID)-XI disease were treated with retrovirus mediated gene therapy.[57] In 2006, two patients with metastatic melanoma were treated using a retrovirus which encoded a T cell receptor and showed sustained levels up to 1 year with metastatic lesions regression.[78] Among several types of viral vectors, adenovirus (23.3%) and retrovirus (19.7%) are the most widely used in gene therapy clinical trials.[78] However, retrovirus-mediated gene therapy is currently decreasing in use.

Nonviral gene therapy is not as widely conducted in clinical trials as viral gene therapy, but nonviral vector applications are in progress. Nonviral vectors have less safety risks, but they have major limitations with regards to efficiently transferring genes. Delivery of naked DNA is the most popular and commonly used nonviral gene therapy in clinical trials followed by lipofection and gene gun.[78] It has been reported that about 14% of the naked DNA injection into a tissue was tested in clinical trials. Lipofection, a lipid-mediated DNA transfection, is the second most popular method within nonviral vector categories. Lipofection makes up about 9% of all gene therapy clinical trials.

In the 1960s, divinylethermaleic anhydride (DIVEMA), a synthetic polymeric anticancer agent, was used in the first clinical trial, and polymer-drug conjugates, micelle, and PEGylated proteins were clinically tested in the 1970s.[80] Furthermore, cationic lipids have been used in clinical trials. For example, DC-Chol/DOPE liposomes, one of the cationic lipids, were approved for a clinical trial in 1992.[81] In 1994, vascular endothelial growth factor (phVEGF) gene transfer driven by a cytomegalovirus (CMV) promoter was performed for limb ischemia patients.[82]

1.4.3. Extracellular Barriers

Extracellular barriers are relevant to the efficacy of gene transfer in *in vivo* applications. The salt concentration in blood changes the physicochemical stability of complexes and induces aggregations between complexes.[83] It has been reported that complex interactions with extracellular anionic glycosaminoglycans also affect the gene release from the vectors and its efficiency.[59, 84] Moreover, negative charged blood components like albumin can cause nonspecific interactions of complexes with serum proteins, and these unwanted interactions will change the surface charge of the complexes which lead to size increase, cellular uptake hindrance, aggregation, and rapid clearance by phagocytosis.[85] Specifically, rapid clearance via the mononuclear phagocyte system (MPS) happens when complexes bind to plasma proteins and are recognized by macrophages which are mostly located in liver, spleen, and bone marrow.[86]

Limited levels of gene expression due to the extracellular barriers can be prolonged by shielding techniques, also known as PEGylation. PEG shielding on the positive surface charge provides steric hindrance and protects against anionic components in

blood as well as physical stability in blood for longer circulation. Thus, PEGylated complexes increase circulation time in blood and enhance the therapeutic index of the complexes as well as the half-life extension. The increase in therapeutic index indicates increase of gene efficacy and toxic effect reduction. More specifically, long circulation of complexes can reduce the MPS uptake rate and complexes are able to accumulate at targeted tumor sites. In addition, long circulating particles are able to accumulate at disease sites due to the EPR (enhanced permeability and retention effect) effect. When particles are more efficiently delivered in specific target sites, toxicity on the nontarget sites can be reduced. Therefore, this will result in the enhancement of the therapeutic plasma concentration and AUCs (area under the plasma concentration time curve) of the complexes.

1.4.4. Intracellular Barriers

Polyplexes or lipoplexes enter the cells via charge mediated interaction with lipid bilayer, receptor-mediated endocytosis, or ligand-receptor binding interactions.[87] However, there are several intracellular obstacles that challenge the gene delivery vectors. The intracellular barriers include cellular internalization, endosome escape, lysosomal trafficking, and nuclear entry. [77, 88]

It has been reported that physicochemical characteristics of polyplexes such as chemical composition of polymer, size, surface charge, and surface chemistry is relevant to cellular internalization. [89] Nanoscale particles are internalized faster than micron size particles,[89] and particles with the positive surface charge are internalized easier than neutral or negative charged particles.[90, 91] In addition, chemical compositions, which

contains amines in the polymers, are easily internalized and number of amines in the polymer repeating units affect the cellular internalization, because the positive charge from amine groups in polymers increased the charge interactions with the cell surface.[92] Several studies demonstrated that DNA complexes with cationic lipids and polymers are internalized by clathrin and caveolae-mediated endocytosis when the particle diameter is 100-200 nm or smaller than 100 nm, as well as macropinocytosis when the complexes are larger than 200 nm.[91]

Rejman *et al.* have demonstrated the internalization of polyplexes and lipoplexes by incubating endocytosis inhibitors and monitored fluorescence colocalization in cells using fluorescent labeled PEI and fluorescent dextran that label the lysosomal compartment.[93] The reported polyplexes uptake is mediated by two pathways which are clathrin-mediated and caveolae-mediated endocytosis, whereas the lipoplexes uptake is mediated by only the clathrin-mediated endocytosis. Depending on the intracellular trafficking pathways, the transfection efficiency was affected. In case of polyplexes, the polyplexes internalized by caveolae-mediated endocytosis was more efficient transfection than the clathrin-mediated pathway.[93]

However, the cellular internalization of polyplexes and lipoplexes can occur both in targeted and nontargeted sites via nonspecific interactions with the cell surface. Therefore, some researchers have been used for targeting gene delivery using receptor-mediated endocytosis for transfection efficiency enhancement. Targeted gene delivery focuses on tumors using receptors like folate, transferrin, antibody, and sugars such as mannose, glucose, and galactose. Coupling of targeting ligands on the complexes will be recognized by a cell surface receptor and leads to cellular uptake. For example,

transferrin coupling to PEI enhanced the transfection efficiency up to hundred-fold, [94] and the folate receptor which is abundantly expressed in human cancers has been used in many polymers such as PLL-folate, PEI-folate, and folate-DOPE conjugates. Folate receptor-mediated pDNA delivery showed that gene transfer efficiency was highly efficient dependent on the folate receptor expression level in the cell and resulted a higher gene expression than control polymers without the folate receptor.[95] In addition, targeting specific cells through sugar conjugations have been studied for gene delivery. Conjugation of sugar moieties to polymers and lipids resulted in a better gene expression through receptor-mediated endocytosis especially galactose for hepatocyte targeting, and mannose for dendritic cells.[94, 96]

Under the process of endocytosis, escaping from endosome is another critical step. Polyplexes are sequestered in intracellular vesicles like endosomes, and inefficient endosomal escape may lead to lysosomal trafficking and undergo degradation due to the presence of degradative enzymes in the acidic vesicles and eventually cause reduction of gene transfer efficiency. However, escaping too early from the endosomes can cause a problem as well, because the distance far away from the nucleus makes it difficult to polyplexes to translocate genes inside the nucleus, and genes that are released in cytoplasm can be degraded by nuclease located in cytoplasm.[97] Mechanisms of endosomal escaping and strategies will be discussed in section 1.5.1.1.

After free pDNA or polyplexes escape from the endolysosomes, pDNA must be transported and localized into the nucleus. The transport of free pDNA through the cytoplasm to the nucleus is also challenging due to the immobility of pDNA in cytoplasm hinders efficient pDNA transfer and it can be degraded by cytosolic nucleases.[98] Thus,

pDNA near the perinuclear region has a high possibility to translocate inside the nucleus.[97] DNA enters the nucleus during mitosis when the nuclear membrane is disrupted or uses specific sequence for active nuclear transport.

Nuclear pore complexes (NPC) act as a gate for the nuclear entry. The NPC diameter is about 9 nm, and it is composed of four different blocks which include ring subunit, column subunit, lumenal subunit, and annular subunit. [99, 100] Small proteins less than 9 nm in diameter or less than 40 kDa in mass can passively diffuse through the NPC, and particles between 9 and 40 nm in diameter of 40 kDa to 60 kDa in mass involve active transport.[100]

Generally, polyplexes with the positive surface charge can interact with anionic microtubules and transport along the microtubules. Many studies have provided evidence that polyplexes conjugated with nuclear localization signal (NLS) or cell penetrating peptides (CPPs) can facilitate nuclear entry.[101, 102] The NLS is a sorting signal that brings nuclear proteins to the nucleus. The signals are consist of one or two short sequences and these sequences have many positively charged lysine and arginine residues. CPPs efficiently facilitate intracellular delivery of cargoes such as plasmid DNA, oligonucleotides, siRNA, peptide nucleic acid, proteins and peptides, and small molecules across the plasma membrane and deliver the cargoes to specific organelles within the cell.[101] Nucleic acids delivery by CPPs provides gene expression regulation and it has been used for siRNA, antisense oligonucleotide, and pDNA.[101] However, there are still limitations for delivering these nucleic acids for high molecular weight and negative charges, because they have low cellular trafficking and uptake.

1.5. Gene Delivery with Stimuli-responsive Polymers

Stimuli-responsive polymers undergo changes of physical or chemical properties of the polymers in response to stimuli in the environmental conditions. The stimuli can be classified into three different subgroups; chemical, physical, or biological/biochemical stimulus. Table. 1.3. summarizes representative stimuli.

Stimuli-responsive polymers have been investigated and applied to many areas such as biosensors, imaging agents, and drug or gene delivery carriers because of their great potential in shape, surface charge, and solubility changes by external or internal stimuli. The benefits of using stimuli-responsive polymers have been reported because of their specific responses to tumors, the side effect reduction, and reversible changes.[103] Among all of the stimuli-responsive polymers, the three main types of stimuli-sensitive polymers are reviewed in this section which will be pH sensitive polymers, temperature-responsive polymers, and biodegradable polymers.

1.5.1. pH-sensitive Polymers

The pH conditions of extracellular and intracellular compartments are different. The pH of blood is 7.4, and the pH of primary tumors and metastasized tumors is lower than the pH of blood and normal tissue. For example, extracellular pH in solid tumors becomes acidic and drops to pH 6.5.[103, 104] The cellular components such as the early/late endosomes, lysosomes, endoplasmic reticulum, cytoplasm, and nucleus have their own pH values. For instance, the early endosome has pH 5.5-7, the late endosome has pH 5-5.5, the lysosome has pH 4-5, and the cytoplasm and nucleus have a pH of 7.2.[110, 111] The variations in extra/intracellular pHs allow designing of pH-responsive gene delivery

Table.1.3. Types of stimuli

Type	Example
Chemical stimulus	pH[109] Salts[110] Ionic strength[111]
Physical stimulus	Magnetic field[103] UV/ visible light[109] Ultrasound[104, 107] Temperature[103] Electric current[109]
Biological/Biochemical stimulus	Antigen[103] Enzymes[103, 107] Temperature[104] pH changes[104] Redox environment[104]

system and applying for pH targeted therapy.[107]

The pH-sensitive polymers contain ionizable functional groups that respond to pH changes.[108] The most typical ionizable functional groups used for pH-sensitive polymer synthesis include carboxylic groups (-COOH), primary amines groups ($-NH_2$), and sulfonic groups ($-SO_3$). Table 1.4 summarizes a few of functional groups, representative polymers, and its pK_a/pK_b values.

The pH-sensitive behavior of polymers is triggered by protonation-deprotonation state of ionizable functional groups. Depending on the difference of environmental pH and intrinsic pKa of polymers, the stability of polymers can be changed and can influence the interaction with genetic materials. The pK_a value of functional groups results in a protonated state when pH values becomes lower than pK_a, and polymer becomes a deprotonated state as pH value becomes higher than pK_a. For instance, the primary amines in PLL have a pK_a value of 10.5 and it becomes protonated at physiological pH 7.4. Therefore, protonated primary amines and phosphate groups in pDNA form polyplexes. bPEI has a high amine density due to the three different types of amine groups. The primary amine groups in bPEI have a pK_a value of 9, and secondary and tertiary amine groups have a pK_a 8 and pK_a 6-7, respectively. The primary amines are used for gene condensation, while secondary and tertiary amines are served for endosomal escaping ability.

The ionization of functional groups upon pH changes not only influences the stability of polymers but also affects conformation change. Poly(amidoamine) (PAMAM) dendrimers are one of the pH-responsive polymers that undergo conformational change due to the local polarity changes via primary amines and tertiary amines protonation.[112]

Table 1.4. Polymer functional groups and pK_a/pK_b

	Functional group	**Polymer**	**pK_a/pK_b**
Acid	-COOH	PAA	4.5[113]
		PET	4.5-5.5[114]
		PMAA	5.5[115]
	$-SO_3H$	PSS	2-3[116]
Base	$-NH_2$	PLL	10.5[117]
		PEI	1º amine 9, 2º amine 8, 3º amine 6-7[118]
		PAMA	7.6[119]
	$-N(CH_3)_2$	PDMAEMA	7.78[120]

PAA: Poly(acrylic acid), PET: Poly(ethylene terephthalate), PMAA: Poly(methacrylic acid), PSS: poly(styrene sulfonate), PLL: Poly ($_L$-lysine), PEI: Polyethylenimine, PAMA: Poly(2-aminoethyl methacrylate), PDMAEMA: poly (N, N- dimethylaminoethyl methacrylate)

At the high pH, primary amines are all protonated and as pH goes down, more amines are protonated and produce either a ‘dense core’ or a ‘dense shell’ conformation. Therefore, the cationic net surface charge of PAMAM dendrimers is also used as a transfection agent which can form stable polyplexes with effective pDNA binding. In addition, enhanced binding of pDNA and efficient gene transfection was demonstrated with higher generation of dendrimers.[121]

The pH-sensitive polymers have been applied to tumor specific targeting, hypoxic disease tissue targeting, and endosomal targeting due to the more acidic pH environments as mentioned above.[104] Polymers will remain stable until they reach the certain targeted pH, and the functional groups in the polymers undergo sharp response to the pH. Further approaches of pH-sensitive polymers have been used for pH-triggered DNA release in DNA vaccination therapy. Wang *et al.* reported that pDNA release can be controlled in a pH-dependent manner by synthesizing poly(ortho esters) (POEs).[122] As pH drops to 5, the DNA release was accelerated due to the degradation of ortho-ester bonds in the POEs. Moreover, efficient targeted delivery was observed via pH sensitive polymer, whereas nonsensitive polymer did not show any pH response and had no effect on tumor mass.[122]

1.5.1.1. Endosomal Targeting Polymers

The pH-dependent disruptive activity of targeting endosomes is one of the important properties for polymeric gene delivery carrier, because poor endosomal escape is one of the major intracellular barriers for gene delivery. Moreover, it has been proposed that the level of gene expression is relevant to endosomal escaping ability.[123] Thus, cationic polymers with endosomolytic activity are important to disrupt the endosomal membrane

and facilitate endosomal escaping for efficient release of pDNA into the cytoplasm before they end up lysosomes and undergo degradation. Some of the endosomolytic polymers that have been used for gene delivery are mentioned in Table 1.5.

Inside the cells, endosome and lysosome have relatively low acidic pH. Within the acidic endosomal compartments, polymers use different types of membrane-destabilization mechanism to escape from the endosomes.[124] The most popular endosomal escaping mechanism is via proton sponge effect. The pH sensitive polymer becomes protonated in acidic endosomal pH and leads to the flow of counter ions and water inside the vesicles that build up osmotic pressure and subsequently rupture the endosomal membrane.[107] PEI is one of the examples that supports the endosomal escaping mechanism. At physiological pH at 7.4, two thirds of amines are not protonated. However, as pH goes down to endosomal pH, the secondary and tertiary amines are protonated due to the pKa values, and more amines become protonated at endosomal pH.[125] Therefore, the powerful proton buffering ability of PEI results in effective endosomal release of gene cargos and leads to high transfection efficiency. Poly(amidoamine) (PAA) is also reported as a gene carrier with a pH-dependent membrane activity which induces a high buffering capacity. Unlike PEI, protonation of tertiary amines in PAA structure undergo conformational change and results in membrane damage at low pH.[126] PAA has been investigated as an endosomolytic polymer that has a high transfection capability. Wang's group reported the synthesis of PAAs with different branched architectures and demonstrated a correlation between branching and gene transfection ability.[127] The transfection studies showed that the level of gene transfection efficiency was improved with increase in branched structure due to

Table 1.5. Endosomolytic polymers and treatment outcomes

Category	Endosomolytic polymer	Nucleic acid type	Outcome
Polymer	Poly(L-histidine)-PEG	pDNA	The level of gene expression was similar to PLL/pDNA, but the cytotoxicity was significantly low due to the uncharged polyhistidine at pH 7.2.[133]
	Histidylated poly(L-lysine)	pDNA	Gene expression revealed 3-4.5 order of magnitude higher than that of PLL/pDNA.[134]
	Polyethylenimine (PEI)	pDNA	Protonable amines provided a strong proton buffering at acidic pHs and widely used as *in vitro* and *in vivo* gene carriers.[135]
	Polyamidoamine (PAMAM)-hydroxyl-terminated dendrimer QPAMAM-OH dendrimers	siRNA	The PAMAM induced a proton sponge effect from tertiary amines and showed a statistically significant gene knockdown efficiency.[136]
	(PPAA)	pDNA	Enhanced pH-dependent hemolysis activity showed an improved gene expression even in serum condition.[137]
	Poly[N-(2 aminoethyl) methacrylamide trifluoroacetate] (PAEMA)	pDNA	The highest transfection efficiency was resulted from polymers containing many primary amino groups which can induce an efficient endosomal release.[138]

Table 1.5. (Continued)

Category	Endosomolytic peptide	Nucleic acid type	Outcome
	Poly(dimethylaminoethyl methacrylate) (pDMAEMA) - chain transfer agent (CTA) pDMAEMA macro CTA	siRNA	Enhanced hemolytic activity at endosomal pH resulted in a strong gene silencing efficiency at charge ratio 8.[139]
	Dynamic polyconjugates	siRNA	A membrane active polymer induced nearly 80% knockdown of apoB mRNA.[140]
Polypeptide	Cys-His-Lys_6-His-Cys	pDNA	His content to 20% in peptides resulted a 10 fold transfection efficiency enhancement than the peptide without His residue.[141]
	Cys-$His_{3/6}$-Lys_3-$His_{3/6}$-Cys	pDNA	His 3 produced a lower transfection efficiency than PEI/pDNA, but higher His content (His 6) induced a superior gene expression activity which was similar to PEI/pDNA.[132]
	H5WYG	pDNA	Selective membrane destabilizing activity at pH 6.2 provided a 93, 215, and 630 fold transfection efficiency enhancement in HepG2, B16, and Rb-1 cells, respectively.[134]
	mellitin	pDNA	A membrane disruption activity of melittin facilitated the release of fluorescein-PEG and increased gene expression up to 5-12 fold higher.[142]

Table 1.5. (Continued)

Category	Endosomolytic peptide	Nucleic acid type	Outcome
	Tat sequence incorporating 10 histidine residue (Tat- 10H)	pDNA	Tat-10 H provided a 7000 fold higher gene expression than that of Tat control, and resulted in a comparable levels of gene activity than that of PEI/pDNA.[143]
	GALA	siRNA	A pH-sensitive membrane disruption activity of GALA enhanced a luciferase gene silencing in the HT 1080 human fibrosarcoma cell line.[144]
	cross-linked KALA cl-KALA	siRNA	Higher gene silencing efficiency was observed due to the membrane destabilizing activity of cl-KALA than that of naked KALA and PEI-mediated gene delivery.[145]

the increasing number of primary and tertiary amines, leading to enhanced buffering ability and pDNA condensation.

Another mechanism of endosomal escaping is via pore formation. Huang *et al.* proposed that some peptides bind to the lipid bilayer with a high affinity in the rim of the pore. Subsequently, the peptide binding induces an internal membrane tension and pores are made under tension in the membrane.[128] Melittin is one of the endosomal escape agents that inserts into the membrane and destabilizes the membrane by its high membrane lytic activity.[124] It was shown that melittin covalently linked to PEI is able to facilitate not only efficient endosomal escape but also the nuclear homing activity after release of polyplexes into the cytoplasm; thus, it leads to significant enhancement of gene expression.[129]

Fusion in the endosomal membrane is another mechanism that destabilizes the endosomal membrane and facilitates endosomal escaping. GALA and KALA are fusogenic amphipathic peptides that undergo a structural transformation upon pH changes. GALA (glutamic acid-alanine-leucine-alanine) is a pH-responsive 30 amino acid peptide that changes its conformation from a random coil to amphipathic α helix when pH drops 7 to 5.[130] At acidic endosomal pH, peptides become hydrophobic, because the glutamic acid residues become protonated and increased hydrophobicity induces the interaction with lipid bilayer that eventually causes membrane disruption.[107, 131] KALA is a similar fusogenic peptide with reduced glutamic acid residues and some alanine residues replacement with lysine residues.[132] It undergoes a similar conformational transition at low pH and shows fusion in the lipid bilayer. These fusogenic peptides have been applied to nonviral gene therapy due to the pH-responsive membrane disruptive behavior and

endosomal targeting polymers that have been studied in gene delivery application due to the presence of a pH-dependent membrane destabilizing activity. Histidinylated polymeric carriers are also known as endosomolytic polymers that destabilize the endosomal membrane because of the imidazole groups in histidine which respond at acidic endosomal pH.[146, 147] The imidazole ring of poly(L-histidine) (polyHis) has a pKa value of 6~7.[147, 148] It is generally hydrophobic and insoluble in aqueous solution at pH 7.4; however, polyHis becomes hydrophilic and more protonated as the pH lowers below 7 and enhances its endosomolytic efficacy via proton sponge effect. Since polyHis is not positively charged at neutral pH, it is hard to make a complex with pDNA. Thus, several researchers have been designed synthesizing polyHis with a polycation PLL. PLL coupled with polyHis was designed to deliver more genes into the cytoplasm by facilitating endosomal escape that PLL lacks. It was demonstrated that a pH-responsive endosomolytic behavior facilitated the release of pDNA from the endosomes and significantly enhanced the transfection efficiency more than with pDNA complexed with PLL.[131, 135] In addition, aminated polyHis was further constructed for gene delivery system. It showed a significant reduction of cytotoxicity and a pH-dependent hemolytic activity at pH 6, which leads to enhanced delivery of pDNA.[147]

The significant improvement of gene therapy via endosomolytic polymers has been demonstrated not only *in vitro* studies but also *in vivo* applications of gene delivery. Rozema *et al.* proposed the efficient *in vivo* siRNA delivery in hepatocytes by using dynamic polyconjugates which contain masking agent and ligand.[140] Once the complexes enter the endosome, the acidic environment inside triggers the polymers to destabilize the endosomal membrane and release siRNA from the endosome. Thus, the endosomolytic

demonstrated efficient release of polyplexes from endosomal vesicles to the cytoplasm.

Histidine containing protonable polycation is one of the intensively investigated polymers that provided highly efficient release of siRNA into the cytoplasm and showed enhanced knockdown in mice.

1.5.2. Biodegradable Polymers

The major benefit of designing and synthesizing biodegradable polymers is a more significant reduction of cytotoxicity than that of nondegraded polymers. Polymer and pDNA should be dissociated after the complexes are released from the endosomes; thus, degradation polymer can be suited as a gene carrier, which is able to release and translocate pDNA into the cytosol.[149] Biodegradable polymers have been synthesized to control release of pDNA upon an intracellular biological stimulus such as redox potential, pH, temperature, and enzyme.[107, 150] In this section, polymers contain hydrolytic sensitive bonds and disulfide bonds will be discussed in detail.

Hydrolytically degradable polymers are one of the biodegradable polymers that have been linked to polycations and used to control release of nucleic acids from the complexes. Hydrolytically sensitive bonds include esters, amides, anhydride, and urethanes.[150, 151] Among these, esters are a widely used biodegradable bond, and the most representative polyesters based polymers for gene delivery systems are poly(lactic-co-glycolic acid) (PLGA) and poly(β-amino esters) (PBAE). PLGA is an attractive pDNA delivery carrier due to its high encapsulation efficiency, and controlled release via biocompatible polyesters that degrades by hydrolysis. However, hydrolytic degradation of PLGA results in low pH within the PLGA particles which can degrade and damage the

DNA.[133, 152] Thus, many studies have been conducted to buffer the intraparticle pH and improve the pDNA stability by adding an excipient to the PLGA microspheres.[152]

PBAE is also known as pDNA delivery vehicles because the polymers have degradable bonds and primary amine end groups that can be protonated and strongly bind to pDNA, which form small complexes under physiological condition. PBAE is degraded by hydrolysis into bis(β-amino esters) which are nontoxic small byproducts.[125] Interestingly, PBAE degrades more rapidly in basic environments and slowly in acidic environments. Lynn *et al.* studied the degradation kinetics of PBAE in two different pHs 7.4 and 5.1, and degradation profiles showed that polymers degraded rapidly in pH 7.4 with half-life less than 2 hr, whereas half-life at pH 5.1 was extended up to 8 hr.[153] The degradability of PBAE not only significantly reduced the cytotoxicity, but also self-assembles with pDNA which produce stable nanoparticles and enhanced transfection efficiency compared to PEI under certain conditions.

Disulfide linked polymers have also been synthesized and applied to gene delivery system by taking advantage of reductive microenvironment.[103] It has been demonstrated in several studies that disulfide linker cleavages induce intracellular disassembly of polyplexes and facilitate release of gene from polyplexes. Generally, disulfide bonds containing bioreducible polymers are stable in the oxidative extracellular environment and degraded in the reductive intracellular environment due to the redox potential between the intracellular and extracellular spaces. Many cationic gene carriers containing disulfide bonds have been synthesized to minimize toxicity and alter the release rate of gene cargo and maximized transfection efficiency.

1.5.2.1. Redox Responsive Polymers

Cationic polymers have been used to protect gene from enzyme degradation; however, high degree of charge density can induce high polymer toxicity and strong interaction with pDNA which affects gene expression. Gene transfection efficiency can be hindered by tight pDNA binding and high toxicity of polyplexes.[154] Thus, the literature emphasizes that unpacking of pDNA from polyplexes is a rate-limiting step that affects the transfection efficiency.[155] The balancing between protection and release of pDNA seems a critical step to selectively release gene into the intracellular compartments. Thus, polymers should be dissociated to release pDNA at the right time.[90, 155]

Disulfide bonds containing reducible polymers are considered ideal gene carriers because of the degradation of the disulfide bonds which can facilitate the unpacking of the polyplexes, minimize toxicity, and accelerate elimination from the body.[156, 157] Generally, cysteine residues or polymers which contain sulfhydryl groups allow disulfide formation when two of sulfhydryl groups undergo oxidation. Disulfide bonds are able to change polymer stability since they have a biodegradable ability under an intracellular environment. Intracellular compartments maintain high concentrations of glutathione (GSH), 0.5-10 mM, and keep a high reducing environment by NADPH and glutathione reductase, whereas GSH concentration is about 2.8 μM.[158-160] Among intracellular compartments, cytosol has a high reducing potential that can facilitate the cleavage rates of the bond and trigger pDNA release mainly in the reducing cytoplasm.[161,162] Therefore, polyplexes remain stable in extracellular compartments and undergo rapid degradation by reduction of disulfide bonds to free thiol in reducing intracellular environments.

Redox potential across the oxidizing extracellular and reducing intracellular

compartment induces thiol-disulfide exchange reaction and it is determined by GSH content in cells. However, there are at least 4 fold differences of GSH levels in normal and tumor tissue.[159] For example, GSH levels in normal breast tissue are 7.2 ± 1.3 nmol/mg protein. On the contrary MCF7 cells show GSH levels of 55 nmol/mg protein, a level more suitable for reducible polymer mediated gene therapy.[159] Moreover, cancer cells display a high glutathione-S-transferase (GST) activity. The glutathione S-transferase (GST) activity in MCF 7 cells show 9.83 ± 0.41 nmol/mg, and other breast cancer cell lines such as T47D and MDA-MB-468 show 4.9 nmol/mg and 2.5 nmol/mg, respectively.[163, 164] Therefore, the high level of GST activity and GSH in cancer cell line provides the optimal conditions for reducible polymer in cancer gene therapy applications due to degradation of bioreducible polymer, which not only triggers the release of DNA, but also reduces cytotoxicity inside cells by preventing accumulation of cationic polymers. Bioreducible polymers, cargo type, and outcome are summarized in Table 1.6.

Reductive sensitive bioreducible polymers have been applied for gene delivery system and tested for gene expression studies *in vitro* and *in vivo*. There are several methods to construct disulfide bonds in polymers. Disulfide linked polymers have been crosslinked in different molecular weights of bPEI using reducible crossing agents such as dithiobis(succinimidylpropionate) (DSP) and dimethyl-3,3´-dithiobispropionimidate-2HCl (DTBP) by many scientists.[156] These crosslinking reagents react with primary amines in PEI and produce disulfide bonds. However, the data showed that DTBP conjugated with PEI demonstrated more enhanced gene expression than that of DSP conjugated with PEI, because DTBP conjugates maintains the net charge and induce stronger interactions with cell membranes, whereas DSP conjugates lead to elimination

Table 1.6. Bioreducible polymers and treatment outcomes

Category	Redox sensitive polymer	Gene type	Outcome
Polymer	Polyethylenimine (PEI)-Dithiobis(succinimidylpropionate)(DSP)/ PEI- Dimethyl·3,3‘-dithiobispropionimidate·2HCl (DTBP) PEI-DSP/PEI-DTBP	pDNA	The transfection efficiency was not greater than that of PEI_{25K}/pDNA, but a significant reduction of toxicity was observed.[156]
	Reducible polycations- branched polyethyleneimine RPC-$bPEI_{0.8\ kDa}$	pDNA	Polymer was 8-19 times less cytotoxic and 1200-1500 fold greater transfection efficiencies than that of $bPEI_{0.8\ kDa}$/pDNA complexes were observed.[166]
	Branched polyethylenimine (BPEI)-SS-polyethylene glycol (PEG)--cyclic NGR (cNGR) BPEI-SS-PEG-cNGR	pDNA	Increased GSH concentration facilitated the pDNA release from the carriers and resulted a transfection efficiency enhancement.[168]
	Lomant's reagent (LR)/Boc-cystine (BC)-linear poly(ethylene imine) (lPEI) LRx-lPEIy/ BCx-lPEIy	pDNA	A maximum transfection efficiency of LR3-lPEI2.6 and BC8-lPEI2.6 were observed at N/P 18 and N/P30, respectively, in CHO-K1 cells.[169]
	linear poly(ethylenimine sulfide) l-PEIS	pDNA	l-PEIS-6 and l-PEIS-8 showed a comparable transfection efficiency to the linear PEI derivatives in Hela and HepG2 cells.[170]
	SS-Poly(amido amine)s (PAAs) SS-PAAs	pDNA	PAAs with disulfide bonds showed up to 1.6 times higher transfection efficiency than those polymers without disulfide bonds.[167]

Table 1.6. (Continued)

Category	Redox sensitive polymer	Gene type	Outcome
	SS–PAAs with oligoamine side chains (PAOAs) SS-PAOAs	pDNA	At N/P 3.5, SS-PAOAs containing tetraethylenepentamine (TEPA) showed a higher tranfection efficiency than that of pDMAEMA and bPEI 25K polyplexes.[171]
	SS-Poly(amido ethylenimine) (PAEI) SS-PAEI	pDNA	SS-PAEIs synthesized from ethylenediamine (EDA) showed a 20 fold higher transfection efficiency that that of bPEI in BACEs cells.[172]
	Poly(N,N-dimethyl-ethylamine methacrylate) PDMAEMA	pDNA	The gene transfection efficiency was enhanced 15-20 fold higher compared to the control groups.[173]
	Arginine-grafted bioreducible poly(disulfide amine) (ABP)	pDNA	The transfection efficiency of ABP at WR 50 was 30 fold higher than that of PEI25K in C2C12 cells.[174]
Polypeptide	Cys-Lys_{10}-Cys	pDNA	A 100 fold enhanced transfection activity was provided by reducible polycations compared to the control PLL.[157]
	Cys-Trp-Lys17-Cys	pDNA	A 60 fold increased gene expression in HepG2 cells.[141]
	PEG-SS-CWK_{18}	pDNA	A 100 fold increase of gene transfer compared to the nonreducible polymers in HepG2 cells.[175]
	Poly(oligo-D-arginine)	pDNA	A 20 fold higher *in vivo* transfection efficiency was obtained with a minimal cytotoxicity compared to the PEI/pDNA complexes.[176]

of the positive charges in PEI.[156]

Sun and coworkers have synthesized reducible SS-PEI via Michael addition polymerization using cysteine bisacrylamide (CBA). Reactive group in CBA reacts with primary amines in PEI to form reducible polymer. The cytotoxicity of disulfide containing polymers were significantly lower than 25 kDa PEI, and polyplexes exposed to reducing agents induced efficient release of pDNA. Therefore, *in vitro* experiments showed that the transfection efficiency of SS-PEI was comparable to that of 25 kDa PEI.[165]

Furthermore, Kang *et al*. reported the formation of disulfide linkages in 800 Da bPEI via thiolation with 2-iminothiolane (2-IT) followed by oxidation under DMSO.[166] 2-IT reacts with primary amines in bPEI and produces amidine groups. Once bPEI is thioloated with 2-IT, DMSO induces oxidative polymerization and synthesizes reducible bPEI. Kang *et al*. tested efficient degradation of disulfide bonds and the release of gene under reducing environment and demonstrated that introduction of disulfide bonds in low molecular weight bPEI significantly enhanced the transfection efficiency up to 1200-1500 fold compared to that of $bPEI_{800}$/pDNA complexes.[166] Thus, the authors emphasized the potential use of reducible bPEI as a gene delivery carrier.

Bioreducible poly(amidoamines) (PAA) also have been synthesized and studied for gene delivery system. Lin and coworkers prepared disulfide linkage polymers via michael addition reaction between CBA and 1-(2-aminoethyl) piperazine (AEP) which is a tri-functional amine monomer and synthesized p(CBA-AEP).[167] p(CBA-AEP) not only displayed high buffering capacity, but also formed stable nano-sized complexes. However, Lin *et al*. claimed that low content of CBA (10-20%) was not efficiently

released pDNA, whereas higher content of CBA (60%) showed complete release of pDNA. Thus, disulfide contents should be optimized to obtain both enhanced levels of gene expression and low cell toxicity. In addition, Lin's group also prepared several SS-PAAs using same methods but various primary amines. Among PAAs, *in vitro* transfection studies showed that reducible polymers made from 4-amino-1-butanol (ABOL), and 5-amino-1-pentanol (APOL) displayed the highest levels of gene expression because of the relatively high charge density which affected the pDNA condensation ability and produced small particle size.[154] The dissociation of disulfide bonds significantly enhanced the transfection activity even in 5% serum condition.

The advantages of a redox triggered dissociation mechanism of reducible polymers also showed superior gene expression activity in *in vivo* studies. Neu *et al.* constructed crosslinked PEI using DSP, and crosslinked PEI/pDNA complexes were delivered via the tail vein in Balb/c mice for systemic plasmid delivery.[177] As a crosslinking degree increased, polyplex stability was enhanced and resulted higher blood levels with longer circulation time. More interestingly, the biodistribution data showed that surface crosslinked polyplexes significantly enhanced liver accumulation, whereas reduced unwanted accumulation in lung. This result might be due to high GSH concentrations in liver cells (0.5-11 mM), which favor degradation of disulfide bonds and facilitate pDNA release in the liver tissue.[178] In a subsequent study, Neu's group designed crosslinked PEI-PEG to improve the polyplexes stability for *in vivo* studies. 2 μg pCMV-Luc plasmids were complexed with the crosslinked PEI-PEG and injected into tail vein for pharmacokinetic studies. In case of crosslinked polyplexes, they were able to observe enhancement of blood levels up to 60 min after IV injection compared to that of PEI and

uncrosslinked PEI-PEG.[178] The pharmacokinetic profile demonstrated that surface crosslinking of PEI-PEG can be beneficial to gene delivery system due to the efficient gene release and high blood levels.

Stimuli-sensitive polymers have been vigorously investigated in gene delivery system due to the change of polymer network structure upon environmental changes. These polymers are designed to change in sharp response to biological stimulus such as pH, temperature, and redox microenvironment to overcome intracellular obstacles and eventually deliver genetic materials to the target sites.

In Chapter 2, a redox-triggered destabilization mechanism was applied in gene delivery system via reducible PLL (RPLL). RPLL containing disulfide linkages was studied in mimicked reductive intracellular environments to test the correlation between disulfide contents and transfection efficiency. Different contents of RPLL regarding gene release rates and kinetics were tested in reducing environments, and its transfection efficiency was demonstrated compared to that of PLL. Depending on the differences in reduction potential, content of the disulfide bonds will affect the release rate of pDNA, toxicity, and gene expression. Therefore, this study will focus on optimizing the protection and release of pDNA via control of disulfide contents to maximize transfection efficiency.

In the following Chapter 3, pH-responsive polymers are constructed in two different ways based on arrangement of imidazole groups in histidine and studied whether an endosomal destabilizing ability from two different polymers can favor efficient gene release and lead to enhanced transfection efficiency. Two types of histidine grafted PLLs, poly(L-histidine) (PLL-*g*-PHis) and a mono-L-histidine (PLL-*g*-mHis), were synthesized

and compared in terms of their endosomolytic activity and transfection efficiency. These experiments are examined in greater details in Chapter 3. The main goal of constructing two different types of PLLs was synthesizing pH-dependent endosomolytic polymers in an effective way for efficient gene delivery and expression. Thus, we performed a comparison study between PLL-*g*-PHis and PLL-*g*-mHis to demonstrate a different pH-responsive disruptive activity regarding endosomal escape, and hemolytic activity, as well as its consequence in rapid release of polyplexes and transfection efficiency.

Based on Chapter 2 and 3, a reducible polymer consisting of PHis and PLL will be developed as an ultimate gene delivery carrier to overcome intracellular barriers and improve gene transfection efficiency. Reducible disulfide bonds into a polymer backbone will be cleaved under a cytosolic reduction condition and lead to enhancement of gene release from the polyplexes in the cytosol. Moreover, degradable bonds will significantly reduce the toxicity in cells. Since imidazole rings in PHis influenced by the degree of ionization, it will contribute to enhance gene delivery by providing superior buffering capacity in endosomes and facilitating polyplexes escape from the endosomes. The details will be discussed in future prospects in Chapter 4.

1.6. References

1. Siegel R, Naishadham D, Jemal A. Cancer statistics, 2012. CA-Cancer J. Clin. 2012;62(1):10-29.

2. Downward J. Targeting RAS signalling pathways in cancer therapy. Nat Rev Cancer. 2003;3(1):11-22.

3. Wicha MS, Liu S, Dontu G. Cancer stem cells: an old idea—a paradigm shift. Cancer Res. 2006;66(4):1883-1890.

4. Visvader JE, Lindeman GJ. Cancer stem cells in solid tumours: accumulating

evidence and unresolved questions. Nat Rev Cancer. 2008;8(10): 755-768.

5. Shackleton M, Quintana E, Fearon ER. Morrison, S. J., Heterogeneity in cancer: cancer stem cells versus clonal evolution. Cell. 2009;138(5):822-829.

6. Brocks D, Assenov Y, Minner S, Bogatyrova O, Simon R, Koop C, Oakes C, Zucknick M, Lipka DB, Weischenfeldt J. Intratumor DNA methylation heterogeneity reflects clonal evolution in aggressive prostate cancer. Cell Rep. 2014;8 (3):798-806.

7. Orive G, Reshkin S, Harguindey S, Pedraz J. Hydrogen ion dynamics and the Na^+/H^+; exchanger in cancer angiogenesis and antiangiogenesis. Br. J. Cancer. 2003;89(8):1395-1399.

8. Vaupel P. Tumor microenvironmental physiology and its implications for radiation oncology. Semin Radiat Oncol. 2004;14(3):198-206.

9. Menon C, Fraker DL. Tumor oxygenation status as a prognostic marker. Cancer Lett. 2005; 221(2):225-235.

10. Bratasz A, Pandian RP, Deng Y, Petryakov S, Grecula JC, Gupta N, Kuppusamy, P. In vivo imaging of changes in tumor oxygenation during growth and after treatment. Magn Reson Med. 2007;57(5):950-959.

11. Fang JS, Gillies RD, Gatenby RA. Adaptation to hypoxia and acidosis in carcinogenesis and tumor progression, Sem Cancer Biol. 2008;18(5):330-337.

12. Denko NC. Hypoxia, HIF1 and glucose metabolism in the solid tumour. Nat Rev Cancer. 2008, 8, (9), 705-713.

13. Carmeliet P, Jain RK. Angiogenesis in cancer and other diseases. nature. 2000, 407, (6801), 249-257.

14. Weis SM, Cheresh DA. Tumor angiogenesis: molecular pathways and therapeutic targets. Nat. Med. 2011;17(11):1359-1370.

15. Sarntinoranont M, Rooney F, Ferrari M. Interstitial stress and fluid pressure within a growing tumor. Ann Biomed Eng. 2003;31(3):327-335.

16. Heldin CH, Rubin K, Pietras K, Östman A. High interstitial fluid pressure—an obstacle in cancer therapy. Nat Rev Cancer. 2004;4(10):806-813.

17. Munson JM, Shieh AC. Interstitial fluid flow in cancer: implications for disease progression and treatment. Cancer Manag Res. 2014; 6:317.

18. Lu P, Weaver VM, Werb Z. The extracellular matrix: a dynamic niche in cancer progression. J. Cell Biol.2012;196(4):395-406.

19. Frantz C, Stewart KM, Weaver VM. The extracellular matrix at a glance. J. Cell Sci. 2010;123(24):4195-4200.

20. Pathak A, Kumar S. Independent regulation of tumor cell migration by matrix stiffness and confinement. Proc. Natl. Acad. Sci. U.S.A. 2012;109 (26):10334-10339.

21. Zitvogel L, Apetoh L, Ghiringhelli F, Kroemer G. Immunological aspects of cancer chemotherapy. Nat Rev Immunol. 2008; 8(1):59-73.

22. Kaufmann SH, Earnshaw WC. Induction of apoptosis by cancer chemotherapy. Exp Cell Res. 2000;256(1):42-49.

23. Baskar R, Lee KA, Yeo R, Yeoh KW. Cancer and radiation therapy: current advances and future directions. Int. J. Med. Sci. 2012;9(3):193.

24. Melero I, Hervas-Stubbs S, Glennie M, Pardoll DM, Chen L. Immunostimulatory monoclonal antibodies for cancer therapy. Nat Rev Cancer. 2007; 7(2):95-106.

25. Weiner LM, Surana R, Wang S. Monoclonal antibodies: versatile platforms for cancer immunotherapy. Nat Rev Immunol. 2010;10(5):317-327.

26. Rosenberg SA, Yang JC, Restifo NP. Cancer immunotherapy: moving beyond current vaccines. Nat. Med. 2004;10(9):909-915.

27. Kerbel R, Klement G, Pritchard K, Kamen B. Continuous low-dose anti-angiogenic/metronomic chemotherapy: from the research laboratory into the oncology clinic. Ann. Oncol. 2002;13(1):12-15.

28. Bentzen SM. Preventing or reducing late side effects of radiation therapy: radiobiology meets molecular pathology. Nat Rev Cancer. 2006;6(9):702-713.

29. Vogelstein B, Kinzler KW. Cancer genes and the pathways they control. Nat. Med. 2004;10(8):789-799.

30. Reles A, Wen WH, Schmider A, Gee C, Runnebaum IB, Kilian U, Jones LA, El-Naggar A, Minguillon C, Schönborn I. Correlation of p53 mutations with resistance to platinum-based chemotherapy and shortened survival in ovarian cancer. Clin. Cancer Res. 2001;7(10):2984-2997.

31. Kuball J, Wen SF, Leissner J, Atkins D, Meinhardt P, Quijano E, Engler H, Hutchins B, Maneval DC, Grace MJ. Successful adenovirus-mediated wild-type p53 gene transfer in patients with bladder cancer by intravesical vector instillation. J. Clin. Oncol. 2002;20(4):957-965.

32. Weiss RH. $p21^{Waf1/Cip1}$ as a therapeutic target in breast and other cancers. Cancer cell. 2003;4(6):425-429.

33. El-Aneed A. An overview of current delivery systems in cancer gene therapy. J Control Release. 2004;94(1):1-14.

34. Davies MA, Kim SJ, Parikh NU, Dong Z, Bucana CD, Gallick GE. Adenoviral-mediated expression of MMAC/PTEN inhibits proliferation and metastasis of human prostate cancer cells. Clin. Cancer Res. 2002;8(6):1904-1914.

35. Huang H, Cheville JC, Pan Y, Roche PC, Schmidt LJ, Tindall DJ. PTEN induces chemosensitivity in PTEN-mutated prostate cancer cells by suppression of Bcl-2 expression. J. Biol. Chem. 2001;276(42):38830-38836.

36. Tanaka M, Grossman H. In vivo gene therapy of human bladder cancer with PTEN suppresses tumor growth, downregulates phosphorylated Akt, and increases sensitivity to doxorubicin. Gene Ther. 2003;10(19):1636-1642.

37. van't Veer LJ, Dai H, Van De Vijver MJ, He YD, Hart AA, Mao M, Peterse HL, van der Kooy K, Marton MJ, Witteveen AT. Gene expression profiling predicts clinical outcome of breast cancer. nature. 2002;415(6871):530-536.

38. Drost R, Bouwman P, Rottenberg S, Boon U, Schut E, Klarenbeek S, Klijn C, van der Heijden I, van der Gulden H, Wientjens E. BRCA1 RING function is essential for tumor suppression but dispensable for therapy resistance. Cancer cell. 2011;20(6):797-809.

39. Zhang Z, Li M, Wang H, Agrawal S, Zhang. R. Antisense therapy targeting MDM2 oncogene in prostate cancer: Effects on proliferation, apoptosis, multiple gene expression, and chemotherapy. Proc. Natl. Acad. Sci. U.S.A. 2003; 100(20):11636-11641.

40. Osborne C, Wilson P, Tripathy D. Oncogenes and tumor suppressor genes in breast cancer: potential diagnostic and therapeutic applications. Oncologist. 2004; 9 (4):361-377.

41. Ménard S, Pupa SM, Campiglio M, Tagliabue E. Biologic and therapeutic role of HER2 in cancer. Oncogene. 2003;22(42):6570-6578.

42. Tai W, Mahato R, Cheng K. The role of HER2 in cancer therapy and targeted drug delivery. J Control Release. 2010;146(3):264-275.

43. Attoub S, Rivat C, Rodrigues S, Van Bocxlaer S, Bedin M, Bruyneel E, Louvet C, Kornprobst M, André T, Mareel M. The c-kit tyrosine kinase inhibitor STI571 for colorectal cancer therapy. Cancer Res. 2002;62(17):4879-4883.

44. Sammarco I, Capurso G, Coppola L, Bonifazi AP, Cassetta S, Delle Fave G, Carrara A, Grassi GB, Rossi P, Sette C. Expression of the proto-oncogene c-KIT in normal and tumor tissues from colorectal carcinoma patients. Int J Colorectal Dis. 2004;19(6);545-553.

45. Birchmeier C, Birchmeier W, Gherardi E, Woude GFV. Met, metastasis, motility and more. Nat. Rev. Mol. Cell Biol. 2003;4(12):915-925.

46. Christensen JG, Burrows J, Salgia R. c-Met as a target for human cancer and characterization of inhibitors for therapeutic intervention. Cancer Lett. 2005;225(1):1-26.

47. Maulik G, Shrikhande A, Kijima T, Ma PC, Morrison PT, Salgia R. Role of the hepatocyte growth factor receptor, c-Met, in oncogenesis and potential for therapeutic inhibition. Cytokine Growth Factor Rev. 2002;13(1):41-59.

48. Adjei AA. Blocking oncogenic Ras signaling for cancer therapy. J Natl Cancer Inst. 2001;93(14):1062-1074.

49. Soussi T. The p53 tumor suppressor gene: from molecular biology to clinical investigation. Ann. N. Y. Acad. Sci. 2000;910(1):121-139.

50. Lang FF, Bruner JM, Fuller GN, Aldape K, Prados MD, Chang S, Berger MS, McDermott MW, Kunwar SM, Junck LR, Phase I trial of adenovirus-mediated p53 gene therapy for recurrent glioma: biological and clinical results. J. Clin. Oncol. 2003;21(13):2508-2518.

51. Xu L, Pirollo K, Chang E. Tumor-targeted p53-gene therapy enhances the efficacy of conventional chemo/radiotherapy. J Control Release. 2001;74(1): 115-128.

52. Gudmundsdottir K, Ashworth A. The roles of BRCA1 and BRCA2 and associated proteins in the maintenance of genomic stability. Oncogene. 2006;25(43):5864-5874.

53. Farmer H, McCabe N, Lord CJ, Tutt AN, Johnson DA, Richardson TB, Santarosa M, Dillon KJ, Hickson I, Knights C. Targeting the DNA repair defect in BRCA mutant cells as a therapeutic strategy. Nature. 2005;434(7035):917-921.

54. Teoh H, Quan A, Creighton A, Bang KA, Singh K, Shukla P, Gupta N, Pan Y, Lovren F, Leong-Poi H. BRCA1 gene therapy reduces systemic inflammatory response and multiple organ failure and improves survival in experimental sepsis. Gene Ther. 2012;20(1):51-61.

55. Slamon DJ, Leyland-Jones B, Shak S, Fuchs H, Paton V, Bajamonde A, Fleming T, Eiermann W, Wolter J, Pegram M. Use of chemotherapy plus a monoclonal antibody against HER2 for metastatic breast cancer that overexpresses HER2. N. Engl. J. Med. 2001;344(11):783-792.

56. Urban-Klein B, Werth S, Abuharbeid S, Czubayko F, Aigner A. RNAi-mediated gene-targeting through systemic application of polyethylenimine (PEI)-complexed siRNA in vivo. Gene Ther. 2004;12(5):461-466.

57. Thomas CE, Ehrhardt A, Kay MA. Progress and problems with the use of viral

vectors for gene therapy. Nat. Rev. Genet. 2003;4(5), 346-358.

58. Sieczkarski SB, Whittaker GR. Dissecting virus entry via endocytosis. J. Gen. Virol. 2002;83(7):1535-1545.

59. Ruponen M, Honkakoski P, Rönkkö S, Pelkonen J, Tammi M, Urtti A. Extracellular and intracellular barriers in non-viral gene delivery. J Control Release. 2003;93(2):213-217.

60. Zhdanov R, Podobed O, Vlassov V. Cationic lipid–DNA complexes—lipoplexes—for gene transfer and therapy. Bioelectrochemistry. 2002;58(1):53-64.

61. Audouy SA, de Leij LF, Hoekstra D, Molema G. In vivo characteristics of cationic liposomes as delivery vectors for gene therapy. Pharm Res. 2002; 19(11):1599-1605.

62. Agrawal A, Min DH, Singh N, Zhu H, Birjiniuk A, Von Maltzahn G, Harris TJ, Xing D, Woolfenden SD, Sharp PA. Functional delivery of siRNA in mice using dendriworms. Acs Nano. 2009;3(9):2495-2504.

63. O'Rorke S, Keeney M, Pandit A. Non-viral polyplexes: scaffold mediated delivery for gene therapy. Prog. Polym. Sci. 2010;35(4):441-458.

64. Merdan T, Kopeček J, Kissel T. Prospects for cationic polymers in gene and oligonucleotide therapy against cancer. Adv. Drug Deliv. Rev. 2002;54(5):715-758.

65. Somia N, Verma IM. Gene therapy: trials and tribulations. Nat. Rev. Genet. 2000;1(2):91-99.

66. Grieger JC, Samulski RJ. Packaging capacity of adeno-associated virus serotypes: impact of larger genomes on infectivity and postentry steps. J. Virol. 2005;79 (15):9933-9944.

67. Monahan PE, Samulski RJ. Adeno-associated virus vectors for gene therapy: more pros than cons?. Mol Med Today. 2000;6(11):433-440.

68. Carew JF, Kooby DA, Halterman MW, Kim SH, Federoff HJ, Fong Y. A novel approach to cancer therapy using an oncolytic herpes virus to package amplicons containing cytokine genes. Mol. Ther. 2001;4(3):250-256.

69. Marconi P, Tamura M, Moriuchi S, Krisky DM, Niranjan A, Goins WF, Cohen J. B, Glorioso JC. Connexin 43-enhanced suicide gene therapy using herpesviral vectors. Mol. Ther. 2000;1(1):71-81.

70. Varghese S, Rabkin SD. Oncolytic herpes simplex virus vectors for cancer

virotherapy. Cancer Gene Ther. 2002;9(12):967-978.

71. Vorburger SA, Hunt KK. Adenoviral gene therapy. Oncologist. 2002;7(1):46-59.

72. Lundstrom K. Latest development in viral vectors for gene therapy. Trends Biotechnol. 2003;21(3):117-122.

73. Shi F, Rakhmilevich AL, Heise CP, Oshikawa K, Sondel PM, Yang NS, Mahvi, DM. Intratumoral injection of interleukin-12 plasmid DNA, either naked or in complex with cationic lipid, results in similar tumor regression in a murine model. Mol. Cancer Ther. 2002;1(11):949-957.

74. Walther W, Stein U, Fichtner I, Malcherek L, Lemm M, Schlag P. Nonviral in vivo gene delivery into tumors using a novel low volume jet-injection technology. Gene Ther. 2001;8(3):173-180.

75. Dass CR, Choong PF. Selective gene delivery for cancer therapy using cationic liposomes: in vivo proof of applicability. J Control Release. 2006;113(2): 155-163.

76. Kaneda Y, Tabata Y. Non-viral vectors for cancer therapy. Cancer Sci. 2006; 97(5):348-354.

77. Morille M, Passirani C, Vonarbourg A, Clavreul A, Benoit JP. Progress in developing cationic vectors for non-viral systemic gene therapy against cancer. Biomaterials. 2008;29(24):3477-3496.

78. Ginn SL, Alexander IE, Edelstein ML, Abedi MR, Wixon J. Gene therapy clinical trials worldwide to 2012–an update. J Gene Med. 2013;15(2):65-77.

79. Cotrim AP, Baum BJ. Gene therapy: some history, applications, problems, and prospects. Toxicol. Pathol. 2008;36(1):97-103.

80. Duncan R. The dawning era of polymer therapeutics. Nat. Rev. Drug Discov. 2003;2(5):347-360.

81. Huang L. LPD Nanoparticles for Gene Delivery. Nat. Biotechnol. 1999;17: 18-18.

82. Isner JM, Pieczek A, Schainfeld R, Blair R, Haley L, Asahara T, Rosenfield K, Razvi S, Walsh K, Symes JF. Clinical evidence of angiogenesis after arterial gene transfer of phVEGF$_{165}$ in patient with ischaemic limb. Lancet. 1996;348(9024):370-374.

83. Mintzer MA, Simanek EE. Nonviral vectors for gene delivery. Chem. Rev. 2008;109(2):259-302.

84. Ruponen M, Rönkkö S, Honkakoski P, Pelkonen J, Tammi M, Urtti, A.

Extracellular glycosaminoglycans modify cellular trafficking of lipoplexes and polyplexes. J. Biol. Chem. 2001;276(36):33875-33880.

85. Pathak A, Patnaik S, Gupta KC. Recent trends in non-viral vector-mediated gene delivery. Biotechnol. J. 2009;4(11):1559-1572.

86. Guo S, Huang L. Nanoparticles escaping RES and endosome: challenges for siRNA delivery for cancer therapy. J Nanomater. 2011;11.

87. Davis ME. Non-viral gene delivery systems. Curr. Opin. Biotechnol. 2002;13(2):128-131.

88. Lechardeur D, Lukacs GL. Intracellular barriers to non-viral gene transfer. Curr. Gene Ther. 2002;2(2):183-194.

89. Gratton SE, Ropp PA, Pohlhaus PD, Luft JC, Madden VJ, Napier ME, DeSimone JM. The effect of particle design on cellular internalization pathways. Proc. Natl. Acad. Sci. U.S.A. 2008;105(33):11613-11618.

90. Lungwitz U, Breunig M, Blunk T, Göpferich A. Polyethylenimine-based non-viral gene delivery systems. Eur. J. Pharm. Biopharm. 2005;60(2):247-266.

91. Verma A, Stellacci F. Effect of surface properties on nanoparticle–cell interactions. Small. 2010;6(1):12-21.

92. Liu Y, Reineke TM. Poly (glycoamidoamine) s for gene delivery. Structural effects on cellular internalization, buffering capacity, and gene expression. Bioconjugate Chem. 2007;18(1):19-30.

93. Rejman J, Bragonzi A, Conese M. Role of clathrin-and caveolae-mediated endocytosis in gene transfer mediated by lipo-and polyplexes. Mol. Ther. 2005; 12(3):468-474.

94. Kircheis R, Wightman L, Wagner E. Design and gene delivery activity of modified polyethylenimines. Adv. Drug Deliv. Rev.. 2001;53(3):341-358.

95. Zhao XB, Lee RJ. Tumor-selective targeted delivery of genes and antisense oligodeoxyribonucleotides via the folate receptor. Adv. Drug Deliv. Rev. 2004; 56(8):1193-1204.

96. Kichler A. Gene transfer with modified polyethylenimines. J Gene Med. 2004; 6(S1):S3-S10.

97. Elouahabi A, Ruysschaert JM. Formation and intracellular trafficking of lipoplexes and polyplexes. Mol. Ther. 2005;11(3):336-347.

98. Pack DW, Hoffman AS, Pun S, Stayton PS. Design and development of polymers for gene delivery. Nat. Rev. Drug Discov. 2005;4(7):581-593.

99. Pouton CW, Wagstaff KM, Roth DM, Moseley GW, Jans DA. Targeted delivery to the nucleus. Adv. Drug Deliv. Rev. 2007;59(8):698-717.

100. Al-Dosari MS, Gao X. Nonviral gene delivery: principle, limitations, and recent progress. AAPS J. 2009;11(4):671-681.

101. Hoyer J, Neundorf I. Peptide vectors for the nonviral delivery of nucleic acids. Acc. Chem. Res. 2012;45(7):1048-1056.

102. Wang F, Wang Y, Zhang X, Zhang W, Guo S, Jin F. Recent progress of cell-penetrating peptides as new carriers for intracellular cargo delivery. J Control Release. 2014;174:126-136.

103. Calderón M, Quadir MA, Strumia M, Haag R. Functional dendritic polymer architectures as stimuli-responsive nanocarriers. Biochimie, 2010;92(9):1242-1251.

104. Ganta S, Devalapally H, Shahiwala A, Amiji M. A review of stimuli-responsive nanocarriers for drug and gene delivery. J Control Release. 2008;126(3):187-204.

105. Kang HC, Samsonova O, Kang SW, Bae YH. The effect of environmental pH on polymeric transfection efficiency. Biomaterials. 2012;33(5):1651-1662.

106. Kim TH, Ihm JE, Choi YJ, Nah JW, Cho CS. Efficient gene delivery by urocanic acid-modified chitosan. J Control Release. 2003;93(3):389-402.

107. Shim MS, Kwon YJ. Stimuli-responsive polymers and nanomaterials for gene delivery and imaging applications. Adv. Drug Deliv. Rev. 2012;64(11):1046-1059.

108. Jeong B, Gutowska A. Lessons from nature: stimuli-responsive polymers and their biomedical applications. Trends Biotechnol. 2002;20(7):305-311.

109. Bawa P, Pillay V, Choonara YE, Du Toit LC. Stimuli-responsive polymers and their applications in drug delivery. Biomed. Mater. 2009;4(2):022001.

110. Mertoglu M, Garnier S, Laschewsky A, Skrabania K, Storsberg J. Stimuli responsive amphiphilic block copolymers for aqueous media synthesised via reversible addition fragmentation chain transfer polymerisation (RAFT). Polymer. 2005;46(18): 7726-7740.

111. De las Heras Alarcón C, Pennadam S, Alexander C. Stimuli responsive polymers for biomedical applications. Chem. Soc. Rev. 2005;34(3):276-285.

112. Chen W, Tomalia DA, Thomas JL. Unusual pH-dependent polarity changes in

PAMAM dendrimers: evidence for pH-responsive conformational changes. Macromolecules. 2000;33(25):9169-9172.

113. Wiśniewska M, Urban T, Grządka E, Zarko VI, Gun'ko VM. Comparison of adsorption affinity of polyacrylic acid for surfaces of mixed silica–alumina. Colloid Polym. Sci. 2014;292(3):699-705.

114. Liu Y, He T, Gao C. Surface modification of poly (ethylene terephthalate) via hydrolysis and layer-by-layer assembly of chitosan and chondroitin sulfate to construct cytocompatible layer for human endothelial cells. Colloids Surf., B. 2005;46(2):117-126.

115. Mebarek N, Aubert-Pouëssel A, Gérardin C, Vicente R, Devoisselle JM, Bégu S. Polymeric micelles based on poly (methacrylic acid) block-containing copolymers with different membrane destabilizing properties for cellular drug delivery. Int. J. Pharm. 2013;454(2):611-620.

116. Grainger SJ, El-Sayed ME. Stimuli-sensitive particles for drug delivery. Biologically-Responsive Hybrid. Biomaterials. 2010;171-190.

117. Bhatia SR, Khattak SF, Roberts SC. Polyelectrolytes for cell encapsulation. Curr. Opin. Colloid Interface Sci. 2005;10(1):45-51.

118. Wang Y, Chen P, Shen J. The development and characterization of a glutathione-sensitive cross-linked polyethylenimine gene vector. Biomaterials. 2006;27(30):5292-5298.

119. Hu X, Tong Z, Lyon LA. Synthesis and physicochemical properties of cationic microgels based on poly (N-isopropylmethacrylamide). Colloid Polym. Sci. 2011;289(3):333-339.

120. Schacher F, Rudolph T, Ulbricht M, Müller AH. Double Stimuli-Responsive Porous Mem-branes from Polystyrene-block-poly (N, N-dimethyl-aminoethyl methacrylate) Diblock Copolymers. ACS. 2009.

121. Dufès C, Uchegbu IF, Schätzlein AG. Dendrimers in gene delivery. Adv. Drug Deliv. Rev. 2005;57(15):2177-2202.

122. Wang C, Ge Q, Ting D, Nguyen D, Shen HR, Chen J, Eisen HN, Heller J, Langer R, Putnam D. Molecularly engineered poly (ortho ester) microspheres for enhanced delivery of DNA vaccines. Nat. Mater. 2004;3(3):190-196.

123. Wiethoff CM, Middaugh CR. Barriers to nonviral gene delivery. J. Pharm. Sci. 2003;92(2):203-217.

124. Varkouhi AK, Scholte. M, Storm G, Haisma HJ. Endosomal escape pathways for delivery of biologicals. J Control Release. 2011;151(3):220-228.

125. Jeong JH, Kim SW, Park TG. Molecular design of functional polymers for gene therapy. Prog. Polym. Sci. 2007;32(11):1239-1274.

126. Richardson SC, Pattrick NG, Stella Man Y, Ferruti P, Duncan R. Poly (amidoamine) s as potential nonviral vectors: ability to form interpolyelectrolyte complexes and to mediate transfection in vitro. Biomacromolecules. 2001;2(3):1023-1028.

127. Wang R, Zhou L, Zhou Y, Li G, Zhu X, Gu H, Jiang X, Li H, Wu J, He L. Synthesis and gene delivery of poly (amido amine) s with different branched architecture. Biomacromolecules. 2010;11(2):489-495.

128. Huang HW, Chen FY, Lee MT. Molecular mechanism of peptide-induced pores in membranes. Phys. Rev. Lett. 2004;92(19):198304.

129. Ogris M, Carlisle RC, Bettinger T, Seymour LW. Melittin enables efficient vesicular escape and enhanced nuclear access of nonviral gene delivery vectors. J. Biol. Chem. 2001;276(50):47550-47555.

130. Li W, Nicol F, Szoka Jr FC. GALA: a designed synthetic pH-responsive amphipathic peptide with applications in drug and gene delivery. Adv. Drug Deliv. Rev. 2004;56(7):967-985.

131. Cho YW, Kim JD, Park K. Polycation gene delivery systems: escape from endosomes to cytosol. J. Pharm. Pharmacol. 2003;55(6)721-734.

132. Martin ME, Rice KG. Peptide-guided gene delivery. AAPS J. 2007;9(1):E18-E29.

133. Putnam D. Polymers for gene delivery across length scales. Nat. Mater. 2006;5(6):439-451.

134. Midoux P, LeCam E, Coulaud D, Delain E, Pichon C. Histidine containing peptides and polypeptides as nucleic acid vectors. Somat. Cell Mol. Genet. 2002;27(1-6):27-47.

135. Midoux P, Pichon C, Yaouanc JJ, Jaffrès PA. Chemical vectors for gene delivery: a current review on polymers, peptides and lipids containing histidine or imidazole as nucleic acids carriers. Br. J. Pharmacol. 2009;157(2):166-178.

136. Patil ML, Zhang M, Taratula O, Garbuzenko OB, He H, Minko T. Internally cationic polyamidoamine PAMAM-OH dendrimers for siRNA delivery: effect of the degree of quaternization and cancer targeting. Biomacromolecules. 2009;10(2): 258-266.

137. Cheung CY, Murthy N, Stayton PS, Hoffman A,S. A pH-sensitive polymer that enhances cationic lipid-mediated gene transfer. Bioconjugate Chem. 2001;12(6):906-910.

138. Reschel T, Koňák Čr, Oupický D, Seymour LW, Ulbrich K. Physical properties and in vitro transfection efficiency of gene delivery vectors based on complexes of DNA with synthetic polycations. J Control Release. 2002;81(1):201-217.

139. Convertine AJ, Benoit DS, Duvall CL, Hoffman AS, Stayton PS. Development of a novel endosomolytic diblock copolymer for siRNA delivery. J Control Release. 2009;133(3):221-229.

140. Rozema DB, Lewis DL, Wakefield DH, Wong SC, Klein JJ, Roesch PL, Bertin SL, Reppen TW, Chu Q, Blokhin AV. Dynamic PolyConjugates for targeted in vivo delivery of siRNA to hepatocytes. Proc. Natl. Acad. Sci. U.S.A. 2007;104(32):12982-12987.

141. McKenzie DL, Smiley E, Kwok KY, Rice KG. Low molecular weight disulfide cross-linking peptides as nonviral gene delivery carriers. Bioconjugate Chem. 2000; 11(6):901-909.

142. Rozema DB, Ekena K, Lewis DL, Loomis AG, Wolff JA. Endosomolysis by masking of a membrane-active agent (EMMA) for cytoplasmic release of macromolecules. Bioconjugate Chem. 2003;14(1):51-57.

143. Lo SL, Wang S. An endosomolytic Tat peptide produced by incorporation of histidine and cysteine residues as a nonviral vector for DNA transfection. Biomaterials. 2008;29(15):2408-2414.

144. Dominska M, Dykxhoorn DM. Breaking down the barriers: siRNA delivery and endosome escape. J. Cell Sci. 2010;123(8):1183-1189.

145. Mok H, Park TG. Self-crosslinked and reducible fusogenic peptides for intracellular delivery of siRNA. Biopolymers. 2008;89(10):881-888.

146. Pack DW, Putnam D, Langer R. Design of imidazole-containing endosomolytic biopolymers for gene delivery. Biotechnol. Bioeng. 2000;67(2):217-223.

147. Park IK, Singha K, Arote RB, Choi YJ, Kim WJ, Cho CS. pH-Responsive Polymers as Gene Carriers. Macromol. Rapid Commun. 2010;31(13):1122-1133.

148. Lee SH, Choi SH, Kim SH, Park TG. Thermally sensitive cationic polymer nanocapsules for specific cytosolic delivery and efficient gene silencing of siRNA: swelling induced physical disruption of endosome by cold shock. J Control Release. 2008;125(1):25-32.

149. Luten J, van Nostrum CF, De Smedt SC, Hennink WE. Biodegradable polymers as non-viral carriers for plasmid DNA delivery. J Control Release. 2008;126(2):97-110.

150. Nair LS, Laurencin CT. Biodegradable polymers as biomaterials. Prog. Polym.

Sci. 2007;32(8):762-798.

151. Wolff JA, Rozema DB. Breaking the bonds: non-viral vectors become chemically dynamic. Mol. Ther. 2007;16(1):8-15.

152. Varde NK, Pack DW. Influence of particle size and antacid on release and stability of plasmid DNA from uniform PLGA microspheres. J Control Release. 2007;124(3):172-180.

153. Lynn DM, Langer R. Degradable poly (β-amino esters): synthesis, characterization, and self-assembly with plasmid DNA. J. Am. Chem. Soc. 2000;122(44):10761-10768.

154. Lin C, Zhong Z, Lok MC, Jiang X, Hennink WE, Feijen J, Engbersen JF. Novel bioreducible poly (amido amine) s for highly efficient gene delivery. Bioconjugate Chem. 2007;18(1):138-145.

155. Grigsby CL, Leong KW. Balancing protection and release of DNA: tools to address a bottleneck of non-viral gene delivery. J. R. Soc. Interface. 2009.

156. Gosselin MA, Guo W, Lee RJ. Efficient gene transfer using reversibly cross-linked low molecular weight polyethylenimine. Bioconjugate Chem. 2001;12(6):989-994.

157. Oupický D, Parker AL, Seymour LW. Laterally stabilized complexes of DNA with linear reducible polycations: strategy for triggered intracellular activation of DNA delivery vectors. J. Am. Chem. Soc. 2002;124(1):8-9.

158. Wu G, Fang YZ, Yang S, Lupton JR, Turner ND. Glutathione metabolism and its implications for health. J. Nutr. 2004;134(3):489-492.

159. Meng F, Hennink WE, Zhong Z. Reduction-sensitive polymers and bioconjugates for biomedical applications. Biomaterials. 2009;30(12):2180-2198.

160. Kim TI, Kim SW. Bioreducible polymers for gene delivery. React. Funct. Polym. 2011;71(3):344-349.

161. Saito G, Swanson JA, Lee KD. Drug delivery strategy utilizing conjugation via reversible disulfide linkages: role and site of cellular reducing activities. Adv. Drug Deliv. Rev. 2003;55(2):199-215.

162. Son S, Namgung R, Kim J, Singha K, Kim WJ. Bioreducible polymers for gene silencing and delivery. Acc. Chem. Res. 2011;45(7):1100-1112.

163. Leyland-Jones BR, Townsend AJ, Tu CPD, Cowan KH, Goldsmith ME. Antineoplastic drug sensitivity of human MCF-7 breast cancer cells stably transfected with a human α class glutathione S-transferase gene. Cancer Res. 1991;51(2):587-594.

164. Dai J, Weinberg RS, Waxman S, Jing Y. Malignant cells can be sensitized to undergo growth inhibition and apoptosis by arsenic trioxide through modulation of the glutathione redox system. Blood. 1999;93(1):268-277.

165. Sun YX, Zeng X, Meng QF, Zhang XZ, Cheng SX, Zhuo RX. The influence of RGD addition on the gene transfer characteristics of disulfide-containing polyethyleneimine/DNA complexes. Biomaterials. 2008;29(32):4356-4365.

166. Kang HC, Kang HJ, Bae YH. A reducible polycationic gene vector derived from thiolated low molecular weight branched polyethyleneimine linked by 2-iminothiolane. Biomaterials. 2011;32(4):1193-1203.

167. Lin C, Zhong Z, Lok MC, Jiang X, Hennink WE, Feijen J, Engbersen JF. Linear poly(amido amine)s with secondary and tertiary amino groups and variable amounts of disulfide linkages: Synthesis and in vitro gene transfer properties. J Control Release. 2006;116(2):130-137.

168. Son S, Singha K, Kim WJ. Bioreducible BPEI-SS-PEG-cNGR polymer as a tumor targeted nonviral gene carrier. Biomaterials. 2010;31(24):6344-6354.

169. Breunig M, Lungwitz U, Liebl R, Goepferich A. Breaking up the correlation between efficacy and toxicity for nonviral gene delivery. Proc. Natl. Acad. Sci. U.S.A. 2007;104(36):14454-14459.

170. Lee Y, Mo H, Koo H, Park JY, Cho MY, Jin Gw, Park JS. Visualization of the degradation of a disulfide polymer, linear poly (ethylenimine sulfide), for gene delivery. Bioconjugate Chem. 2007;18(1):13-18.

171. Lin C, Blaauboer CJ, Timoneda MM, Lok MC, van Steenbergen M, Hennink WE, Zhong Z, Feijen J, Engbersen JF. Bioreducible poly (amido amine) s with oligoamine side chains: synthesis, characterization, and structural effects on gene delivery. J Control Release. 2008;126(2):166-174.

172. Christensen LV, Chang CW, Kim WJ, Kim SW, Zhong Z, Lin C, Engbersen JF, Feijen J. Reducible poly (amido ethylenimine) s designed for triggered intracellular gene delivery. Bioconjugate Chem. 2006;17(5):1233-1240.

173. Dai F, Sun P, Liu Y, Liu W. Redox-cleavable star cationic PDMAEMA by arm-first approach of ATRP as a nonviral vector for gene delivery. Biomaterials. 2010;31(3): 559-569.

174. Kim TI, Ou M, Lee M, Kim SW. Arginine-grafted bioreducible poly (disulfide amine) for gene delivery systems. Biomaterials. 2009;30(4):658-664.

175. Kwok KY, Mckenzie DL, Evers DL, Rice KG. Formulation of highly soluble poly (ethylene glycol)-peptide DNA condensates. J. Pharm. Sci. 1999;88(10):996-1003.

176. Won YW, Kim HA, Lee M, Kim YH. Reducible poly (oligo-D-arginine) for enhanced gene expression in mouse lung by intratracheal injection. Mol. Ther. 2009;18(4):734-742.

177. Neu M, Germershaus O, Mao S, Voigt KH, Behe M, Kissel T. Crosslinked nanocarriers based upon poly (ethylene imine) for systemic plasmid delivery: in vitro characterization and in vivo studies in mice. J Control Release. 2007;118(3): 370-380.

178. Neu M, Germershaus O, Behe M, Kissel T. Bioreversibly crosslinked polyplexes of PEI and high molecular weight PEG show extended circulation times in vivo. J Control Release. 2007;124(1):69-80.

CHAPTER 2

BIOREDUCIBLE POLYMERS AS A DETERMINING FACTOR FOR POLYPLEX DECOMPLEXATION RATE AND TRANSFECTION*

2.1 Abstract

Polyplex formation (complexation) and gene release from the polyplexes (decomplexation) are major events in polymeric gene delivery, however the effect of the decomplexation rate on transfection has been rarely investigated. This study employed mixed polymers of poly($_L$-lysine) (PLL: MW ~7.4 kDa) and reducible PLL (RPLL) (MW ~3.75 kDa) to design decomplexation rate-controllable $PLL_{100-x}RPLL_x$/pDNA complexes (PRL_x polyplexes). The transfection efficiency of a model gene (luciferase) in MCF7 and HEK293 cell lines increased with increasing x (RPLL content) in the PRL_x polyplexes until peaking at x=2.5 and x=10, respectively, at which point transfection efficiency declined rapidly. In MCF7 cells, $PRL_{2.5}$ polyplex produced 3 or 223 times higher gene expression than PLL or RPLL polyplexes, respectively. Similarly, the transfection efficiency of PRL_{10} polyplex-transfected HEK293 cells was 3.8 or 67 times higher than that of PLL or RPLL polyplexes, respectively. The transfection results were not apparently related to the particle

*Modified with permission from HS Hwang, HC Kang, YH Bae. Biomacromolecules 2013; 14: 548-556. Hwang managed the project, completed all of the experiments, and analyzed the data. Kang provided key insights into the project and organized the data. Bae is the PI responsible for the project.

size, surface charge, complexation/compactness, cellular uptake, or cytotoxicity of the tested polyplexes. However, the decomplexation rate varied by RPLL content in the polyplexes, which in turn influenced the gene transfection. The nuclear localization of pDNA delivered by PRLx polyplexes showed a similar trend to their transfection efficiencies. This study suggests that an optimum decomplexation rate may result in high nuclear localization of pDNA and transfection. Understanding in decomplexation and intracellular localization of pDNA may help develop more effective polyplexes.

2.2 Introduction

Interest in polymeric gene carriers has been steadily increased due to their tailored structural characteristics (e.g., charges and architectures) and versatile design components endowing required functionalities (e.g., endosomal disruption, cytosolic transport, nuclear import, triggering drug release, and biocompatibility).[1-4] Such functionalities have been thought to overcome various extracellular and intracellular barriers encountered in the gene delivery process, anticipating enhanced therapeutic effects of an exogenous gene delivered by polymeric carriers. In addition, it is critical for optimal transfection that the decomplexation to release genes from the carriers should occur at a right intracellular place and the right time.[5]

Our group has discovered that high transfection efficiency can be obtained by tuning the pH at which the polyplex is released from the endolysosome and that pH-tunable sulfonamide-based oligomers/polymers loaded in polyplexes affected gene expression but not gene silencing in gene delivery.[6,7] Despite the recognized significance of intracellular location and timing of gene, the related investigation is seldom conducted.

The release or decomplexation of plasmid DNA (pDNA) from electrostatically driven polyplexes is mostly induced by competitive interactions with charged biological components, which disrupt the ionic bond that binds the gene to the carrier and protects from degradation. For most cationic polyplexes, such as anionic polymers or molecules such as glycosaminoglycans in plasma,[8-10] RNA in the cytoplasm,[11] DNA in the nucleus,[12] heparin,[6,13,14] poly(acrylic acid) and sodium dodecyl sulfate in test tubes, it is difficult to control the unpacking process of polyplexes under a given extracellular and intracellular environment because their concentrations cannot be manipulated by extrinsic factors.

Longer polycations generally cause stronger attraction with negatively charged genes than shorter polycations, resulting in tighter polyplexes.[6,14,15] Thus, to facilitate polyanion-induced decomplexation of polyplexes especially in intracellular environments, degradable polymers responding to acidic pHs in the endolysosomes[16] or glutathione in the cytoplasm and the nucleus[14,17,18] have been developed. These polyplexes resulted in improved transfection efficiency, but the genes are susceptible to lytic enzymes in the endolysosomes. For pDNA, transfection efficiency could be dependent on the distance between its releasing site and the nucleus due to its poor mobility[19] in intracellular environment. In addition, pDNA is deactivated or degraded by cytosolic nucleases, giving pDNA a 60-90 min half-life in HeLa and COS cells.[20] Therefore, it is hypothesized that the intracellular release rate of genes affects transfection.

It has been generally recognized that the low transfection efficiency of poly($_L$-lysine) (PLL) polyplexes is caused by lack of endosomolytic activity of PLL. However, PLL polyplexes showed much slower decomplexation rate than poly(cyclooctene-*g*-oligolysine) (i.e., comb-shaped PLL) with nuclear localization signal (NLS), despite the fact that the

former had a more nuclear uptake than the latter.[21] Nondegradable and degradable PLL polymer-based polyplexes also showed molecular weight (MW)-dependent decomplexation and transfection efficiency.[12,15] For example, when forming linear polylysine/pDNA complexes, longer polylysine chains, (180 lysine units, MW 28 kDa) showed slower dissociation than shorter polylysine chains, (19 or 36 lysine units, 2.3 kDa or 4.4 kDa, respectively) due to the greater positive charge of the longer chains tightly binds the pDNA that interferes the release of the genes from the carrier, thus leading to increased inhibition of RNA synthesis and lower gene expression.[12] However, reducible PLL (RPLL)-based polyplexes showed contradictory *in vitro* transfection results depending on their MWs compared with polyplexes prepared by PLL with comparable MWs. High MW RPLL (187 kDa) showed more effective transfection than PLL (205 kDa),[21] whereas moderate MW RPLL (65 kDa) showed lower gene transfection efficiency than PLL (54 kDa).[23] on the basis of these results, it appears that either “too fast” or “too slow” release of genes from polyplexes would bring low transfection efficiency.

This study investigated the effect of the decomplexation rate of pDNA on transfection efficiency. Commercial PLL with 7.4 kDa and synthesized reducible PLL (RPLL) with a comparable MW were selected. Using the polyplexes formed from a model gene and mixed PLL and RPLL, the influence of RPLL content on physicochemical characteristics (e.g., size, surface charge, complexation, and decomplexation) and biological characteristics (e.g., cellular uptake, cytotoxicity, transfection efficiency, and intracellular localization) was studied.

2.3. Materials and Methods

2.3.1. Materials

Poly($_L$-lysine) hydrogen bromide (PLL·HBr; Mw 12 kDa), dimethyl sulfoxide (DMSO), 4-(2-hydroxy-ethyl)-1-piperazineethanesulfonic acid (HEPES), 3-(4,5-dimethylthiazol-2-yl)-2,5-diphenyltetrazolium bromide (MTT), $_D$-glucose, cystamine, sodium bicarbonate, recombinant human insulin, ethidium bromide (EtBr), paraformaldehyde (PFA), deuterium oxide (D_2O), dithiothreitol (DTT), heparin sodium salt (139 USP units/mg), Hoechst 33342, RPMI-1640 medium, Dulbecco's phosphate buffered saline (DPBS), Dulbecco's modified eagle's medium (DMEM), fetal bovine serum (FBS) were purchased from Sigma-Aldrich (St. Louis, MO). LysoTracker®Green dye and YOYO-1 were received from Invitrogen, Inc. (Carslbard, CA). A pDNA that encodes firefly luciferase (gWiz-Luc or pLuc) was bought from Aldevron, Inc. (Fargo, ND). A decapeptide (Cys-Lys_8-Cys) was synthesized by American Peptide Company (Sunnyvale, CA). Luciferase assay kit and GSH-Glo^{TM} glutathione assay kit were purchased from Promega Corporation (Madison, WI) and BCA protein assay kit was bought from Pierce Biotechnology. (Rockford, IL). Cy5-labeled pDNA was prepared by using *Label* IT® nucleic acid labeling kit of Cy5 dye (Mirus Bio LLC; Madison, WI).

2.3.2. Cell Culture

HEK293 cells (human embryonic kidney cell line) and MCF7 cells (human breast adenocarcinoma cell line) were used in this study. HEK293 cells were cultured in DMEM supplemented with 10% FBS and $_D$-glucose (4.5 g/L). MCF7 cells were cultured in RPMI-1640 supplemented with 10% FBS, $_D$-glucose (2 g/L), and insulin (4 mg/L). The

cells were maintained and grown under a humidified air with 5% CO_2 at 37 °C.

2.3.3. Synthesis and Characterization of Reducible Poly(Cys-Lys$_8$-Cys) (RPLL)

As previously reported,[21, 23] a decapeptide (Cys-Lys$_8$-Cys) was oxidized to form reducible poly(Cys-Lys$_8$-Cys) (RPLL) (Figure 2.1). Cys-Lys$_8$-Cys (50 mg; 40 μmol) was dissolved in deionized water (DIW; 1 mL) and then cystamine (0.31 mg; 4 μmol) as a chain closer was added into the peptide solution. On adding DMSO (0.33 mL) into the solution, oxidative polymerization of the decapeptide was performed to form RPLL at room temperature (RT). After 1 day polymerization, the synthesized RPLL was dialyzed using a dialysis MWCO of 1 kDa for 2 days and then was lyophilized.

As shown in Figure 2.2, the ^{1}H-NMR spectra of RPLL in D_2O were characterized and confirmed by characteristic peaks at δ 1.32 (–CH-CH_2-C**H$_2$**–), δ 1.57 (–CH-C**H$_2$**-CH_2–), δ 2.59 (–CH-C**H$_2$**-NH_2), δ 3.1 (–C**H$_2$**-NH_2CH-CO–), δ 3.25 (–S-CH_2C**H$_2$**-NH_2), δ 3.8 (–S-C**H$_2$**CH_2-NH_2), δ 4.17 (–NH-C**H**CH_2-CO–), δ 4.3 (–CH_2-NH_2C**H**-CO–). To estimate repeating units of decapeptide (n), integrated peaks which correspond to cysteamine and decapeptide were compared. Based on the relative integration values of the peaks, the repeating units of decapeptide were n=3. Thus, the molecular weight of polymers estimated by ^{1}H NMR was 3.75 kDa (2 x 75 + 3 x 1200=3750).

In vitro cytotoxicity of RPLL was evaluated by MTT-based cell viability as previously reported to determine the polymer amount used for cell experiments.[6, 13] HEK293 cells and MCF7 cells were seeded at (2 and 5) $\times 10^3$ cells per well of a 96-well plate, respectively and then were incubated for 24 hr in serum-containing culture medium.

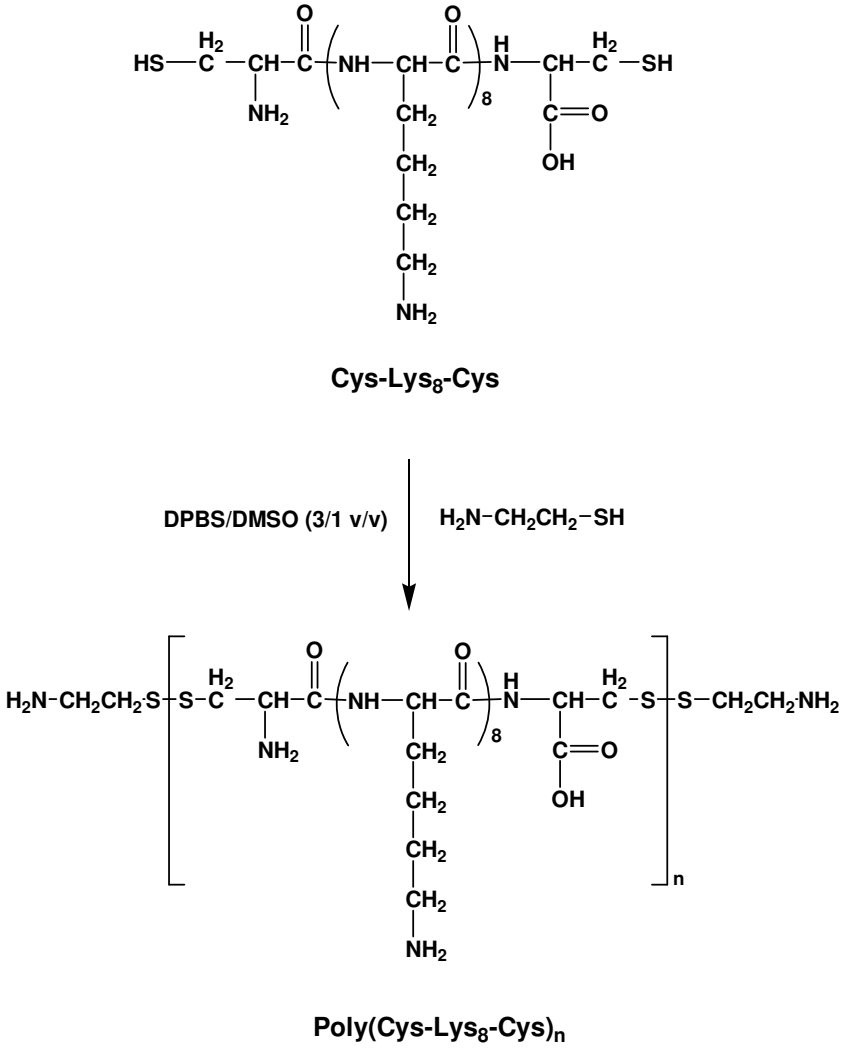

Figure 2.1. Synthetic scheme of reducible poly(Cys-Lys$_8$-Cys) (RPLL)

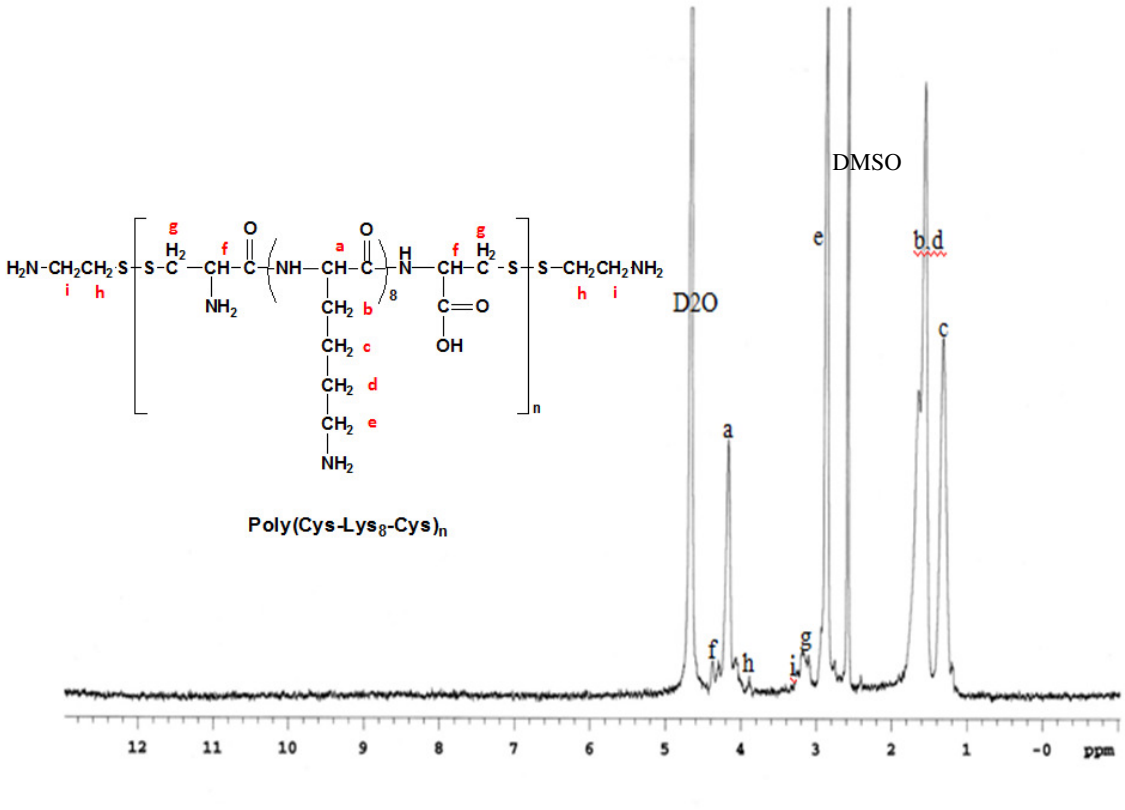

Peak No.	No. of protons	Integration value	Peak No.	No. of protons	Integration value
a	24	0.54	f	6	0.12
b	48	1	g	12	0.32
c	48	1	h	4	0.11
d	48	1	i	4	0.08
e	48	1.08			

Figure 2.2. ^{1}H-NMR analysis of RPLL in D_2O

The cells were exposed to RPLL having different concentrations (0-100 μg/mL) for 24 hr. Then, MTT solution (10 μL; 5 mg/mL) was treated to the cells in the culture medium (0.1 mL) for additional 4 hr. After discarding the culture medium, DMSO was added to dissolve the formazan crystals which are produced by living cells. Their absorbance was measured at 570 nm to estimate the cell viability and was compared with that of PLL as a nonreducible counterpart.

2.3.4. Preparation and Physicochemical Characterization of Polyplexes

As previously reported,[6,14,25] a cationic solution having polymers (*i.e.*, PLL and RPLL) and an anionic solution containing pDNA were separately prepared by using HEPES buffer (20 mM, pH 7.4). Two solutions with an equivalent volume were mixed and then incubated for 30 min at RT. The formed polyplexes (20 μL per 1 μg of pDNA) were further evaluated. Complexation ratio of polyplexes was expressed based on the N/P ratio using amines (N) of polymers and phosphates (P) of pDNA.

Particle sizes and surface charges of polyplexes were evaluated as previously reported.[6,14,25] After preparing polyplexes (100 μL; 5 μg pDNA), they were diluted with HEPES buffer (20 mM, pH 7.4) and pDNA in the polyplex solution was 2.5 μg/mL. The polyplexes were then monitored by using a Zetasizer 3000 (Malvern Instrument, UK) with a wavelength of 677 nm and a constant angle of 90° at RT.

The complexation ability of pDNA with PLL and RPLL was evaluated by a gel electrophoresis assay. After loading polyplexes (10 μL; 0.5 μg of pDNA) in 0.8% agarose gel having EtBr, the gel was run in 0.5x TBE buffer at a constant voltage (80 V) for 90 min. A UV illuminator was used to detect whether pDNA was exposed.

Compactness of pDNA was tested by using quenching fluorescent YOYO-1 dye intercalated with pDNA in polyplexes. Fluorescent intensity of YOYO-1 in the polyplexes was measured at 495 nm (excitation) and 515 nm (emission). Compactness (%) of pDNA in polyplexes was calculated as a following equation.

$$\text{Compactness of pDNA (\%)} = (1 - \frac{\text{RFU}_{\text{Polyplex}} - \text{RFU}_{\text{Buffer}}}{\text{RFU}_{\text{pDNA}} - \text{RFU}_{\text{Buffer}}}) \times 100\ (\%)$$

where $\text{RFU}_{\text{Polyplex}}$, RFU_{pDNA}, and $\text{RFU}_{\text{Buffer}}$ are relative fluorescent units (RFU) of polyplexes, YOYO-1-intercalated pDNA, and HEPES buffer, respectively.

Decomplexation of pDNA from polyplexes was monitored by a gel electrophoresis assay in the presence of DTT and/or heparin. Polyplexes were exposed to 150 mM NaCl solution supplemented with heparin sodium salt (0-100 μg/mL) and/or DTT (20 mM) for 1 hr at 37 °C and a final concentration of pDNA was 25 μg/mL. Then the polyplexes were run and evaluated in 0.8% agarose gel as previously described in the complexation ability of polyplexes.

In addition, decomplexation kinetics of polyplexes was monitored by a dye-dequenching technique. The polyplexes with YOYO-1-intercalated pDNA (5 μg/mL) were treated with 150 mM NaCl solution having heparin (6.5 μg/mL) and DTT (10 mM) as a decomplexation solution (0.2 mL) at RT. Time-dependent decomplexation was evaluated by changing RFU of YOYO-1-intercalated pDNA exposed from the polyplexes using a plate reader. Free YOYO-1-intercalated pDNA and the decomplexation solution were set as 100% RFU and 0% RFU, respectively.

$$\text{Decomplexation of pDNA (\%)} = \frac{\text{RFU}_{\text{Polyplex}} - \text{RFU}_{\text{Buffer}}}{\text{RFU}_{\text{pDNA}} - \text{RFU}_{\text{Buffer}}} \times 100\ (\%)$$

2.3.5. Biological Characterizations of Polyplexes

HEK293 cells and MCF7 cells were seeded at (1 and 5) $\times 10^5$ cells/well (of a six-well plate), respectively, for cellular uptake, *in vitro* transfection efficiency, and intracellular trafficking study, whereas their cell densities were 5×10^4 HEK293 cells/well and 2.5×10^5 MCF7 cells/well (of a 12-well plate) for *in vitro* cytotoxicity. The seeded cells were incubated for 24 hr in serum-containing culture medium and then were used for further studies.

For *in vitro* transfection study, cells were cultured in a six-well plate and the transfection experiments were performed as previously described.[14,25,26] One hour before the addition of polyplexes, serum-containing culture medium was replaced with serum-free and insulin-free transfection medium. After transfecting with polyplexes, the transfected cells were incubated for 4 hr. The transfection medium was then replaced with serum-containing culture medium and the cells were incubated for additional 44 hr. After the transfection experiments were completed, the cells transfected with pLuc were rinsed with DPBS and then lysed in a reporter lysis buffer. Relative luminescent unit (RLU) and protein content of transfected cells were evaluated by luciferase assay kit and BCA protein assay kit, respectively.

To evaluate whether transfection procedure of polyplex is toxic, we evaluated *in vitro* cytotoxicity of polyplexes by MTT-based cell viability, and its experimental procedure mostly followed the aforementioned *in vitro* transfection study except for its cell density and pDNA dose (0.5 μg pDNA per well). After completing transfection procedures for 48 hr, MTT solution (0.1 mL; 5 mg/mL) was added to cells incubated in serum-containing culture medium (1 mL) for an additional 4 hr. The *in vitro* cytotoxicity of the polymer, was

evaluated using formazan crystals, which are metabolized by live cells. The formazan crystals were dissolved in DMSO and added to the cultured cells; their absorbance was subsequently monitored at 570 nm for converting cytotoxicity of polyplexes.

Cellular uptake of polyplexes was evaluated as previously reported.[6,14] Polyplexes prepared with YOYO-l-intercalated pDNA (1 μg pDNA per well) were treated to cells. After 4 hr of incubation, the cells were detached and fixed with 4% PFA solution. The fluorescent polyplex-containing cells were monitored using flow cytometry (FACScan Analyzer, Becton–Dickinson; Franklin Lakes, NJ) with a primary argon laser (488 nm) and a fluorescence detector (530 ± 15 nm) to detect YOYO-1. Uptake levels of polyplexes in the cells were analyzed with a gated population of living 10,000 cells.

For intracellular trafficking of polyplexes, MCF7 cells were seeded on a coverglass in a six-well plate at 5×10^5 cells/well. Polyplexes prepared with Cy5-labeled pDNA (1 μg pDNA per well) were treated to the cells in serum-free transfection medium. After 3.5 hr of transfection, Hoechst 33342 and LysoTracker®Green dye were added to stain the nuclei and the acidic vesicles (mostly relevant to late endosomes and lysosomes), respectively. At 4 hr incubation with polyplexes the cells were rinsed with DPBS and fixed with 4% PFA solution for 5 min. The cells were evaluated using a laser scanning confocal microscope. In particular, nuclear localization of Cy5-labeled pDNA was quantified from fluorescence (FL) of two regions of interest (ROIs). The first region of fluorescence was obtained from the whole cell, indicated as FL_{cell}, and the second region is from the nuclei, FL_{nuclei}. Fluorescence intensity of Cy5-labeled pDNA was measured by using Image J software and the nuclear localization of Cy5-labeled pDNA was calculated from the following equation.[26]

$$\text{Nuclear Localization of pDNA (\%)} = \frac{\text{FL}_{\text{nuclei}}}{\text{FL}_{\text{cell}}} \times 100\ (\%)$$

2.3.6. Evaluation of Intracellular Glutathione Concentration

HEK293 cells and MCF7 cells were seeded at 5×10^3 cells/well and 2.5×10^4 cells/well (of a 96-well plate), respectively and were cultured for 1 day. After the culture medium was discarded, the cells were rinsed and then were treated by following GSH Glo™ glutathione assay protocol.

2.3.7. Statistical Analysis

The statistical significance of the data was evaluated by conducting an one way ANOVA and unpaired Student t-test at a confidence level of $p<0.05$.

2.4. Results and Discussion

To control the decomplexation rates of pDNA in intracellular environments such as the cytoplasm and nucleus, this study designed pDNA complexes using lysine-based polycation mixtures comprising nonreducible PLL and RPLL as a decomplexation controller of polyplexes. PLL with MW 7.4 kDa (MW 12 kDa of PLL·HBr) and synthesized RPLL with a MW of 3.75 kDa were used to minimize MW effects of polycations on size and complexation of polyplexes. In ($PLL_{100-x}RPLL_x$)/pDNA complexes, (100-x)% and x% of primary amines for complexation with phosphate groups in pDNA were from PLL and RPLL, respectively and PRL_x polyplexes as code names were used. Also, PRL_x polyplexes were prepared at a fixed N/P ratio of 5 due to an optimum condition for transfection efficiency of PLL/pDNA complexes[25] and polyplex formation based on

electrophoresis (Figure 2.3).

2.4.1. Effects of RPLL Content (x) in Transfection Efficiency of PRLx Polyplexes

To demonstrate the different responses of PRL_x polymers in cancer and noncancerous cell lines, MCF7 and HEK 293 cells were selected as cancer and noncancerous cell line, respectively. Prior to detailed analyses of various physicochemical and biological characteristics of PRL_x polyplexes, we first examined whether the presence of RPLL in PRL_x polyplexes affects their transfection efficiency in MCF7 and HEK293 cells.

When we applied PRL_x polyplexes to the cells, their transfection efficiencies increased, had a peak value at x=2.5 for MCF7 cells and x=10 for HEK293 cells, and then decreased with increasing concentration of RPLL compared with that of PRL_0 polyplexes (*i.e.*, PLL/pDNA complexes) (Figure 2.4). Using MCF7 cells, $PRL_{2.5}$ and PRL_5 polyplexes showed three fold and two times higher transfection efficiencies than PRL_0 polyplexes, respectively and their differences were statistically significant ($p=0.017$ for $PRL_{2.5}$ polyplexes and $p=0.036$ for PRL_5 polyplexes compared with PRL_0 polyplexes) by one-way ANOVA posthoc test. (Figure 2.4(a)). PRL_x polyplex-transfected HEK293 cells produced 3.8 fold ($p=0.042$) higher transgene expression using PRL_{10} polyplexes and 2.9-fold ($p=0.048$) and 2.6 fold ($p=0.066$) higher transgene expression using PRL_5 and $PRL_{7.5}$ polyplexes, respectively, compared with PRL_0 polyplexes (Figure 2.4(b)).

When the transfection efficiencies of PRL_x polyplexes in MCF7 cells were normalized with that of PRL_{100} polyplexes (i.e., RPLL/pDNA complexes), PRL_0, $PRL_{2.5}$, and PRL_5 polyplexes, 74, 223, and 151 times higher luciferase expression were observed, respectively (Figure 2.5). For HEK293 cells, PRL_0, PRL_5, $PRL_{7.5}$, and PRL_{10} polyplexes

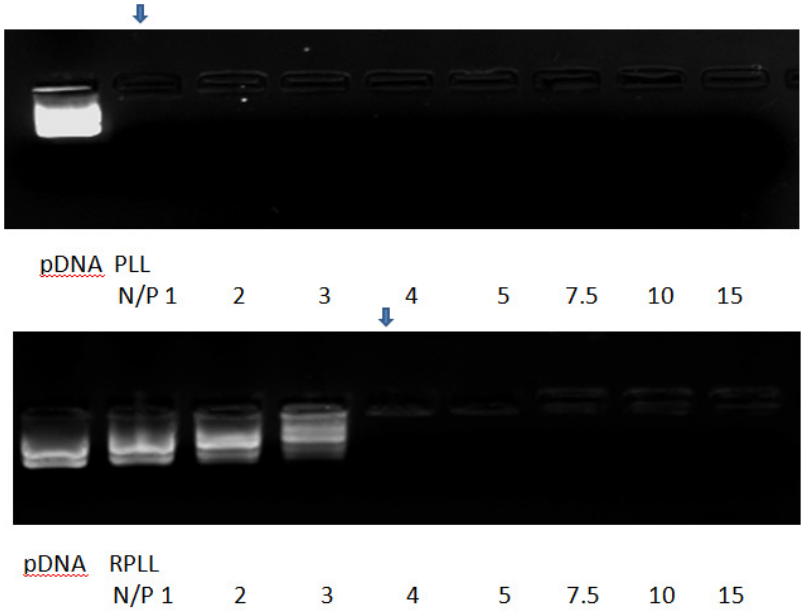

Figure 2.3. Condensation of pDNA with either PLL or RPLL in agarose gel

(a)

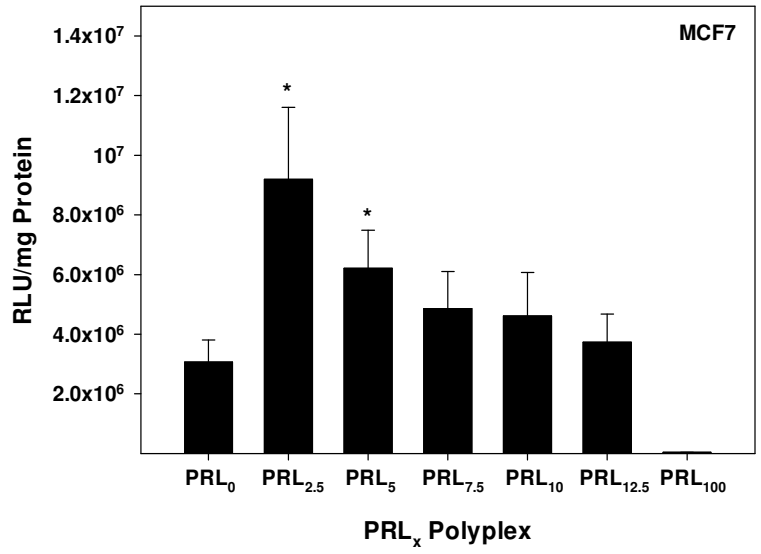

(b)

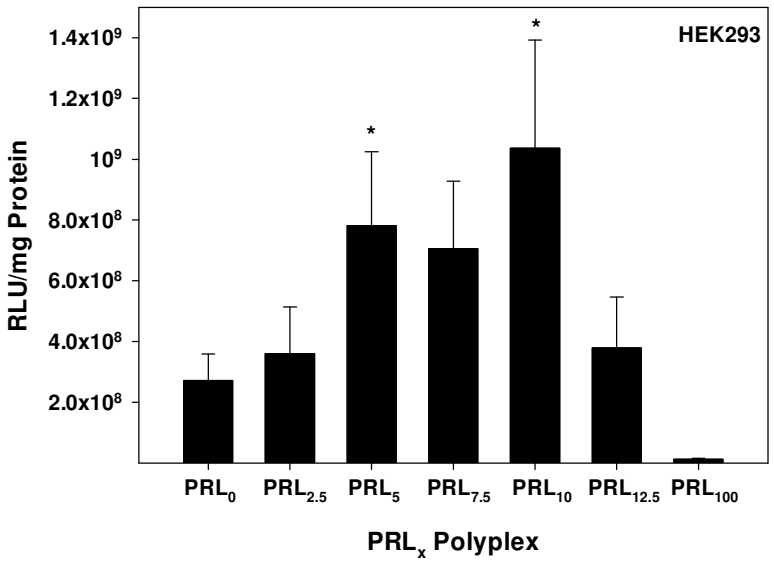

Figure 2.4. Transfection efficiencies of $PLL_{100-x}RPLL_x$/pDNA complexes (PRL_x polyplexes) (at N/P 5, 1 µg of pDNA) in (a) MCF7 cells and (b) HEK293 cells. PLL/pDNA and RPLL/pDNA complexes were denominated as PRL_0 and PRL_{100} polyplexes, respectively. * means $p<0.05$ compared with PRL_0 polyplex by one-way ANOVA. (Mean ± SD; $n \geq 4$)

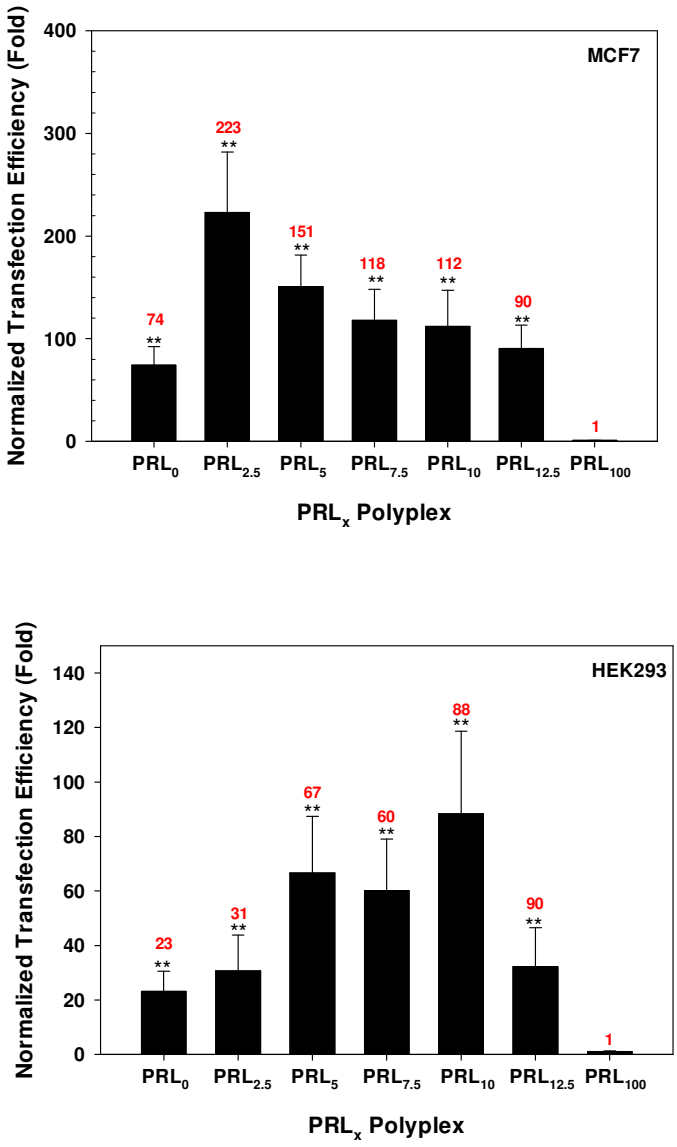

Figure 2.5. Normalized transfection efficiencies of $PLL_{100-x}RPLL_x$/pDNA complexes (PRL_x polyplexes) (at N/P 5, 1 µg of pDNA) in MCF7 cells and HEK293 cells. PLL/pDNA and RPLL/pDNA complexes were denominated as PRL_0 and PRL_{100} polyplexes, respectively. Transfection efficiency of PRL_x/pDNA complexes were normalized by dividing with transfection efficiency of PRL_{100} complexes. ** $p<0.01$ vs. PRL_{100} polyplex (Mean ± SD; $n \geq 4$)

resulted in 23, 67, 60, and 88 times better gene expression than RPL_{100} polyplexes (Figure 2.5). The transfection results suggest that RPLL content in PRL_x polyplexes influences the transfection efficiencies. Neither the fast decomplexation of RPLL/pDNA complexes nor the slow decomplexation of PLL/pDNA complexes appear to be optimal for high transfection efficiency. It seemed that non-degradable PLL helps to slow decomplexation of RPLL-rich PRL_x polyplexes compared with RPLL polyplexes and that degradable RPLL induces faster decomplexation of PLL-rich PRL_x polyplexes than PLL polyplexes. This led to efforts to determine how the change in RPLL content affects the physicochemical and biological characteristics of PRL_x polyplexes.

2.4.2. Effects of RPLL on Particle Size, Surface Charge, and Complexation/Compactness

The compactness and surface charge of pDNA polyplexes are affected by complexation conditions (e.g., dose of polymers, N/P ratios) and polymer characteristics (e.g., architectures, charge density, flexibility, hydrophobicity).[4] Although the MW of RPLL used in this study is similar to that of PLL, the chain structure of RPLL is different from that of PLL (Figure 2.1). Thus, it is important to determine whether RPLL causes significant changes in particle size, surface charge, and complexation of PRL_x polyplexes compared with those of PLL polyplexes.

The particle size of RPL_0 polyplex was ~100 nm in diameter. Particle sizes were slightly increased with increasing RPLL content in PRL_x polyplexes, growing to about 120 nm for PRL_5 polyplex ($p=0.02$) and then to around 150 nm ($p<0.01$) for PRL_x polyplexes with x=10-50 (Figure 2.6). It might be due to the weaker pDNA complexation

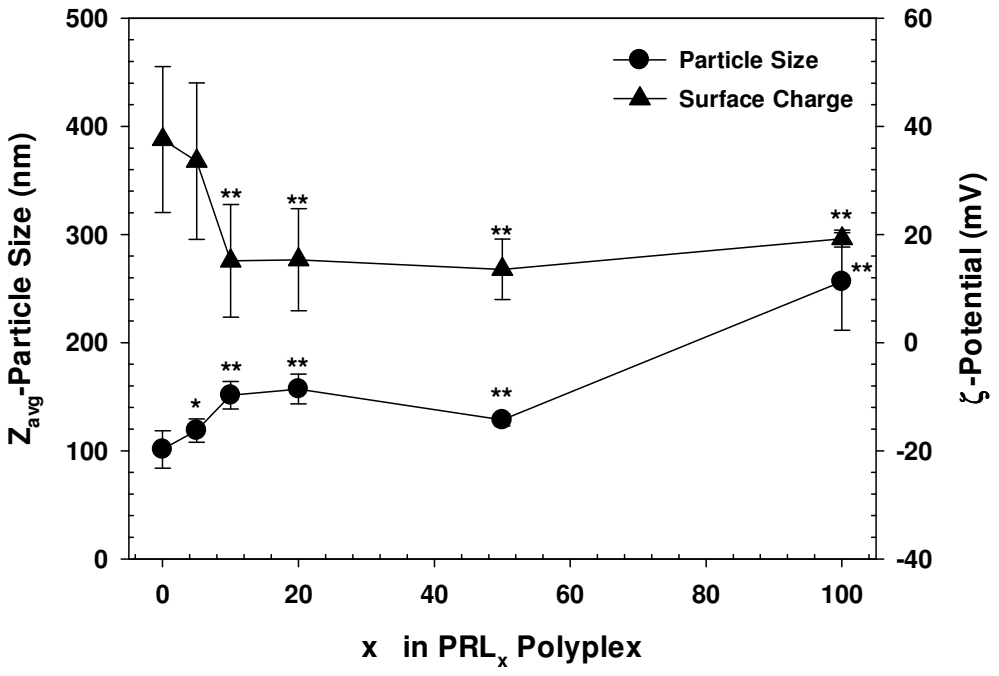

Figure 2.6. Particle size and surface charge of PRL_x polyplexes (at N/P 5) in HEPES buffer (25 mM, pH 7.4). * and ** mean $p<0.05$ and $p<0.01$, respectively, compared with PRL_0 polyplex by two-way ANOVA. (Mean ± SD; n = 10)

of RPLL compared with PLL resulting from the lower charge density of RPLL (157 Da per one primary amine) than PLL (129 Da per one primary amine). This conclusion is supported by the large particle size (250 nm diameter) of RPL100 polyplex.

PRL0 polyplex had a zeta-potential ~40 mV. Introducing RPLL to PRLx polyplexes, decreased the surface charge to about 35 mV at x=5 ($p=0.53$) and then reached a saturated value (~20 mV) at x=10-100 ($p<0.01$) (Figure 2.6). This observation is due to the presence of one carboxylic group associated with the cysteine on each decapeptide unit which negates the positive charge of the primary amine on the lysine. The presence of free carboxylic groups in RPLL provides a possible explanation for the increased particle size of PRLx polyplexes with higher RPLL content.

Condensation of pDNA in PLL and RPLL polyplexes (N/P 5) prepared in a HEPES buffer was confirmed by a gel electrophoresis method in 0.8% agarose gel (Figure 2.3). At N/P 5, both cationic polymers completely shielded pDNA on the polyplex surface. In addition, the compactness of pDNA in PRLx polyplexes was monitored by tracking quenching of YOYO-1-intercalated pDNA. As shown in Figure 2.7, the fluorescent intensity of unquenched YOYO-1-intercalated pDNA was set to 0% and complete quenching was given a value of 100%. All tested PRLx polyplexes (x=0-100) showed above 90% compactness of pDNA. The results indicate that different amounts of RPLL did not cause serious difference in the compactness of pDNA in PRLx polyplexes.

2.4.3. Effects of RPLL in Cellular Viability and Cell Uptake

The surface charge and particle size of polyplexes influence cellular uptake, which can further affect transfection efficiency. Also, excessively high positive surface charges

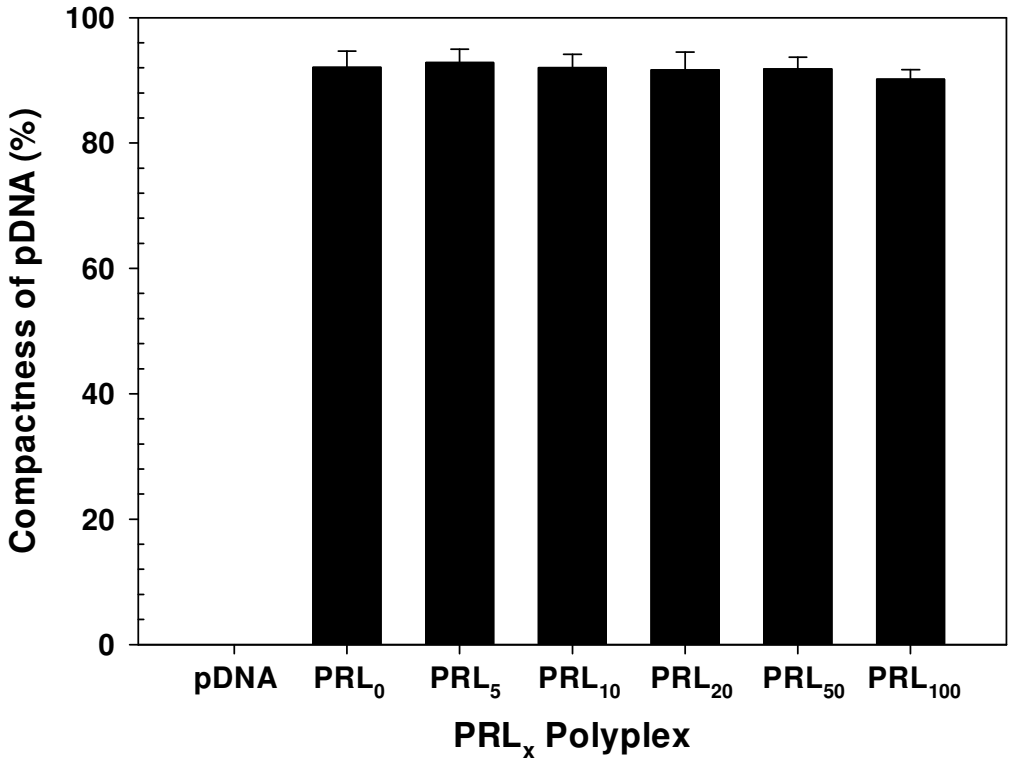

Figure 2.7. Compactness (%) of pDNA in PRL_x polyplexes (at N/P 5) prepared in a HEPES buffer (25 mM, pH 7.4). (Mean ± SD; n = 3)

of polyplexes could damage the cell membrane, resulting in cellular toxicity and leading to reduced transfection efficiency. Thus, cellular uptake studies of PRLx polyplexes were performed by flow cytometry in MCF7 and HEK293 cells (Figure 2.8), and cytotoxicity of PRLx polyplexes was evaluated by MTT-based cell viability assay (Figure 2.9).

After forming PRLx polyplexes (x=0-12.5) with YOYO-1-intercalated pDNA, the cells were incubated with the polyplexes in serum-free and protein-free transfection medium for 4 hr. It was expected that cellular uptake of PRL0 polyplexes would be much higher than those of other PRL_x polyplexes (x=2.5-12.5) because PRL_0 polyplexes had much higher positive surface charges than other PRL_x polyplexes (x=2.5-12.5). However, with both the cells, PRL_x polyplexes showed similar uptake regardless of the amount of RPLL present (Figure 2.8). The results indicate that different transfection efficiencies of PRL_x polyplexes (Figure 2.4) might be not caused by the cellular uptakes of PRL_x polyplexes (Figure 2.8).

The cytotoxicity of polycations is influenced by their length, charge, degradability, hydrophobicity, and architecture[1,4,17,27] and strongly affects the cytotoxicity, and thus transfection efficiency, of their polyplexes. PLL·HBr with MW 12 kDa showed more toxicity than RPLL 3.75 kDa in MCF7 and HEK293 cells (Figure 2.10). The IC_{50} of PLL·HBr was about 80 μg/mL for MCF7 cells and about 65 μg/mL for HEK293 cells. RPLL showed negligible cytotoxicity with above 80% cell viability in the tested range of polymer (0~100 μg/mL). Different cytotoxicities of PLL and RPLL might result from different degradation characteristics in intracellular environments because RPLL is degraded much more quickly than RPLL in the cytoplasm and the nucleus. The cytotoxicity of PRL_x polyplexes during a 48 hr transfection process was evaluated by an

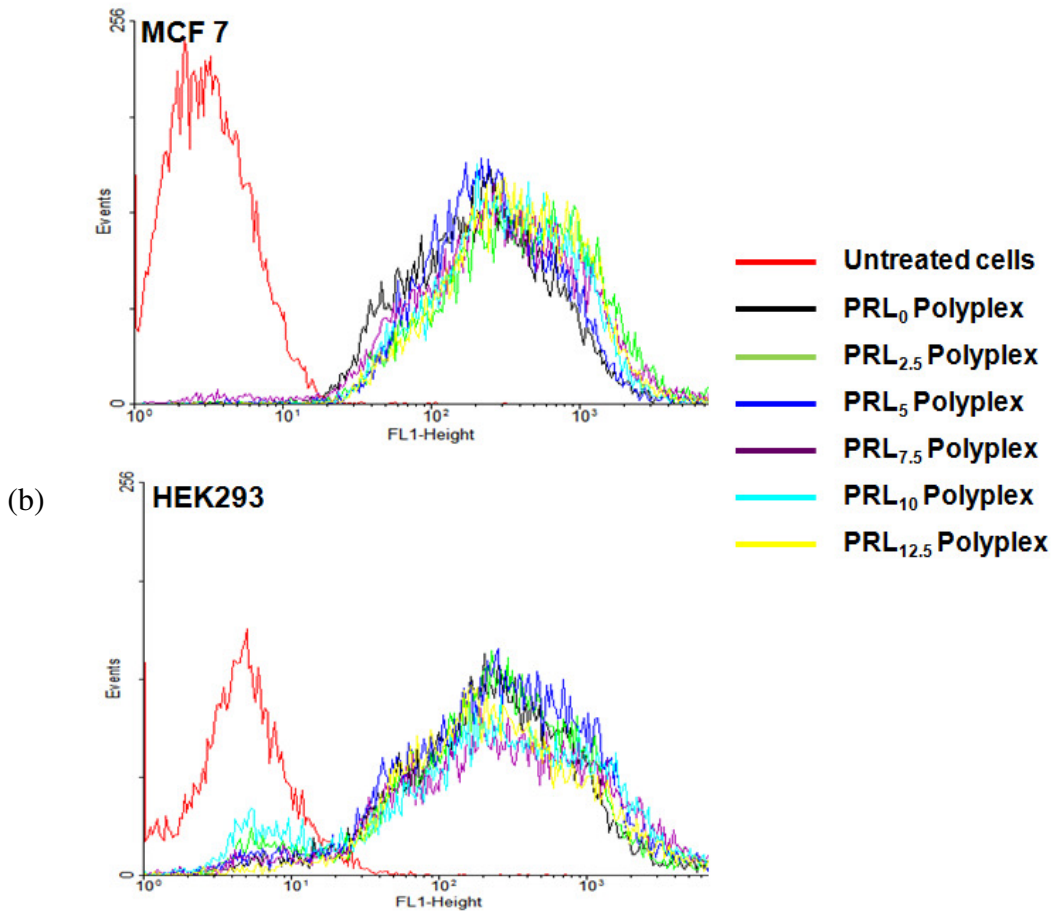

Figure 2.8. Cellular uptake of PRL_x polyplexes (at N/P 5) after 4 hr transfection in (a) MCF7 and (b) HEK293 cells. The x-axis represents YOYO1 fluorescence from YOYO1-labeled pDNA in polyplex. Control (red line) was obtained by cells with no treatments.

(a)

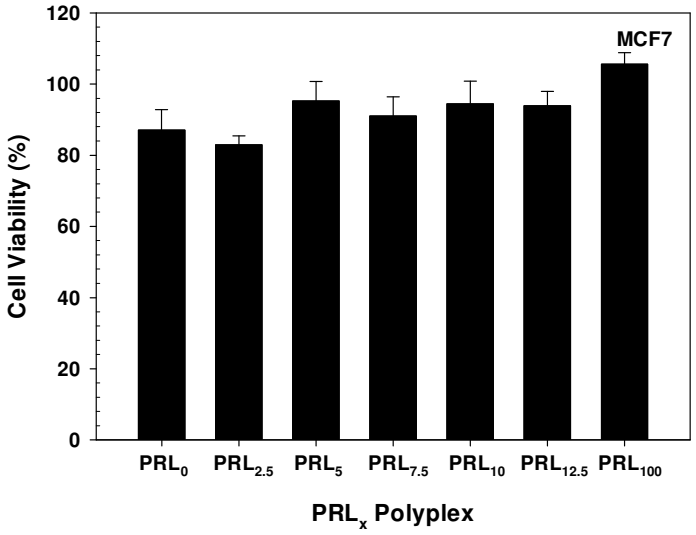

(b)

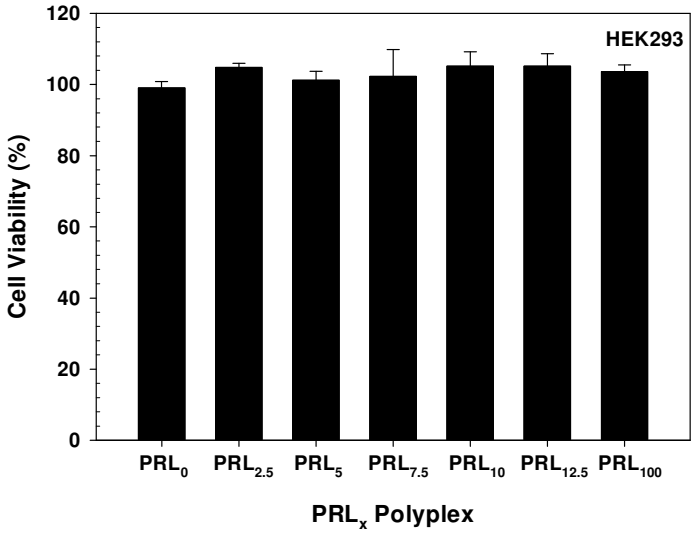

Figure 2.9. Cytotoxicity of PRL_x polyplexes (at N/P 5, 0.5 µg of pDNA) detection by MTT assay after 48 hr transfection in (a) MCF7 and (b) HEK293 cells. Cells were incubated with MTT solution for 4 hr and the absorbance was measured at 490 nm. (Mean ± SD; n = 6)

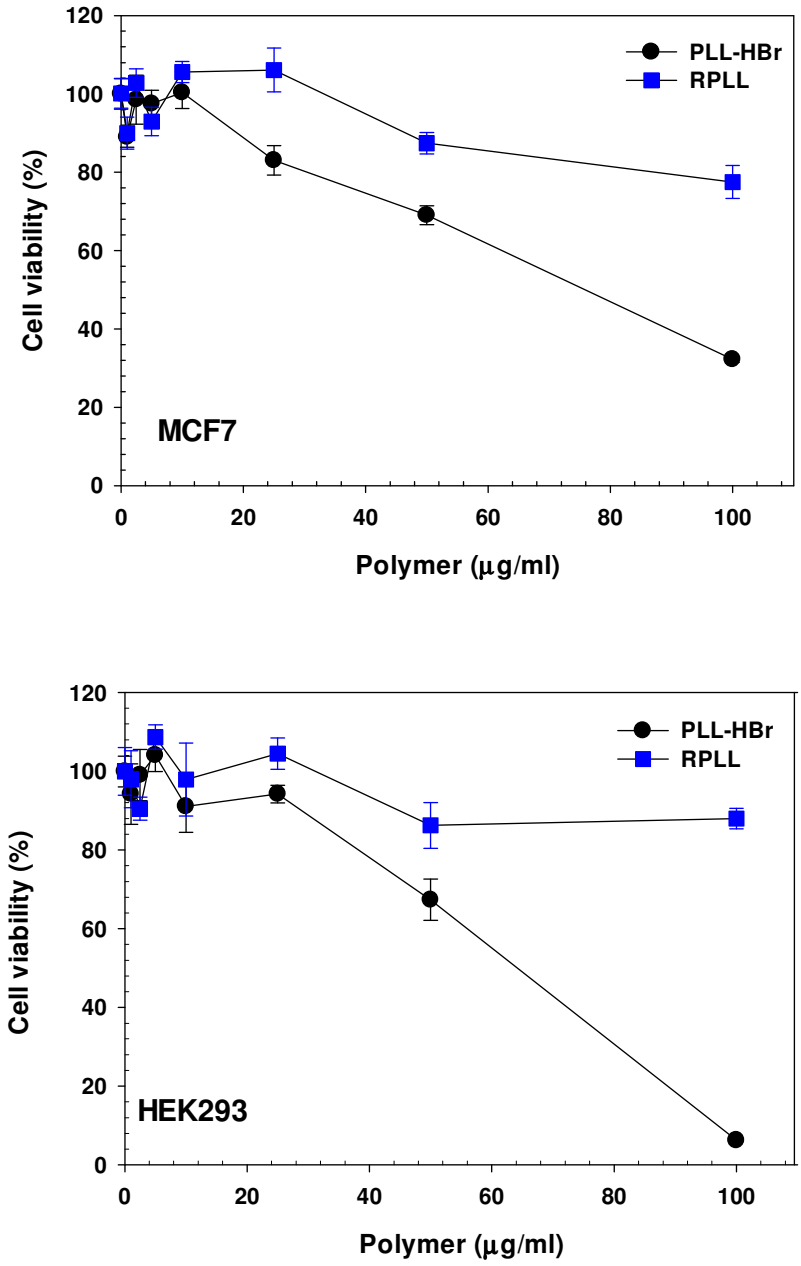

Figure 2.10. MTT-based dose-dependent cytotoxicity assay of PLL and RPLL (0-100 µg/mL) in MCF7 and HEK293 cells. The cells were exposed to the polymers for 24 hr in the serum-containing medium, incubated with MTT solution for 4 hr and the absorbance was measured at 490 nm. (Mean ± SD; n = 6)

MTT-based cell viability assay using MCF7 and HEK293 cells. PRL_0 and PRL_{100} polyplexes had ~88% and almost 100% cell viability against MCF7 cells, respectively. The difference might be caused by lower toxicity of RPLL than PLL. However, cell viability in the presence of PRL_x polyplexes (x=2.5-12.5) differed only negligibly from PRL_0 polyplexes. When applying the polyplexes into HEK293 cells, all tested PRL_x polyplexes (x=0-100) were nontoxic compared with untreated control cells. Thus, the findings indicate that PRL_x polyplex-dependent transfection efficiencies (Figure 2.4) were not influenced by the toxicity results of PRL_x polyplexes.

2.4.4. Effects of RPLL in Decomplexation of pDNA

pDNA must be decomplexed from the polyplex within the cell if the encoded protein is to be expressed. If pDNA release is too slow or absent, gene expression will hardly occur due a lack of accessibility of transcriptional machinery to pDNA.[5] Also, if polyplexes release pDNA too early, then it may not reach the nucleus due to its limited mobility and vulnerability to enzymatic degradation.[5,19] Although PLL and RPLL had similar MW, their polyplexes caused very different transfection efficiencies. PLL/pDNA complexes (N/P 5) showed 74 and 23 times higher luciferase expression than RPLL/pDNA complexes (N/P 5) in MCF7 and HEK293 cells, respectively (Figure 2.4 and Figure 2.5). With the hypothesis of the presence of relationship between the release rate of pDNA from a given system and transfection, decomplexation of pDNA from PRL_x polyplexes was monitored in heparin- and DTT-containing NaCl solution.

First, PRL_x polyplexes (x=0, 5, 10, 20, 50, and 100) were incubated in 150 mM NaCl solution with DTT (20 mM) and different concentrations of heparin (0-100 μg/mL) at 37°C for 1 hr and then were electrophoresed in 0.8% agarose gel with EtBr. The stronger anionic

character of heparin induced the release of weaker anionic pDNA when interacting with polyplexes.[14] When reducible bonds in a polycation exist, DTT degrades disulfide bonds of reducible polymeric backbone. The static interaction strength with pDNA of the fragmented polycations becomes weaker, resulting in facilitated pDNA release.[14] As shown in Figure 2.11, 50 μg/mL of heparin induced pDNA exposure of PRL_0 polyplexes (i.e., PLL polyplexes) in the loading well and 75 μg/mL of heparin caused complete decomplexation of pDNA from PRL_0 polyplexes. However, pDNA complexed in PRL_{100} polyplexes (i.e., RPLL polyplexes) was exposed at 0 μg/mL and was released at 10 μg/mL of heparin. With increasing the amount of RPLL in PRL_x polyplexes, the required heparin concentration for complete decomplexation of pDNA was decreased. However, pDNA release from PRL_x polyplexes with x=0-10 is difficult to discern under these experimental conditions due to the static analysis of the experiment.

PRL_x polyplexes (x=0-10) were exposed to a weakly reducing decomplexation solution (i.e., 150 mM NaCl solution with DTT (10 mM) and of heparin (6.5 μg/mL)) at RT, and their pDNA release kinetics were monitored by dequenching of YOYO-1-intercalated pDNA. Compared with the decomplexation kinetics of pDNA from PRL_0 polyplexes, pDNA releases from PRL_x polyplexes (x=2.5-10) were slightly accelerated with increasing RPLL content (Figure 2.12). These static and dynamic decomplexation results may support the transfection efficiency data of PRL_x polyplexes and also indicate significance of decomplexation optimization regarding release of pDNA from polyplexes.

Transfection results of PRL_x polyplexes (Figure 2.1) showed the highest transfection efficiency at a different amount of RPLL in PRL_x polyplexes depending on cell type. That is, $PRL_{2.5}$ polyplexes and PRL_{10} polyplexes showed maximum transfection

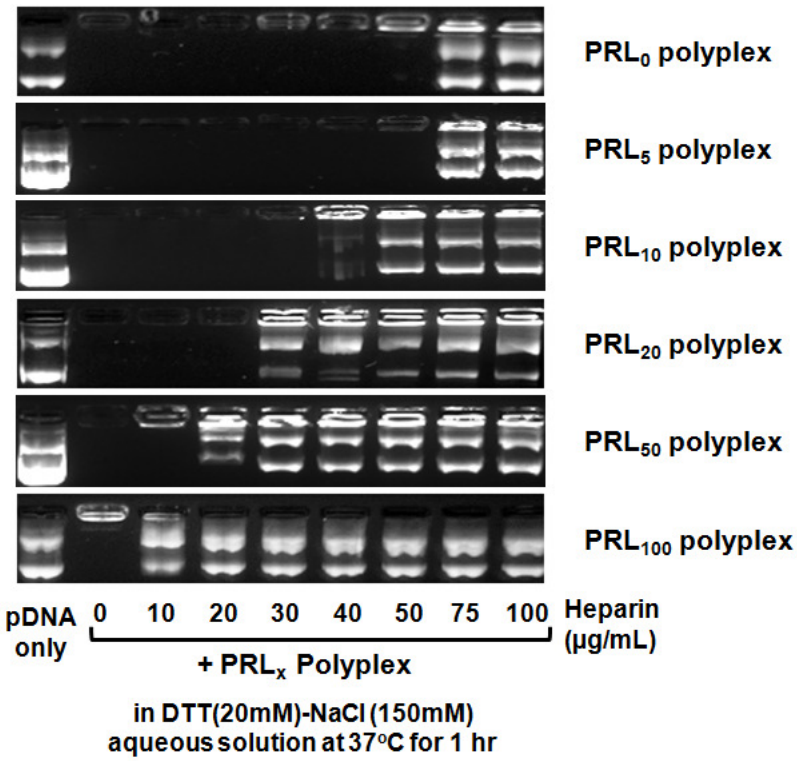

Figure 2.11. Decomplexation (or pDNA release) of PRL_x polyplexes (at N/P 5). After the polyplexes with pDNA (25 μg/mL) were exposed to DTT (20 mM) and heparin sodium salt (0-100 μg/mL) in 150 mM NaCl aqueous solution at 37°C for 1 hr, the polyplex solution was loaded into 0.8% agarose gel and then was electrophoresed at 80 V for 90 min.

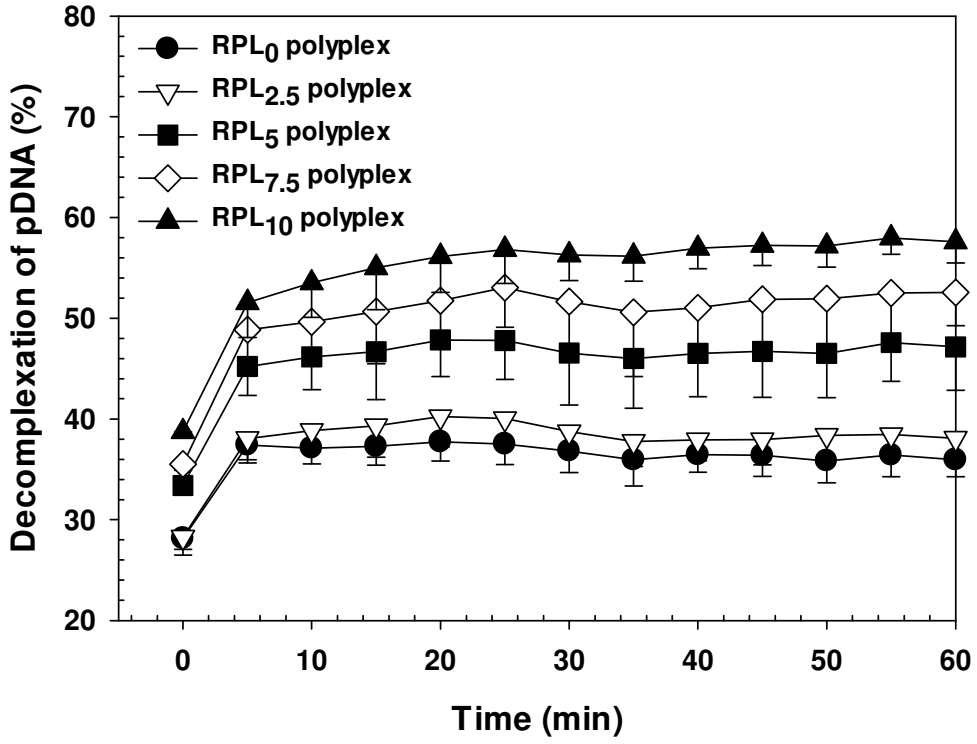

Figure 2.12. Decomplexation (or pDNA release) kinetics of PRL_x polyplexes (at N/P 5) using YOYO-1-labeled pDNA. The polyplexes with pDNA (5 μg/mL) were exposed to DTT (10 mM) and heparin (6.5 μg/mL) in 150 mM NaCl aqueous solution (0.2 mL) at RT. (n = 3; Mean ± SD).

efficiency in MCF7 and HEK293 cells, respectively. This result might be explained by different decomplexation rates of PRLx polyplexes which are further influenced by cell-dependent intracellular glutathione levels, which may accelerate RPLL degradation and thus pDNA release. In fact, tumor cells may have about four times more intracellular glutathione levels than normal cells,[28] and although tumor cell lines are originated from an identical organ, intracellular glutathione levels are different.[29] Thus, to understand clearly why MCF7 cells required a smaller amount of RPLL in PRL_x polyplexes to reach maximum transfection efficiency than HEK293 cells, we monitored intracellular glutathione levels of these two cells were monitored by a GSH-Glo glutathione assay protocol. As shown in Figure 2.13, MCF7 and HEK293 cells had 51.7 ± 0.7 nmol/25000 cells and 4.0 ± 0.1 nmol/5000 cells, respectively. As expected, MCF7 tumor cells represented higher glutathione contents in the cells than the noncancerous HEK293 cells. When applying the same PRL_x polyplexes, lower intracellular glutathione concentrations may cause the slower decomplexation rate of PRL_x polyplexes. Thus, to achieve a similar decomplexation rate of PRL_x polyplexes in MCF7 cells, PRL_x polyplexes in HEK293 cells require higher RPLL contents because higher RPLL contents induce faster decomplexation rate of PRL_x polyplexes. These factors help to explain why that $PRL_{2.5}$ polyplexes and PRL_{10} polyplexes reached a maximum transfection efficiency in MCF7 and HEK293 cells, respectively.

In addition, when PLL with higher MWs than 7.4 kDa (used in this study) is applied for PRL polyplexes, RPLL content in the polyplexes should be increased to represent similar decomplexation rate of PLL 7.4 kDa-based PRL polyplexes because higher MW PLL makes stronger binding affinity with pDNA.

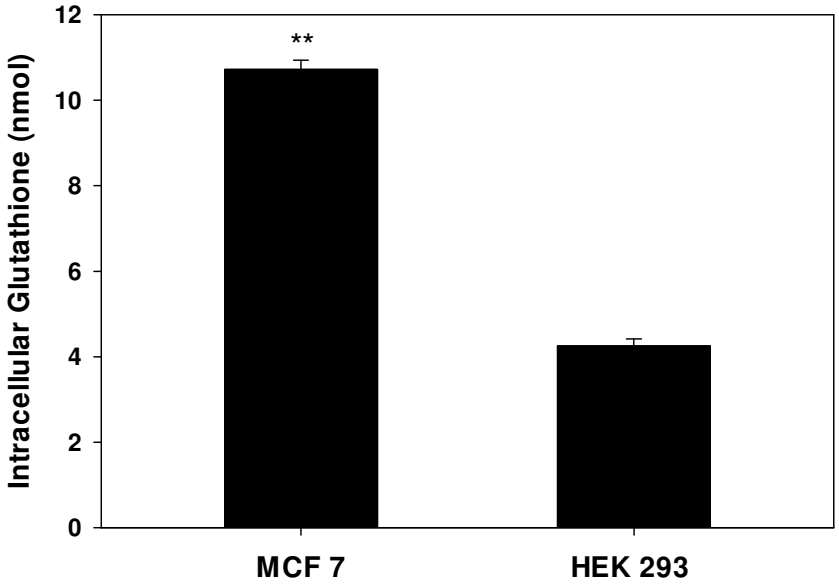

Figure 2.13. Intracellular glutathione levels of MCF7 and HEK293 cells. 5000 cells of MCF7 or HEK293 cells were evaluated. ** means $p<0.01$ compared with HEK293 cells by unpaired Student t-test. (Mean ± SD; n = 3)

2.4.5. Effects of RPLL in Intracellular Localization

After pDNA is internalized into cells, nuclear localization of pDNA is a significant step required for transfection to take place. The polyplexes of polylysine having 28 kDa (about 180 repeating units) delivered pDNA in the nucleus and perinuclear area, whereas polylysines with 19 and 36 repeating units (about 2.3 kDa and 4.4 kDa, respectively) delivered pDNA in the nucleus.[5,12] Lower MW polylysine-mediated polyplexes expressed higher transfection efficiency than higher MW polylysine-mediated polyplexes.[12] However, when using PLL with an intermediate MW (e.g., PLL with MW 7.4 kDa used in this study) to form polyplexes, it is unclear whether pDNA is localized only in the nucleus. It is also unclear how degradable polymers influence intracellular localization of pDNA.

Thus, to understand these significant localization issues of pDNA delivered with degradable polycations, we labeled pDNA with Cy5 and stained the nucleus and acidic vesicles (i.e., late endosomes and lysosomes) were stained with Hoechst 33342 and LysoTracker Green, respectively. As shown in Figure 2.14, all tested PRL_x polyplexes-transfected cells showed similar distributions of acidic vesicles in the cytoplasm based on similar fluorescent intensity of LysoTracker Green. The presence of strong acidic vesicles was caused by weak endosomolytic function of PLL and RPLL. For intracellular distribution of pDNA, it was dependent on RPLL contents in PRL_x polyplexes. In PRL_0, $PRL_{7.5}$, and PRL_{10} polyplexes, pDNA was mostly localized in the cytoplasm and little pDNA was found in the nucleus. However, it seemed that pDNA in $PRL_{2.5}$ and PRL_5 polyplexes distributed almost evenly throughout the cytoplasm and the nucleus.

To understand clearly the nuclear localization of pDNA in PRL_x polyplex-transfected MCF7 cells, the fluorescent intensity of pDNA was separately measured in the whole cell and in the nucleus (Figure 2.15). When transfecting MCF7 cells with PRL_0 polyplexes, 22%

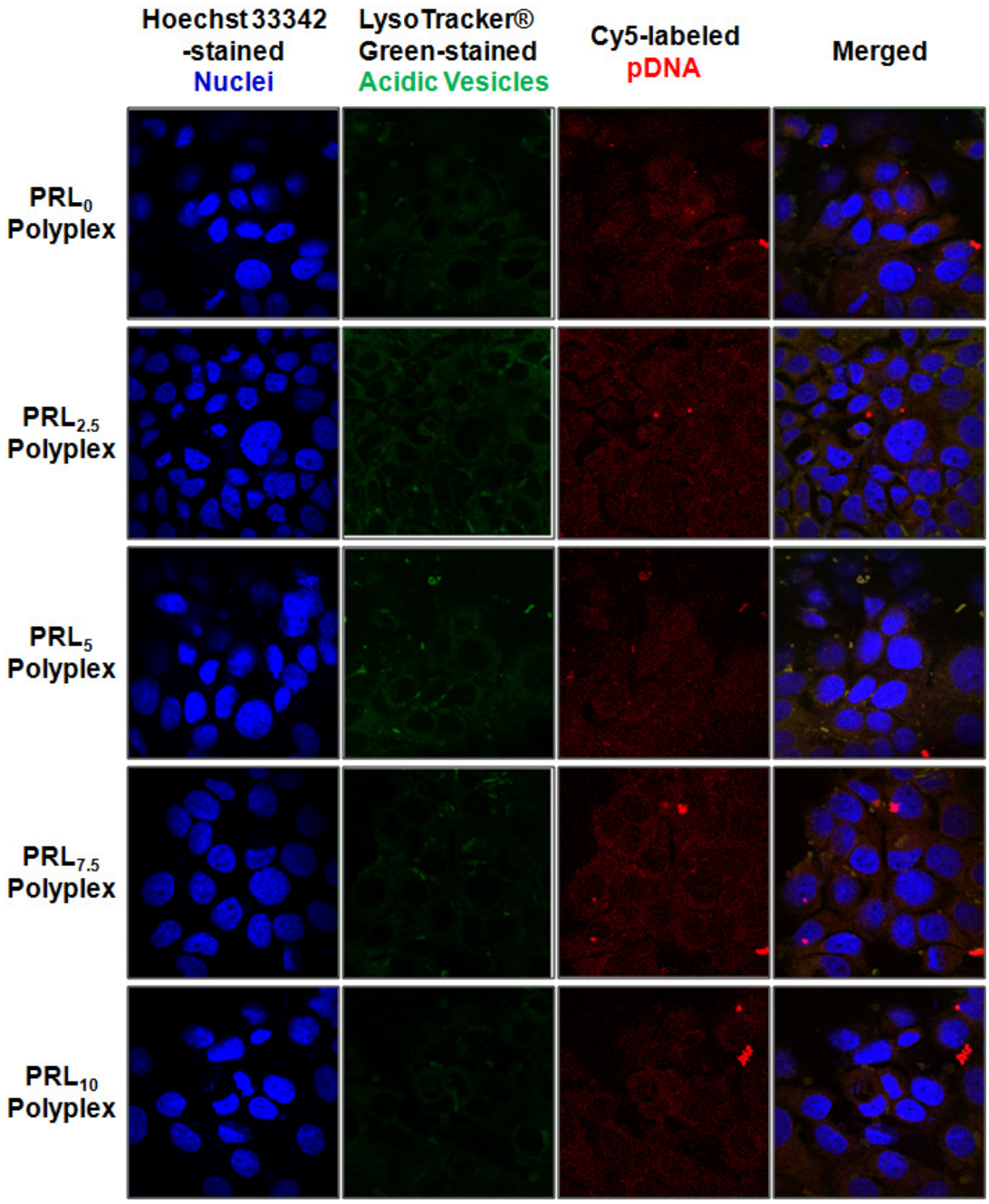

Figure 2.14. Intracellular distribution of Cy5-labeled pDNA delivered by PRL_x polyplexes (at N/P 5) at 4 hr posttransfection in MCF7 cells.

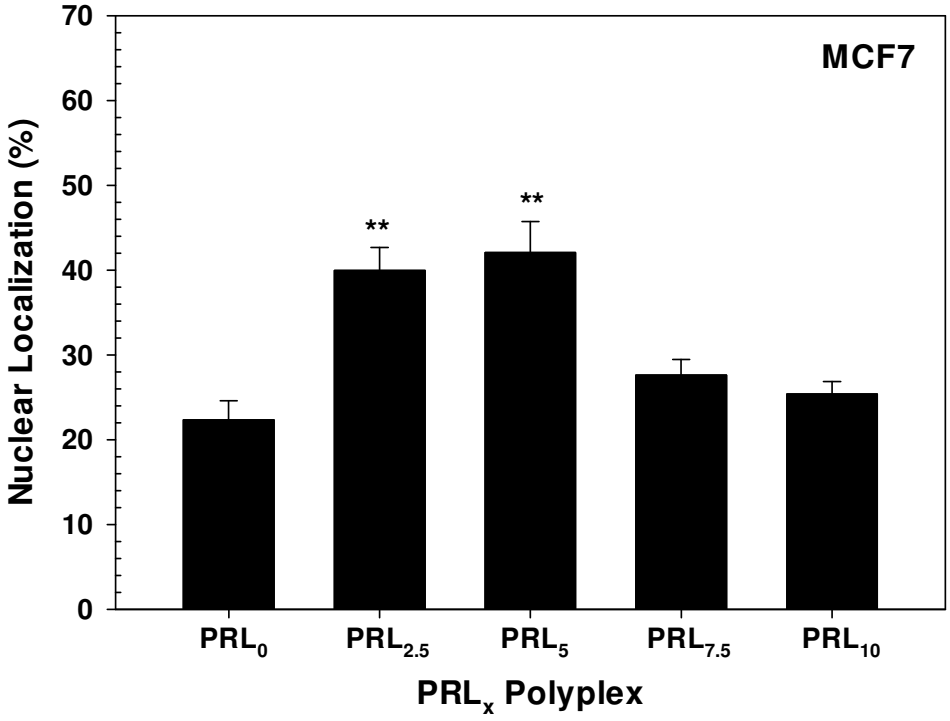

Figure 2.15. Nuclear localization of Cy5-labeled pDNA delivered by PRL_x polyplexes (at N/P 5) at 4 hr posttransfection in MCF7 cells. Nuclear localization was calculated using relative fluorescence intensity ratio in cell and the nucleus generated from a z-stack of confocal images ** mean $p<0.01$ compared with PRL_0 polyplex by one way ANOVA (n = 10; Mean ± SD).

of pDNA was found in the nucleus and the remaining 78% in the cytoplasm and acidic vesicles. Similarly, $PRL_{7.5}$ and PRL_{10} polyplexes-transfected MCF7 cells had ~25% of pDNA in the nucleus. These PRL_x polyplexes (x=0, 7.5, and 10) delivered three to four times more pDNA in the cytoplasm and acidic vesicles than in the nucleus, but, as estimated in confocal microscope, $PRL_{2.5}$ and PRL_5 polyplexes delivered 40~42% of pDNA in the nucleus which is 1.8 to 1.9 times more than that of PRL_0 polyplexes. The different nuclear localization of pDNA may cause their different transfection efficiencies.

Most researches for developing effective polymeric gene carriers have focused on new polymers with functionalities that can overcome various extracellular and intracellular hurdles during a journey of polyplexes from an administration site to the nucleus as a subcellular organelle of interest.[1, 2] Although the significance of timely release of pDNA in the cytosol or the nucleus in polymeric transfection efficiency is recognized,[5] the relationship between decomplexation rate, intracellular localization, and transfection efficiency of pDNA delivered with polymeric carriers has been widely ignored or not investigated.

This study has shown that the pDNA contents in the nucleus is influenced by decomplexation rates of pDNA from polyplexes, and in turn influences the transfection efficiency of the polyplexes. These findings will give greater understanding in polymer-based gene delivery systems and will help to design effective functionalized polyplexes.

2.5. Conclusion

Polyplexes prepared with a mixture of PLL and RPLL were used to understand the relationship between decomplexation rate, intracellular localization, and transfection efficiency. Although the size and surface charge of PRL_x polyplexes were influenced by

the RPLL content, these characteristics did not influence cellular uptake of PRL_x polyplexes. However, the highest transfection efficiency of PRL_x polyplexes in this study may be caused by an optimal decomplexation rate (faster than that of PLL polyplexes and slower than that of RPLL polyplexes) and more nuclear localization of pDNA. These findings will help to design decomplexation-tunable polyplexes made of various combinations of nondegradable and degradable polymers.

2.6. References

1. Kang HC, Lee M, Bae YH. Polymeric gene carriers. Crit Rev Eukaryot Gene Expr. 2005;15(4):317-342.

2. Kang HC, Huh KM, Bae YH. Polymeric nucleic acid carrier: Current issues and novel design approaches. J Control Release. 2012;164(3):256-264.

3. Wagner E. Polymers for siRNA delivery: inspired by viruses to be targeted, dynamic, and precise. Acc Chem Res. 2012;45(7):1005-1013.

4. Son S, Namguang R, Kim J, Singha K, Kim WJ. Bioreducible polymers for gene silencing and delivery. Acc Chem Res. 2012;45(7), 1100-12.

5. Grigsby CL, Leong KW. Balancing protection and release of DNA: tools to address a bottleneck of non-viral gene delivery. J R Soc Interface. 2010;7:S67-82.

6. Kang HC, Bae YH. Co-delivery of small interfering RNA and plasmid DNA using a polymeric vector incorporating endosomolytic oligomeric sulfonamide. Biomaterials. 2011;32(21):4914-24.

7. Kang HC, Bae YH. pH-Tunable endosomolytic oligomers for enhanced nucleic acid delivery. Adv Funct Mater. 2007;17(8):1263-1272.

8. Ruponen M, Yla-Herttuala S, Urtti A. Interactions of polymeric and liposomal gene delivery systems with extracellular glycosaminoglycans: physicochemical and transfection studies. Biochim Biophys Acta. 1999; 1415(2):331-41.

9. Moret I, Esteban Peris J, Guillem VM, Benet M, Revert F, Dasi F, Crespo A, Alino SF. Stability of PEI-DNA and DOTAP-DNA complexes: effect of alkaline pH, heparin and serum. J Control Release. 2001;76(1-2):169-81.

10. Lu H, McDowell LM, Studelska DR, Zhang L. Glycosaminoglycans in human and

bovine serum: detection of twenty-four heparan sulfate and chondroitin sulfate motifs Including a novel sialic acid-modified chondroitin sulfate linkage hexasaccharide. Glycobiol Insights. 2010;(2):13-28.

11. Huth S, Hoffmann F, von Gersdorff K, Laner A, Reinhardt D, Rosenecker J, Rudolph C. Interaction of polyamine gene vectors with RNA leads to the dissociation of plasmid DNA-carrier complexes. J Gene Med. 2006;8(12):1416-24.

12. Schaffer DV, Fidelman NA, Dan N, Lauffenburger DA. Vector unpacking as a potential barrier for receptor-mediated polyplex gene delivery. Biotechnol Bioeng. 2000; 67(5):598-606.

13. Mishra D, Kang HC, Bae YH. Reconstitutable charged polymeric $(PLGA)_2$-b-PEI micelles for gene therapeutics delivery. Biomaterials. 2011, 32, 3845-3854.

14. Kang, H. C.; Kang, H. J.; Bae, Y. H., A reducible polycationic gene vector derived from thiolated low molecular weight branched polyethyleneimine linked by 2-iminothiolane. Biomaterials. 2011;32(15):1193-1203.

15. Mann A, Thakur G, Shukla V, Singh AK, Khanduri R, Naik R, Jiang Y, Kalra N, Dwarakanath BS, Langel U, Ganguli M. Differences in DNA condensation and release by lysine and arginine homopeptides govern their DNA delivery efficiencies. Mol Pharmaceutics. 2011;8(5):1729-1741.

16. Kim YH, Park JH, Lee M, Kim YH, Park TG, Kim SW. Polyethylenimine with acid-labile linkages as a biodegradable gene carrier. J Control Release. 2005;103(1):209-19.

17. Ou M, Xu R, Kim SH, Bull DA, Kim SW. A family of bioreducible poly(disulfide amine)s for gene delivery. Biomaterials. 2009;30(29):5804-14.

18. Lee Y, Koo H, Jin GW, Mo H, Cho MY, Park JY, Choi JS, Park JS, Poly(ethylene oxide sulfide): new poly(ethylene glycol) derivatives degradable in reductive conditions. Biomacromolecules. 2005;6(1):24-6.

19. Lukacs GL, Haggie P, Seksek O, Lechardeur D, Freedman N, Verkman AS. Size-dependent DNA mobility in cytoplasm and nucleus. J Biol Chem. 2000; 275(3):1625-1629.

20. Lechardeur D, Sohn KJ, Haardt M, Joshi PB, Monck M, Graham RW, Beatty B, Squire J, O'Brodovich H, Lukacs GL. Metabolic instability of plasmid DNA in the cytosol: a potential barrier to gene transfer. Gene Ther. 1999;6:482-97.

21. Parelkar SS, Chan-Seng D, Emrick T. Reconfigurating polylysine architectures for controlling polyplex binding and non-viral transfection. Biomaterials. 2011;32(9): 2432-2444.

22. Oupicky D, Parker AL, Seymour LW. Laterally stabilized complexes of DNA with linear reducible polycations: strategy for triggered intracellular activation of DNA delivery vectors. J Am Chem Soc. 2002;124(1):8-9.

23. Read ML, Singh S, Ahmed Z, Stevenson M, Briggs SS, Oupicky D, Barrett LB, Spice R, Kendall M, Berry M, Preece JA, Logan A, Seymour LW. A versatile reducible polycation-based system for efficient delivery of a broad range of nucleic acids. Nucleic Acids Res. 2005;33(9):e86.

24. Read ML, Bremner KH, Oupicky D, Green NK, Searle PF, Seymour LW. Vectors based on reducible polycations facilitate intracellular release of nucleic acids. J Gene Med. 2003;5(3):232-45.

25. Kang HC, Samsonova O, Kang SW, Bae YH. The effect of environmental pH on polymeric transfection efficiency. Biomaterials. 2012;33(5):1651-62.

26. Kang HC, Samsonova O, Bae YH. Trafficking microenvironmental pH of gene vector polycation in drug-sensitive and multidrug-resistant MCF7 breast cancer cell. Biomaterials. 2010;31(11):3071-3078.

27. Jeong JH, Kim SH, Christensen LV, Feijen J, Kim SW. Reducible poly (amido ethylenimine)-based gene delivery system for improved nucleus trafficking of plasmid DNA. Bioconjugate Chem. 2010;21(2):296-301.

28. Kuppusamy P, Li H, Ilangovan G, Cardounel AJ, Zweier JL, Yamada K, Krishna MC, Mitchell JB. Noninvasive imaging of tumor redox status and its modification by tissue glutathione levels. Cancer Res. 2002;62:307-12.

29. Manickam DS, Li J, Putt DA, Zhou QH, Wu C, Lash LH, Oupicky D. Effect of innate glutathione levels on activity of redox-responsive gene delivery vectors. J Control Release 2010;141(4):77-84.

CHAPTER 3

ROLE OF POLYMERIC ENDOSOMOLYTIC AGENTS IN GENE TRANSFECTION: A COMPARATIVE STUDY OF POLY(L-LYSINE) GRAFTED WITH MONOMERIC L-HISTIDINE ANALOGUE AND POLY(L-HISTIDINE)*

3.1 Abstract

Endosomal entrapment is one of the main barriers that must be overcome for efficient gene expression along with cell internalization, DNA release, and nuclear import. Introducing pH-sensitive ionizable groups into the polycationic polymers to increase gene transfer efficiency has proven to be a useful method; however, a comparative study of introducing equal numbers of ionizable groups in both polymer and monomer forms, has not been reported. In this study, we prepared two types of histidine-grafted poly(L-lysine) (PLL), a stacking form of poly(L-histidine) (PLL-*g*-PHis) and a mono- L-histidine (PLL-*g*-mHis) with the same number of imidazole groups. PLL-*g*-PHis and PLL-*g*-mHis showed profound differences in hemolytic activity, cellular uptake, internalization and transfection efficiency. Cy3-labeled PLL-*g*-PHis showed strong fluorescence in the nucleus after internalization, and high hemolytic imidazole groups from PHis also provided higher

*Modified with permission from HS Hwang, J Hu, K Na, YH Bae. Biomacromolecules 2014; 15: 3577-3586. Hwang managed the project, completed part of the experiments, and analyzed the data. Hu completed part of the experiments, and analyzed the data. Na provided key insights into the project. Bae is the PI responsible for the project.

gene expression than mHis due to its ability to escape the endosome. mHis or PHis grafting reduced the cytotoxicity of PLL and changed the rate of cellular uptake by changing the quantity of free ε-amines available for gene condensation. The subcellular localization of PLL-*g*-PHis/pDNA measured by YOYO1-pDNA intensity was highest inside the nucleus, while the lysotracker, which stains the acidic compartments was lowest among these polymers. Thus, the polymeric histidine arrangement demonstrate the ability to escape the endosome and trigger rapid release of polyplexes into the cytosol, resulting in a greater amount of pDNA available for translocation to the nucleus and enhanced gene expression.

3.2 Introduction

Most polymeric gene carriers gain access to target cells via endocytic pathways and must escape from the endosomes before they merge with the lysosomes, rich in digestive enzymes that degrade the therapeutic genes.[1, 2] Polymers synthesized with pH-sensitive groups serve as proton sponges and provide endosomolytic ability that helps escape from the endosome and significantly enhances the potential of gene delivery.[3, 4] The "proton sponge effect" underlies a common strategy for endosomal escape in which the high buffering capacity of the gene carrier agents, *i.e.*, proton absorption by carrier protonation, induces an influx of counterions and water into the endosomes.[5-7] The resulting osmotic pressure build-up subsequently leads to rupture of the endosomal membrane and releases the entrapped components into the cytosol.[8, 9] However, the proton sponge effect is still under debate, and contradictory reports insist this hypothesis is not the dominant mechanism of endosomal escape.[10-12] Benjaminsen *et al*. has argued that polymer concentration inside the endosomes is not sufficient to generate the necessary osmotic

gradient to facilitate polyplex escape from the endosomes.[13] Many other papers do not rule out the proton sponge effect, but have proposed a charge density of polymer that affects the interaction with the endosomes and may destabilize the endosomal membrane inducing membrane disruption, thinning and erosion to facilitate the polyplexes escaping from the endosomes.[11, 14]

Histidine (His) analogues having imidazole group grafted to various polymers including PLL[15] and gluconic acid[16] have become popular materials to deliver pDNA. A study conducted by Singh *et al*. showed that conjugating histidine which has a pK_a near endosomal pH provided effective buffering for strong endosomolytic activity in the endosomal compartments,[17] increased endosomal escape,[18, 19] and enhanced the transfection efficiency and gene expression.[20, 21] The protonation state of the imidazole group is determined by a lone electron pair of the unprotonated nitrogen atom in the imidazole ring of the His analogues, which has a pK_a around 7.[22] Poly($_L$-histidine) (PHis), known as an effective pH-buffering and endosomal pH targeting agent,[23, 24] has been developed and applied for more than a decade as a component of pH-sensitive polymeric carriers. When introduced into the early endosomes, the micelles containing PHis blocks demonstrate strong endosomolytic activity and the ability to produce therapeutic cytosolic drug concentrations in a relatively short time period.[22, 25, 26] These properties have led us to hypothesize that nanocarriers containing PHis blocks result in enhanced gene delivery by inducing endosomal swelling via the proton sponge effect and simultaneously interacting with and disrupting the lipid bilayer membrane of the endosome and facilitating release of the cargo.[25, 27, 28]

Poly($_L$-lysine) (PLL) was the first polycationic nonviral vector used for gene delivery[8]

numerous variations have been explored for the purpose due to its biodegradability into benign products.[29] However, the high positive charge density of PLL still causes cytotoxicity and prevents the release of plasmid DNA (pDNA) from PLL polyplexes. PLL also lacks endosomolytic activity due to the absence of secondary and tertiary amines which results inasmuch as a 10-fold low transfection efficiency *in vitro,*[30, 31] than a standard branched poly(ethylenimine) (bPEI 25 K) in polymeric gene transfection.[32]

We constructed two histidylated PLLs in this study: PLL modified with monomeric histidine analogue (mHis) (PLL-*g*-mHis) and PLL grafted with short PHis blocks (PLL-*g*-PHis) with an equivalent number of imidazole groups in the two architectures. We propose that polymers with high positive charge density are capable of binding to the negatively charged endosomal membrane. As the membrane swells due to the increased osmotic pressure, local stress at the point where the polymer is bound can cause the membrane to be disrupted and release the gene cargo into the cytosol.

3.3. Materials and Methods

3.3.1. Materials

Dimethyl sulfoxide (DMSO), *N*, *N*-dimethylformamide (DMF), 4-(2-hydroxy-ethyl)-1-piperazine (HEPES), 3-(4, 5-dimethylthiazol-2-yl)-2,5-diphenyltetrazolium bromide (MTT), D-glucose, sodium bicarbonate, recombinant human insulin, ethidium bromide (EtBr), heparin sodium salt (139 USP units/mg), paraformaldehyde (PFA), Hoechst 33342, RPMI 1640 medium, Dulbecco's phosphate buffered saline (DPBS), Dulbecco's modified Eagle's medium (DMEM), Poly(L-lysine) hydrogen bromide (PLL·HBr), Cy3-NHs, and FITC were purchased from Sigma-Aldrich (St. Louis, MO). LysoTracker-Red

dye and YOYO-1 were purchased from Invitrogen (Carslbard, CA). A firefly luciferase (gWiz-Luc or pLuc) pDNA was bought from Aldevron (Fargo, ND). Rabbit whole blood cells were purchased from Hemostat (Hemostat Laboratories, CA) and dialysis membranes were obtained from Spectrum Laboratories, Inc. (Rancho Dominguez, CA). Boc-His (DNP, dinitrophenyl)-OH·isopropanol (>99%) was purchased from Bachem.

3.3.2. Synthesis of Boc-Poly (Nim-DNP-histidine), Poly(L-lysine)-graft-(PLL-*g*-PHis) poly(L-histidine), and PLL-graft-monomeric L-histidine (PLL-*g*-mHis)

·*Boc-Poly (N^{im}-DNP-histidine):* Before the conjugation with polymers and poly(L-histidine), DNP protected poly(L-histidine) was first prepared according to our previous report.[26] Briefly, the PHis block was prepared by a ring-opening polymerization method using amine-containing small molecules, N-Boc-1,4 butanediamine, as an initiator, and the number average molecular weight (MW) of PHis was determined to be 3.7 kDa by its ^{1}H-NMR spectrum.

·*Poly(L-lysine)-graft-poly(L-histidine)(PLL-g-PHis):* Poly(L-lysine) (100 mg), succinic anhydride (4.1 mg) and DMAP (10 mg) were first dissolved in 10 mL of anhydrous DMSO. After 2 days stirring at 40 °C, the modified poly(L-lysine) was added with NHS (9.4 mg) and DCC (17 mg). After 1 day stirring, Boc-Poly (N^{im}-DNP-histidine) was added into the DMSO solution under nitrogen airflow. Then 2-mercaptoethanol (3 mL) was added after 2 days dropwise into the mixture for overnight stirring. The product was precipitated in ether: ethanol (50:50%, V/V) and purified by dialyzing against DMSO for 2 days and DI water for 2 days with a dialysis membrane of MWCO 3500 g/mol. The final yellow product was

obtained after lyophilization, and the yield of the product was 65%.

·*Poly(L-lysine)-graft-mono- L-histidine(PLL-g-mHis):* The synthesis of PLL-*g*-mHis is started with 0.5 g poly(L-lysine) and 0.212 g L-histidine. These materials were dissolved in 30 mL of DI water, and after adjusting the pH to 5.0, 0.262 g EDC·HCl was added to the solution. After stirring the mixture overnight, the solution was dialyzed against deionized water for 2 days with at least four changes using dialysis membrane (MWCO 6000-8000 g/mol). The final product was collected after lyophilization and the yield of the product was 89%.

3.3.3. Characterization of Polymers

^{1}H-NMR spectra were recorded on a Varian Unity 400 at 9 T with NaLoRAc Z-spec broadband probe for the modified polymers in D_2O/DCl mixed solvent with 10 v% DCl and chemical shifts were given in parts per million from tetramethylsilane.[15]

The average number of imidazole molecules bound per polylysine was calculated according to $x = 6 \times h_{8.7}/h_{lys} \times 100\%$, where x was the percentage of imidazole repeat to lysine repeat, $h_{8.7}$ was the value of the integration of the signal at 8.7 ppm corresponding to the proton of histidine, h_{lys} was in the range 1.3-1.9 ppm corresponding to the six methylene protons of lysine residues.

Gel permeation chromatography (GPC) measurement of the PHis was performed on an Agilent 1100 Series high performance liquid chromatography (HPLC) system equipped with a TSKgel G3000HHR GPC column equilibrated at 30 °C and a refractive index detector. DMF with 10 mM LiBr solution was used as the eluent at a flow rate of 1 mL/min for PHis before deprotection.[26]

The buffering capacity of polymers was measured via acid-base titration.[33] Polymers were dispersed in 150 mM NaCl, and pH of solutions was adjusted to 10 using 1 N NaOH. Then the solutions (1 mg/mL, total volume 2 mL) were titrated with 0.1 N HCl to monitor the pH changes of the polymer solution. The proton buffering capacity of polymers was compared at a pH of 7.4 to 5.1 and calculated using the equation below, where ΔV_{HCl} is the volume of HCl that used to titrate the pH, C_{HCl} is the concentration of HCl which was 0.1 N, and m is the mass of the polymer, which was 2 mg.

$$Buffering\ capacity = \frac{\Delta V_{HCl} \times C_{HCl}}{m}$$

The membrane-disruptive activity of the difference between PLL-*g*-PHis and PLL-*g*-mHis was measured using a red blood cell (RBC) hemolysis assay.[34] RBCs were harvested by centrifuging whole blood to remove serum and resuspended in 100 mM dibasic sodium phosphate at pH 7.4 and 5.5 at 5×10^8 cells/mL. A total of 200 µL of RBC suspension and 800 µL of buffer solution of polymers were mixed at final concentration of polymers 50 µg/mL and incubated at 37 ^{0}C for 1.5 hr. Buffer only and deionized water were used as negative and positive control separately. After centrifuge, lysis was determined by measuring the absorbance of the supernatant at 541 nm. The percent

$$\text{Hemolysis } (\%) = \frac{Abs_{sample} - Abs_{blank}}{Abs_{positive\ control}} \times 100$$

hemolysis was calculated by the above formulation.

3.3.4. Physicochemical Characterization of Polyplexes

A solution of cationic polymers and solution of pDNA (20 µL per 1 µg of pDNA) in HEPES buffer (20 mM, pH 7.4) were prepared separately and mixed to form polyplexes.

After 30 min incubation at RT, the prepared polyplexes were used for further experiments. Polyplexes were expressed based on the N/P ratio; the mole ratio of the amines (N) of polycation per phosphate group (P) of pDNA.

Condensation of DNA (0.5 μg of pDNA) with polymers was monitored using a gel electrophoresis assay. Polyplexes with several complexation ratios were loaded into a 0.8 % agarose gel containing ethidium bromide (EtBr), and a constant voltage (95 V) was applied to the polyplex-loaded gel in 0.5xTBE buffer for 40 min. Shielded or exposed pDNA from the polyplexes was detected using a UV illuminator. Polyplexes at N/P ratio 5 were then prepared in 20 mM HEPES buffer at pH 7.4 and 5.5 followed by incubation in solutions of various heparin (used as the competing polyanion) concentrations at 37 ^{o}C for 30 min to monitor the pH-dependent pDNA release. The release of pDNA was analyzed in 0.8 % agarose gel containing EtBr (95 V, 40 min). In addition, decomplexation of pDNA from polyplexes was monitored by a YOYO 1-intercalated pDNA containing heparin. Relative fluorescent units (RFUs) of polyplexes was measured using a plate reader at 495 (excitation) and 515 nm (emission). Free YOYO 1-intercalated pDNA and the buffer solution were set as 100% and 0%, respectively and pDNA release was calculated by the following equation. [30]

$$\text{pDNA release (\%)} = \frac{\text{RFU}_{\text{Polyplex}} - \text{RFU}_{\text{Buffer}}}{\text{RFU}_{\text{pDNA}} - \text{RFU}_{\text{Buffer}}} \times 100\ (\%)$$

The particle sizes and zeta potential of polyplexes were monitored using a Zetasizer Nano ZS (Malvern Instrument, U.K.) at a wavelength of 677 nm and a constant angle of 90^{o} at RT (25 ^{o}C). Polyplexes were diluted in HEPES buffer (20 mM, pH 7.4) with the concentration of pDNA set to 2.5 μg/mL.

3.3.5. Cells and Cell Culture

Hela cells (human cervical carcinoma cell line) were cultured in DMEM supplemented with 10% FBS and $_{D}$-glucose (4.5 g/L). MCF7 cells (human breast adenocarcinoma cell line) were cultured in RPMI supplemented with 10% FBS, D-glucose (2 g/L), and insulin (4 mg/L). Both cells were grown and maintained under humidified air containing 5% CO_2 at 37 ^{o}C.

3.3.6. Biological Characterization of Polymer and Polyplexes

To visualize the localization of Cy3 labeled polymers under a confocal microscope, 1 mL× 2.4 mg/mL DPBS solution of PLL-*g*-PHis, PLL-*g*-mHis or PLL was mixed with 40 μL× 1 mg/mL DMSO solution of Cy3-NHS separately, after stirring overnight, the mixtures were dialyzed against DPBS for one day with two changes using dialysis membrane (MWCO 3,500 g/mol). The final concentration of polymers in DPBS almost kept constant at 2.4 mg/mL. For fluorescence labeling with FITC and Cy3 together, 2 mL× 1 mg/mL DPBS solution of PLL-*g*-PHis, PLL-*g*-mHis or PLL was mixed with 40 μL× 1 mg/mL DMSO solution of Cy3-NHS and 60 μL× 1mg/mL ethanol solution of FITC at the same time, after stirring overnight, the mixtures were dialyzed against DPBS for 1 day with two changes using dialysis membrane (MWCO 3,500 g/mol). The final concentration of polymers in DPBS almost kept the same as 1 mg/mL.

The intracellular pH environments of polymers were monitored using fluorescence method, as reported by articles.[35, 36] For the construction of pH calibration curve, Hela cells were seeded in six-well plates at a density of 2 x 10^5cells/well and cultured for 24 hr before treatment. After treated with FITC+Cy3 labeled PLL-*g*-PHis and PLL-*g*-mHis 4

hr, the cells were suspended in one of four pH clamping buffers (130 mM KCl, 1 mM $MgCl_2$, 15 mM HEPES, and 15 mM MES) with pH adjusted to 5, 5.5, 6 and 7.4. The cells containing fluorescent polymers were monitored using flow cytometry. The correlation between pH and average Cy3/FITC ratios of pH clamp cells was calibrated. Based on the pH calibration curve, the intracellular pH of polymers at different time were calculated.

To determine the polymer cytotoxicity *in vitro*, a MTT-based cell viability test was performed in 96 well plates as previously reported.[33] Hela and MCF7 cells were seeded at a density of 2 x 10^3 and 5 x 10^3 cells per well and the cells were cultured for 24 hr in serum containing culture medium (100 μL of medium per well). Different concentration ranges (0 - 100 μg/mL) of polymers were exposed to the cells for 24 hr, then the cells in the culture medium of 0.1 mL were treated with MTT solution (5 mg/mL, 10 μL) to measure cell survival. After 4 hr incubation, the culture medium was aspirated and 100 μl of DMSO was added to dissolve the formazan crystals. The absorbance of the solution was monitored at 570 nm using a microplate reader.

YOYO1-labeled pDNA was used to monitor cellular uptake of polyplexes. Cells were treated with 1μg pDNA (1mg/ml) per well, and 4 hr post-transfection, the cells were washed with DPBS, detached and fixed using PFA 4% solution. Analysis was performed using a flow cytometry (FACScan Analyzer, Becton−Dickinson; Franklin Lakes, NJ) equipped with a primary argon laser (488 nm) and a fluorescence detector (530 ± 15 nm) for YOYO-1 detection. The uptake of the polyplexes was analyzed through 10000 gated events per sample.

In vitro transfection studies were performed in MCF7 and Hela cells, and both cells

were seeded in 6-well plates at a density of 5 x 10^5 cells/well and 1 x 10^5 cells/well, respectively. After 24 hr, the culture medium was replaced with serum-free transfection medium 1 hour before the addition of polyplexes. Then the polyplexes (1 µg of pDNA per 20 µl) are transfected in cells and incubated for 4 hr, and serum-containing culture medium was added in cells and incubated for additional 44 hr. When the transfection experiments were completed, the cells were rinsed with DPBS for twice and then lysed in a reporter lysis buffer. The relative luminescence unit (RLU) was evaluated by luciferase assay kit (Promega), protein content of the transfected cells were monitored by BCA protein assay kit (Thermo scientific). Transfection experiments with chloroquine (Sigma -Aldrich, 100 µM) were performed as below. The drug was added to the cells 30 min prior to polyplexes addition and polyplexes were exposed to media for 3.5 hr, and the medium was changed to serum containing DMEM for an additional 44 hr. Then the cells were lysed and assayed by luciferase assay kit and BCA protein assay kit for RLU and protein content, respectively as described above.

For studying the intracellular trafficking of polyplexes, Hela cells were seeded at 1 x 10^5 cells/well on sterile cover glasses in a six-well plate. YOYO1- intercalated pDNA was used to prepare polyplexes and added to the cells in serum-free media. Hoechest 33342 and LysoTrackerRed dyes were added 30 min before the incubation termination to stain the nuclei and the acidic vesicles. After 4 hr of incubation, the cells were washed twice with PBS and fixed with 4% paraformaldehyde in PBS. The cover glasses were mounted on the slide glasses with a drop of antifade mounting media. The fixed cells were examined under a confocal microscope (FV1000-XY, Olympus) for the detection of the YOYO1-labeled pDNA, Hoechest 33342, and LysoTrackerRed. Fluorescence

intensity of YOYO1-intercalated pDNA and red lysotracker was quantified by using ImageJ software.

3.3.7. Statistical Analysis

ANOVA and unpaired Student's *t*-test were performed for statistical analysis and $p < 0.01$ considered statistically significant.

3.4. Results and Discussion

3.4.1. Preparation and Characterization of Histidylated PLLs

The chemical structures of PLL-*g*-PHis and PLL-*g*-mHis polymers are shown in Figure 3.1, and the synthetic schemes and ^{1}H-NMR spectra are in Figure 3.1. The 3.7 kDa PHis with a polydispersity 1.2 was prepared by the same method mentioned in our previous paper[26] and the GPC curve is provided in Figure 3.2. As reported previously, the transfection efficiency of histidylated PLL was optimal with 38±5% of the ε-amino groups in PLL being substituted with histidyl residues [16] In this study the percentage of total imidazole groups per lysine residue (Lys) was set at 30%.

3.4.2. Buffering Capacity of Polymers in the pH Range

Endosomal escape via the proton sponge effect requires that gene carriers have a high buffering capacity. The buffering capacity of the modified PLL was evaluated as shown in Figure 3.3 to investigate the change of buffering capacity of PLL upon either mHis or PHis incorporation. As expected, acid base titration revealed that unmodified PLL showed the least buffering capacity, whereas introducing imidazole groups

(a) PLL-*g*-PHis

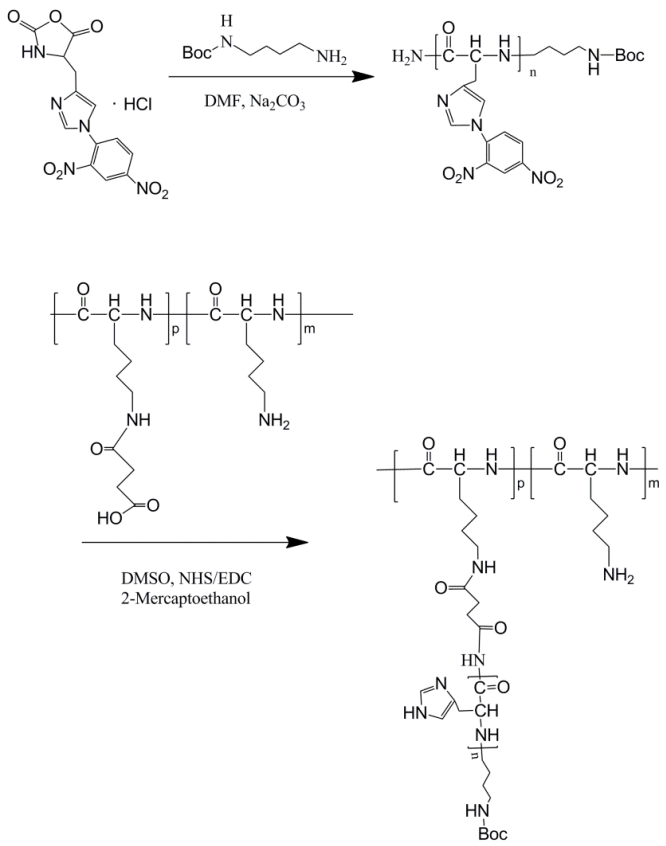

(b) PLL-*g*-mHis

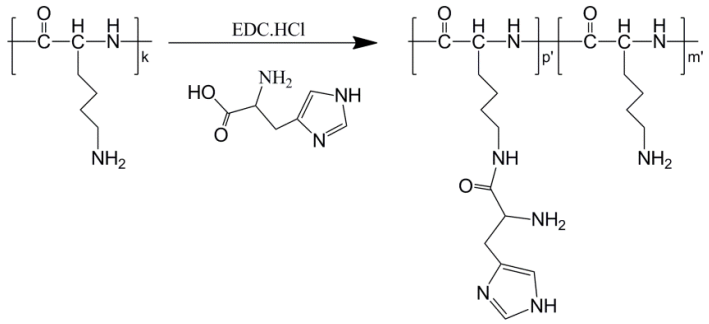

Figure 3.1. Synthetic schemes of polymers and ^{1}H-NMR analysis of PLL-*g*-PHis in D_2O. Alphabets in the figure represent each proton in the polymer chemical structure which corresponds to ^{1}H-NMR peaks.

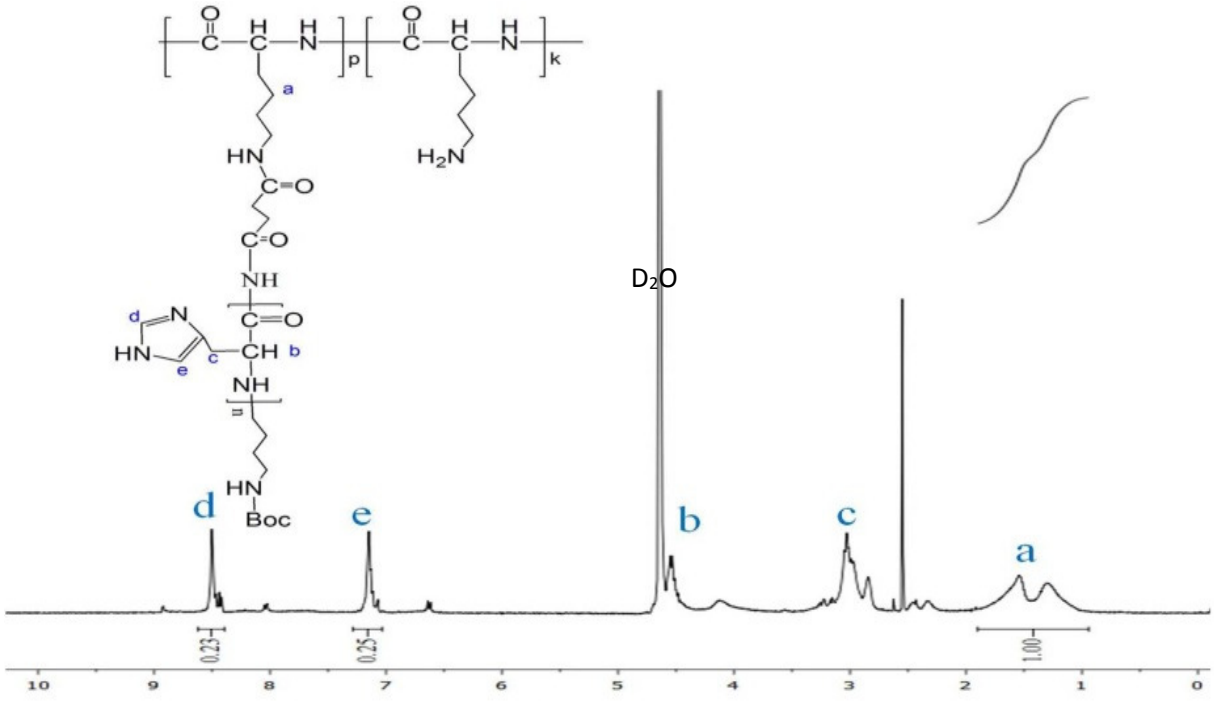

Figure 3.1. (Continued)

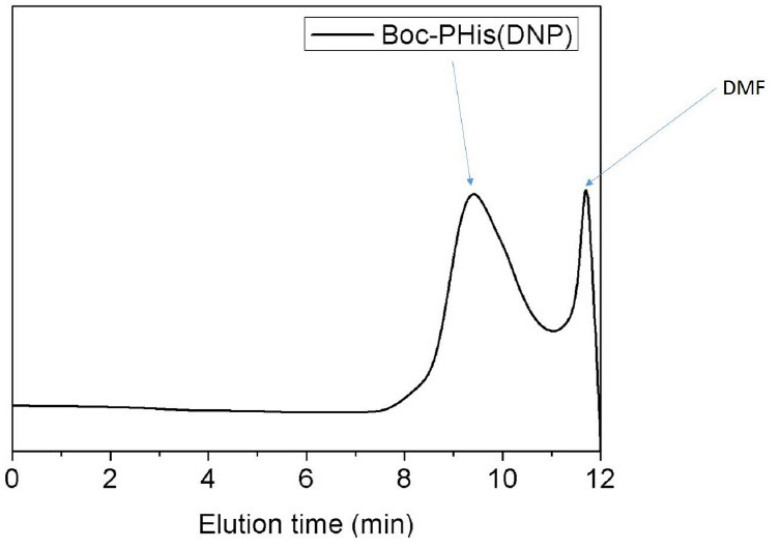

Figure 3.2. GPC curve of poly(L-histidine) (PHis).

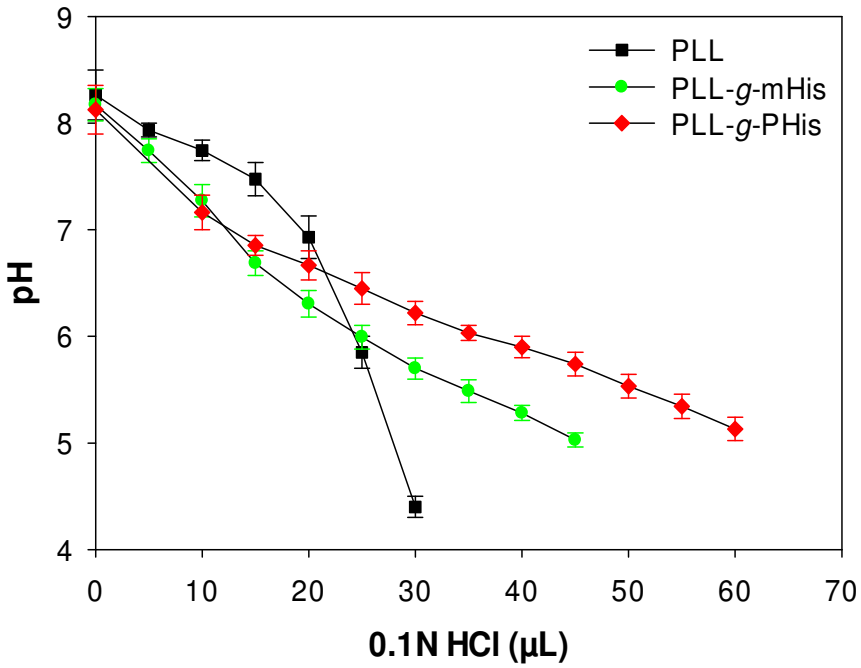

Figure 3.3. Acid-base titration curves of PLL and histidine modified PLLs in 150 mM NaCl.

increased the buffering capacity between lysosomal (pH 5) and cytoplasmic (pH 7.2) pH. The buffering capacity of PLL-*g*-PHis was slightly higher than PLL-*g*-mHis though both had an equivalent number of imidazole groups (Figure 3.4). The higher buffering capacity of PLL-*g*-PHis may be attributed to the short distance between imidazole groups in PHis. The imidazole ring in the His residue contains two ionizable nitrogens (Nδ1 and Nδ2). The pKa values and the degree of ionization of imidazole rings are influenced by neighboring groups, making them tunable to specific environmental conditions.[37] Titration data also suggests that the pK_a values of the ionizable groups in mHis and PHis are different, which implies that the protonation of the imidazole groups are different depending on the connectivity of His residues. Differential protonation behavior may result from the different distances between imidazole groups in PLL-*g*-mHis and PLL-*g*-PHis. The distance between imidazole groups in PHis is ~3 Å, whereas, the closest distance in PLL-*g*-mHis is at least 4.5 Å (or even longer), the shorter distance favors more rapid proton transfer via a hydrogen bridge.[38] Multiple adjacent imidazole rings in PHis influence each other and effectively produce an electron rich environment that stabilizes positive charges on imidazole groups and allows higher protonation state.

3.4.3. The Hemolysis Activity of Polymers

The pH in the late endosomal compartment ranges from 5 to 6 and from 5 to 5.5 in the lysosomal compartment.[39] The membrane damage should be restricted to endosomal vesicles in a pH-dependent manner, avoiding nonspecific membrane disruption. His becomes fully protonated in the endosomal pH range, thus providing pH-responsive membrane destabilizing activity. Though PLL has been widely used as a gene carrier, it

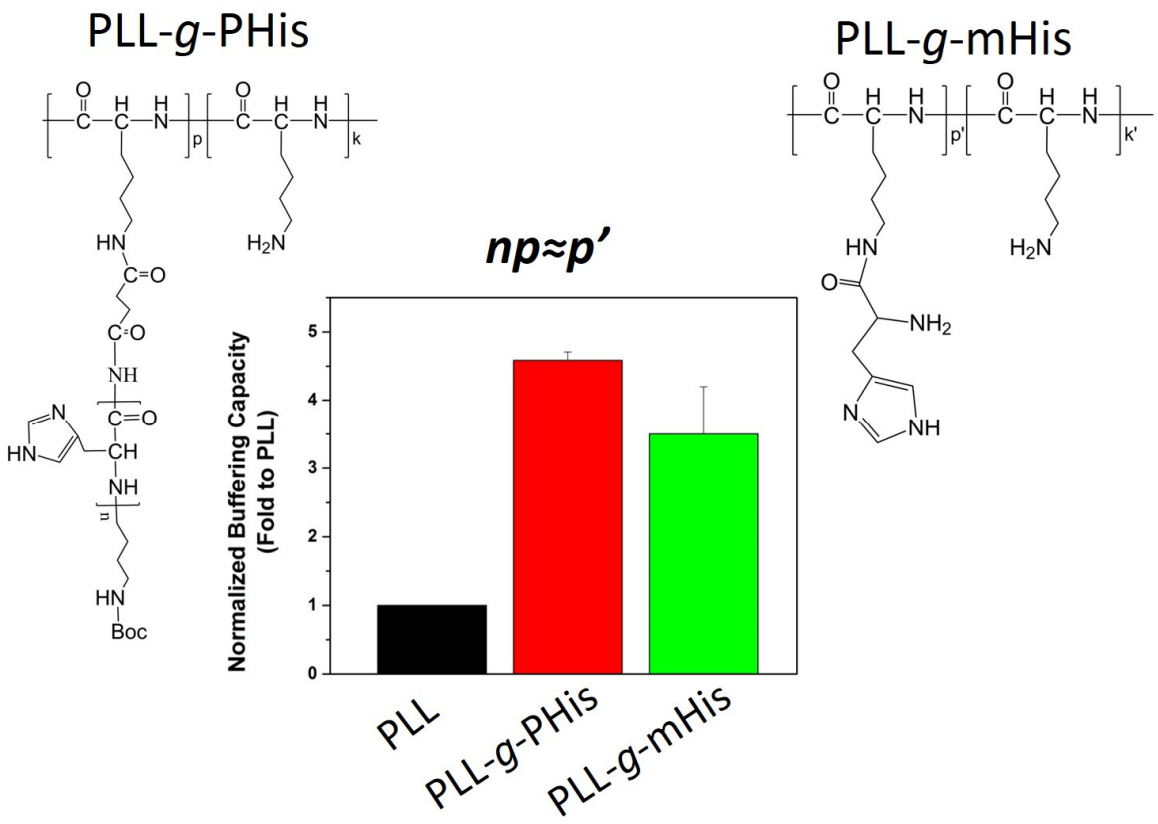

Figure 3.4. Poly(L-lysine)-*g*-poly(L-histidine) (PLL-*g*-PHis) and poly(L-lysine)-*g*-mono-L-histidine (PLL-*g*-mHis) chemical structures and comparison of buffering capacity.

shows no apparent pH-dependent hemolysis.[40]

The hemolysis activity of PLL and two His grafted polymers was tested with rabbit red blood cells at two pHs. As shown in Figure 3.5, PLL at pH 7.4 caused 10% hemolysis, which showed less hemolysis than the His containing polymers. In addition, there was no significant change in the hemolytic activity of PLL as pH dropped from 7.4 to 5.5. This explains PLL is absence of pH-dependent hemolysis. On the other hand, the hemolytic activity of PLL-*g*-mHis changed from 18% at pH 7.4 to 42% at pH 5.5, and PLL-*g*-PHis changed from 27% at pH 7.4 to 75% at pH 5.5. Both histidylated polymers contained an equivalent number of imidazole groups showed pH-responsive membrane disruption, but PLL-*g*-PHis caused more hemolysis at pH 5.5 than PLL-*g*-mHis. Based on the hemolysis assay, PLL-*g*-PHis displayed much higher membrane disruption activity at pH 5.5 compared to PLL-*g*-mHis, making it a potentially better carrier with higher endosome disruption property for gene delivery than PLL-*g*-mHis.

The hemolysis activity appears to be dependent on interactions between the cell membranes and cationic polymers that results local stress on the membrane. In more detail, the hemolytic activity of the polymers is governed by the electrostatic stress force applied to the membrane surface as it swells, and the electrostatic forces produced between the polymers and cell membranes causes a charge imbalance on the membrane. It eventually disrupts the electric fields formed on the RBC membrane to create pores or holes leading to osmotic lysis.[41-43] The external stress forces that destabilize membrane come from the density of electrostatic interactions of protonated polymers per the membrane surface area[43], and it has been reported that different protonation states of polymer affect the disruption of RBCs lipid bilayers.[44] The significant difference

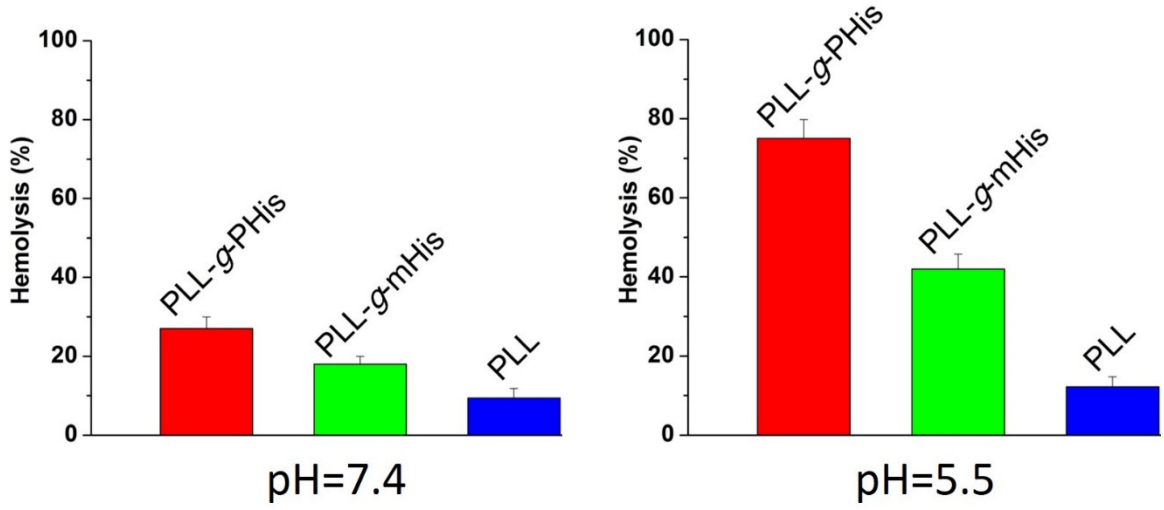

Figure 3.5. pH dependence of hemolytic activity of PLL-*g*-PHis and PLL-*g*-mHis in pH 7.4 and pH 5.5. (Data shown are the Mean ± SD; n = 3).

in hemolytic activity of PHis and mHis suggests that the strength of the stress force induced by PLL-*g*-PHis per the area of the membrane is stronger than that of mHis because the higher charge density on PLL-*g*-PHis at lower pHs produces stronger interactions with the membrane, whereas, the more diffuse imidazole groups in PLL-*g*-mHis result in a weaker stress force intensity. Therefore, it is thought that a more protonated state of PLL-*g*-PHis will produce higher electrostatic interactions and induce higher stress forces by interacting more strongly with the membrane increasing the probability of destabilization and endosomal escape. The observed hemolytic activities of pH sensitive polymers show a great potential to disrupt endosomal membranes and aid endosomal escape.[45]

3.4.4. Gel Electrophoresis Study of Polymer/pDNA Complexation

A gel retardation assay was performed to investigate the complexation capability of PLL and PLL-*g*-mHis/PLL-*g*-PHis with pDNA. Polyplexes were prepared at N/P ratios ranging from 1 to 8 and loaded in agarose gel (Figure 3.6). Data showed that PLL was able to completely condense genes at N/P 1, while PLL-*g*-mHis and PLL-*g*-PHis based polyplexes did the same at N/P 4 and 2, respectively. PLL has a high charge density from primary ε-amino groups, enabling it to condense the genes at a very low N/P ratio. The ε-amino groups are the histidine grafting sites for both PLL-*g*-mHis and PLL-*g*-PHis, resulting in a lower charge density. Grafted histidine may also pose some steric hindrance to DNA binding. Therefore, complete gene condensation required more PLL-*g*-PHis molecules than PLL and the PLL-*g*-mHis needed even more molecules to condense the same amount of genes since 30 % ε-amines in Lys residues are modified

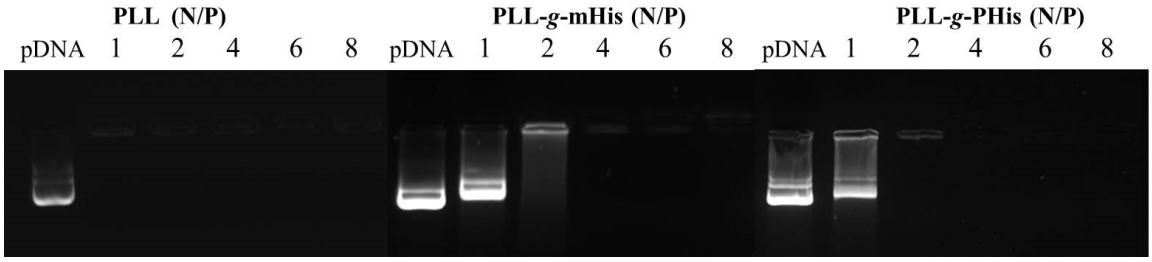

Figure 3.6. Gene condensation ability of polymers with pDNA in 0.8% agarose gel at 80 V for 90 min.

with mHis.

To determine the binding strength and stability of polyplexes at different pHs, polyplexes were incubated with increasing concentrations of heparin, which is a competing polyanion with pDNA for the binding to polymers (Figure 3.7(a)). PLL/pDNA polyplexes remained stable and showed no pH-dependent change of binding strength. In contrast, PLL-*g*-mHis/pDNA and PLL-*g*-PHis/pDNA polyplexes in pH 7.4 buffer required less heparin to expose pDNA compared to PLL/pDNA polyplexes. At pH 5.5, both polyplexes were more resistant to dissociation upon heparin incubation, because the more protonated state of the imidazole groups enhances interactions with pDNA and forms more stable polyplexes. As shown in Figure 3.7(b), PLL-*g*-PHis/pDNA polyplexes revealed more change in the DNA binding strength as pH drops, indicating that the higher degree of protonation is due to the more fully protonated imidazole groups.

The results suggest that decomplexation of histidylated polyplexes provides pH-dependent pDNA release. This will prevent premature pDNA release and effectively protect genes against enzymatic (nuclease) degradation.[46, 47] Thus, the different binding strength between PLL-*g*-mHis and PLL-*g*-PHis will influence pDNA release kinetics and plays a critical role in determining transfection efficiency after endosomal escape.

3.4.5. Particle Size and Zeta Potential Profiles of Polyplexes at Various N/P Ratios

PLL-*g*-PHis formed a micelle at physiological pH because of the amphiphilicity of the polymer. The average diameter of PLL-*g*-PHis in HEPES buffer at pH 7.4 was about 60 nm (Figure 3.8). The size of micelles increased as the pH dropped and grew sharply at

(a)

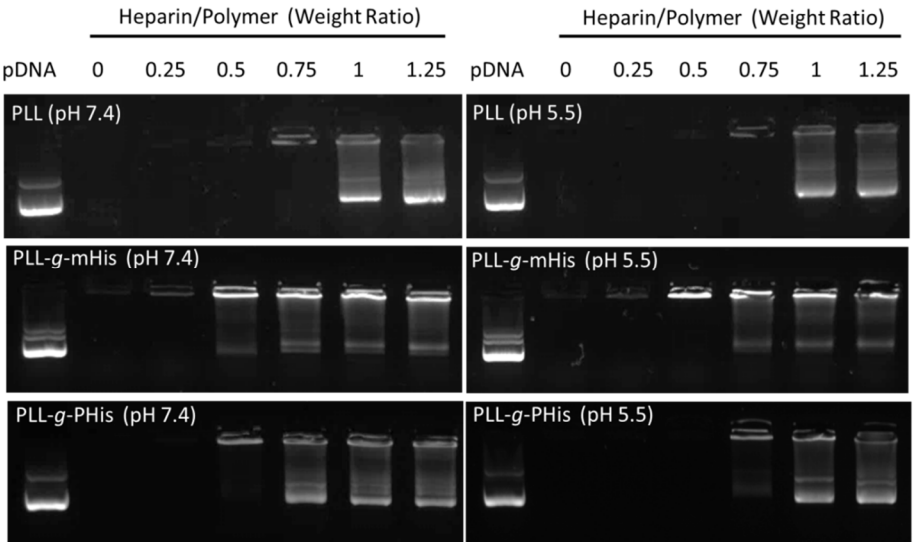

(b)

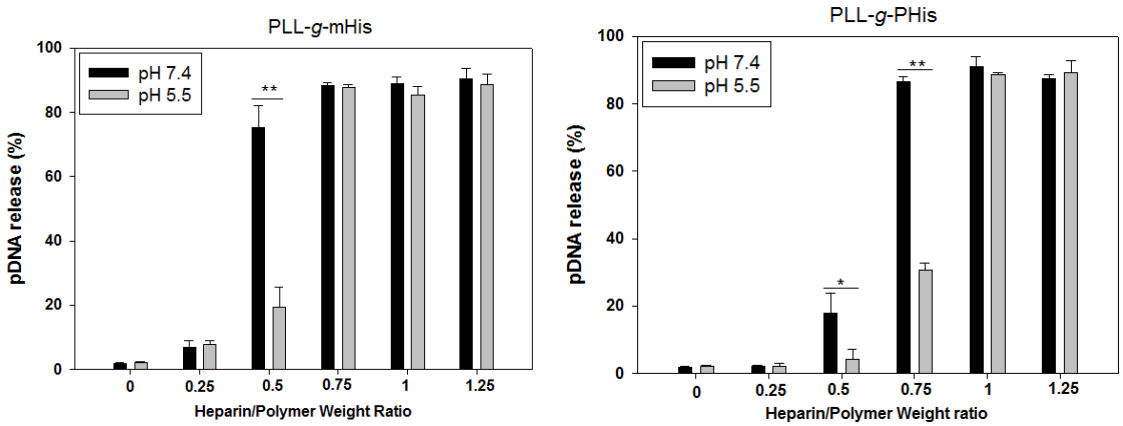

Figure 3.7. pH-dependent pDNA release test using a heparin competition assay. (a) The binding strength of the polyplexes (N/P 5) at pH 7.4 and pH 5.5 under heparin incubation (b) A quantification of the release of pDNA using a YOYO-1-labeled pDNA at increasing concentration of heparin under pH 7.4 and pH 5.5. (* $p<0.01$, ** $p<0.001$; Mean ± SD; n = 3)

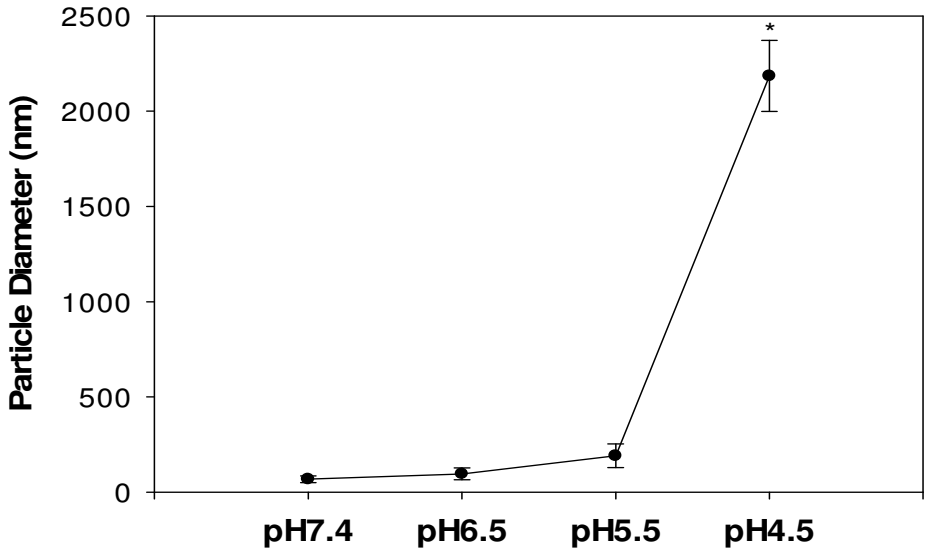

Figure 3.8. The particle size changes of PLL-*g*-PHis upon pH reduction (Mean ± SD; n = 10) * indicates $p<0.05$ compared with particle sizes at pH7.4.

pH 4.5 as the micelles became sufficiently protonated to cause dissociation. To characterize complexation with pDNA, the particle size and zeta potential were monitored at various N/P ratios ranging from 4 to 10 (Figure 3.9). PLL polyplexes showed the smallest particle size (60-90 nm), whereas, PLL-*g*-mHis and PLL-*g*-PHis were larger (80-120 nm and 70-80 nm, respectively). The size and charge of the polyplexes depends on the number of free primary amino groups on the PLL backbone which can alter the electrostatic interactions with the genes. Thus, PLL can make a compact particle, but this in turn retards the dissociation between PLL and pDNA once located inside the cells and leads to low transfection efficiency.[48]

3.4.6. Cell Viability Analysis Using MTT Assay

Grafting His into PLL reduces the cytotoxicity of the polymer as assessed in MCF7 and Hela cells using an MTT assay (Figure 3.10). The cytotoxicity of PLL was significantly higher in both cell lines, but PLL-*g*-mHis and PLL-*g*-PHis showed negligible cytotoxicity within the tested concentration range.

The difference between PLL and PLL grafted with histidine is mainly due to the reduced numbers of free ε-amines. Since 30 Lys residues are grafted with mHis in PLL-g-mHis, it has the lowest surface charge and the highest cell viability of the three polymers followed by PLL-g- PHis and PLL. This MTT data suggests that the hemolytic activity of PLL-*g*-PHis was induced by a pH sensitive mechanism at pH 5.5 without compromising cell viability. Thus, PLL-g-PHis becomes more protonated at lower pH, and strongly interacts with the RBCs membrane where it causes membrane disruption.

(a)

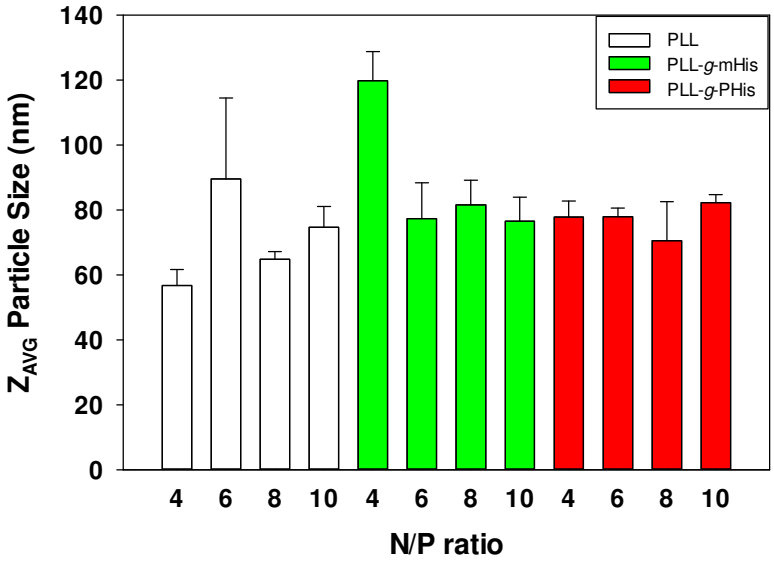

(b)

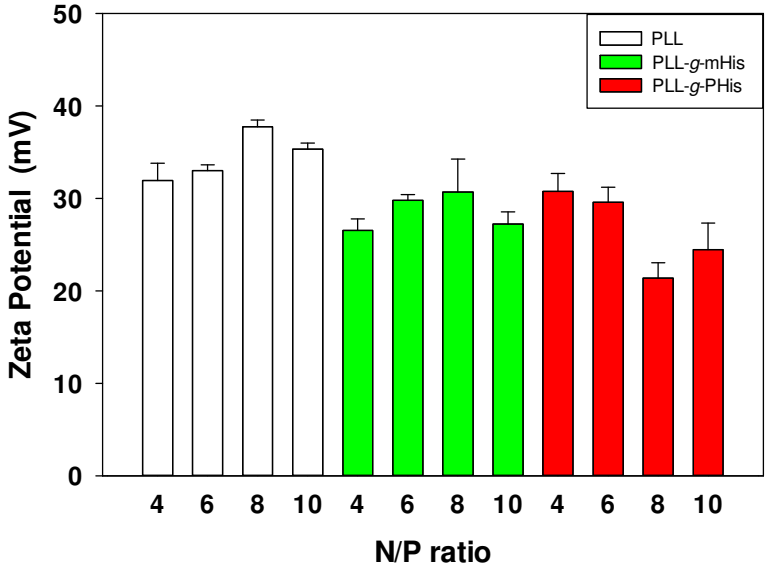

Figure 3.9. Physicochemical characterization of polyplexes. (a) Particle size and (b) zeta potential of complexes from PLL, PLL-*g*-mHis, and PLL-*g*-PHis with pDNA at different ratios (Mean ± SD; n = 10).

(a)

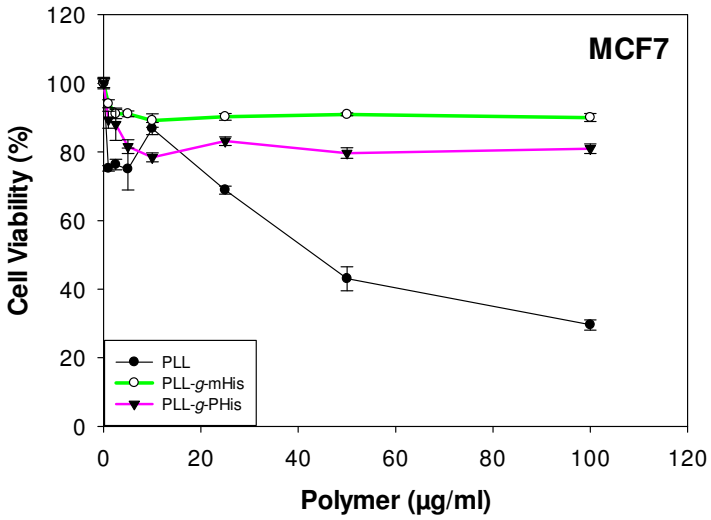

(b)

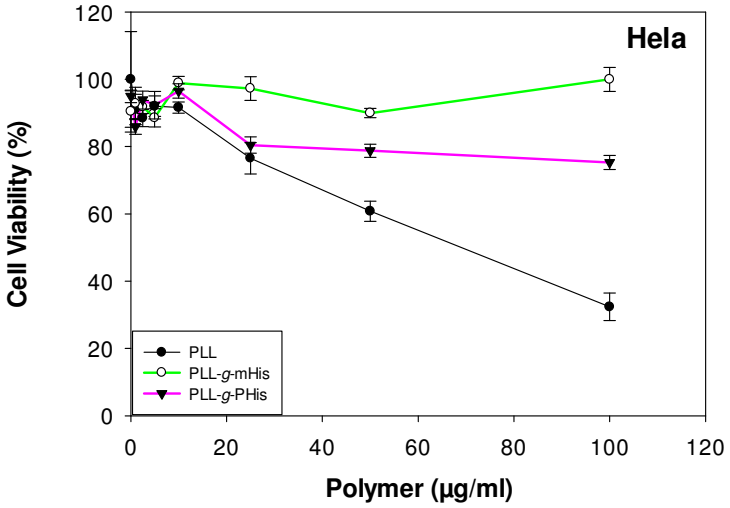

Figure 3.10. Dose-dependent cytotoxicity of polymers in (a) MCF7 and (b) Hela cells. The cells were exposed to the polymers for 24 hr in the serum-containing medium (Mean ± SD; n = 6).

3.4.7. *In vitro* Transfection Efficiency Evaluation of Polyplexes

The *in vitro* transfection efficiency of the genes carried by PLL-*g*-mHis and PLL-*g*-PHis was compared to PLL using a luciferase activity in MCF7 (Figure 3.11(a)) and Hela cells (Figure 3.11(b)). PLL-*g*-mHis/pDNA polyplexes in MCF7 cells had lower transfection efficiency than PLL up to N/P 8, but the efficiency was enhanced about 2 fold at N/P 10 with statistical significance ($p<0.01$); however, 6.5 fold higher gene expression was observed with PLL-*g*-PHis/pDNA than PLL even at N/P 4. In Hela cells, both PLL-*g*-mHis (statistically not significant) and PLL-*g*-PHis showed enhanced transfection efficiency compared to PLL. mHis modification resulted in a minor improvement in luciferase activity without statistical significance ($p=0.32$), but PHis showed up to a tenfold enhancement in transfection efficiency even at the lowest N/P ratio ($p<0.001$). Incorporation of histidine groups enhanced luciferase activity by providing buffering capacity in PLL, but the degree to which transfection efficiency improves depends on the arrangement of imidazole groups. PLL-*g*-mHis requires more polymer per quantity of gene (higher N/P ratio) than other polymers, because there are fewer ε-amines available for gene interactions due to the substitution of histidine monomers on the PLL backbone. Higher transfection efficiency compared to PLL and PLL-*g*-mHis was observed via PLL-*g*-PHis, since PHis can provide stronger endosomolytic activity during transfection as was demonstrated in the hemolysis assay (Figure 3.5). We conclude that given an equivalent number of histidine residues attached to PLL for buffering capacity, PHis grafting provided better performance in terms of endosomal disruption and transfection efficiency.

Since the final transfection efficiency levels are strongly associated with the ability

(a)

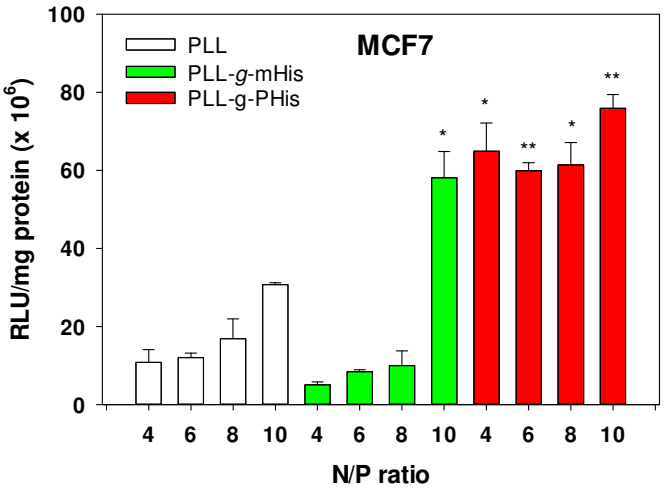

(b)

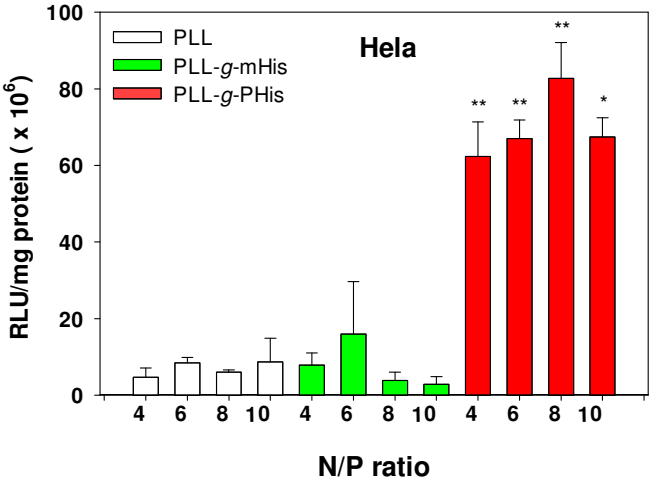

Figure 3.11. Luciferase expression of polyplexes at various N/P ratios in (a) MCF7 and (b) Hela cells. * and ** means $p<0.01$ and $p<0.001$ vs. PLL polyplexes (Mean ± SD; $n \geq 4$)

of polyplexes to escape the endosome, transfection of the polyplexes was evaluated with the treatment of chloroquine (CQ) to evaluate the ability of polyplexes to escape from the endosomes in Hela cells (Figure 3.12). CQ is a weak base endosomolytic agent that mainly accumulates in the late endosome and lysosomes, and causes a reduction of protonation. Thus, CQ acts as a proton buffer and enhances the release of genes into the cytoplasm.[49] As shown in Figure 3.12, the presence of CQ enhanced the transfection efficiency of PLL/pDNA polyplexes by bolstering the weak endosomolytic activity of PLL. PLL-*g*-mHis/pDNA transfection activity was slightly boosted by CQ, because it was able to escape the endosomes on its own but slowly. On the other hand, the preincubation of CQ did not enhance the transfection efficiency of PLL-g-PHis/pDNA. We can conclude PLL-*g*-PHis helps pDNA escapes into the cytoplasm from the early endosomes before the gene degradation in the late endosome or lysosomal phases occurs.

3.4.8. Intracellular Localization and pH Environment of the Polymers

To investigate the impact of the polymers inside the cell, confocal microscopy and flow cytometry were used to track intracellular localization and pH environment of the polymers in the cells. As shown in Figure 3.13(a), Cy3 labeled PLL-*g*-PHis and PLL-*g*-mHis yielded discernible localization results after 1.5 hr incubation. After 1.5 hr incubation PLL at a concentration of 50 μg/mL killed most of the cells due to high polymer toxicity. It was obvious that the Cy3 red from PLL-*g*-mHis was mostly located around the cell nucleus, whereas a higher portion of red fluorescence was found inside of the nucleus for PLL-*g*-PHis. Interestingly, PLL-*g*-PHis was able to translocate inside the nucleus, which is an advantage for gene delivery and gene expression. The fluorescence

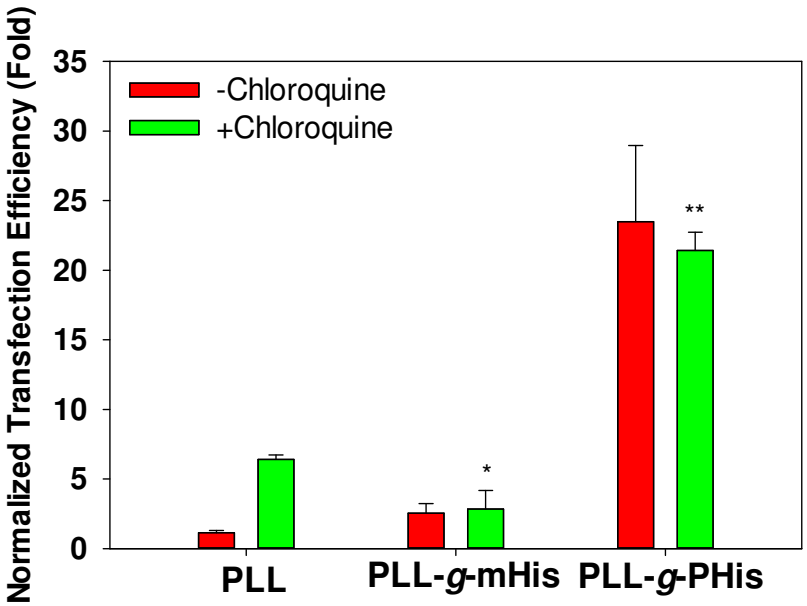

Figure 3.12. Normalized transfection efficiency of polyplexes in Hela cells (N/P 4). Transfections were performed in the absence (-) and presence (+) of Chloroquine. Result expressed as Mean ± SD; $n \geq 4$, where * $p<0.01$ and ** $p<0.001$ compared with (-) CQ.

(a)

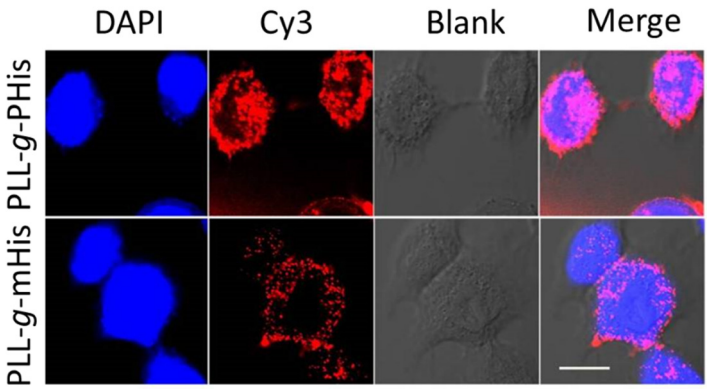

(b)

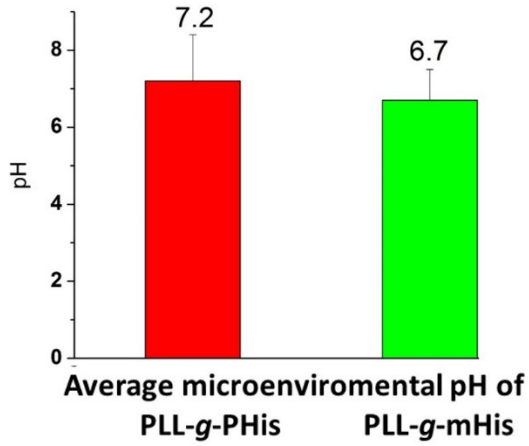

Figure 3.13. Polymers treated in Hela cells (a) confocal images of PLL-*g*-PHis and PLL-*g*-mHis at 50 μg/mL after 1.5 hr incubation. Scale bar: 20 μm. (b) Intracellular pH of PLL-*g*-PHis and PLL-*g*-mHis at 50 μg/mL after 1.5 hr incubation. Data shown are the Mean ± SD; n = 3.

intensity ratio of pH-sensitive and pH-insensitive dyes is linearly related to the pH environment of the labeled polymers. After conjugation with Cy3 (pH-insensitive) and FITC (pH-sensitive), flow cytometry data (Figure 3.13(b)) demonstrated that the average pH around PLL-*g*-mHis was pH 6.7, suggesting that most polymer molecules are trapped in the early endosomes (pH 5.5-6.5).[39] However, the average pH, where PLL-*g*-PHis located was 7.2, implying that the polymer escaped from the endosomal/lysosomal compartments and entered into the cytoplasm and nucleus (pH 7.2) after 1.5 hr incubation. In more detail, the narrow time points of PLL-*g*-PHis were monitored to track the fluorescence changes over time. As shown in Figure 3.14, after 0.5 hr and 1 hr incubation, the fluorescence was located around the cell nucleus, and after 1.5 hr incubation, most of the fluorescence translocated into the nucleus. The pH remained almost the same for the first 1 hr (pH 6.7~6.8) and slightly changed to 7.2 after 1.5 hr, which not only confirmed the endosomal escape of PLL-*g*-PHis, but also showed the exact time point when PLL-*g*-PHis escapes from the acidic compartment while PLL-*g*-mHis was still entrapped. This observation is the evidence of the powerful membrane disruption and cell permeability ability of PLL-*g*- PHis.

3.4.9. Intracellular Localization of pDNA Delivered by Polymers

To verify efficient functional transfection by the His grafted PLL, Hela cells were treated with the polyplexes carrying YOYO1-pDNA at N/P 4, and the intracellular localization of the fluorescently tagged DNA was monitored for each polymer. As shown in Figure 3.15(a), the results indicated that the YOYO1-pDNA from PLL polyplexes was localized in both the nucleus and cytoplasm, and red lysotracker staining was more

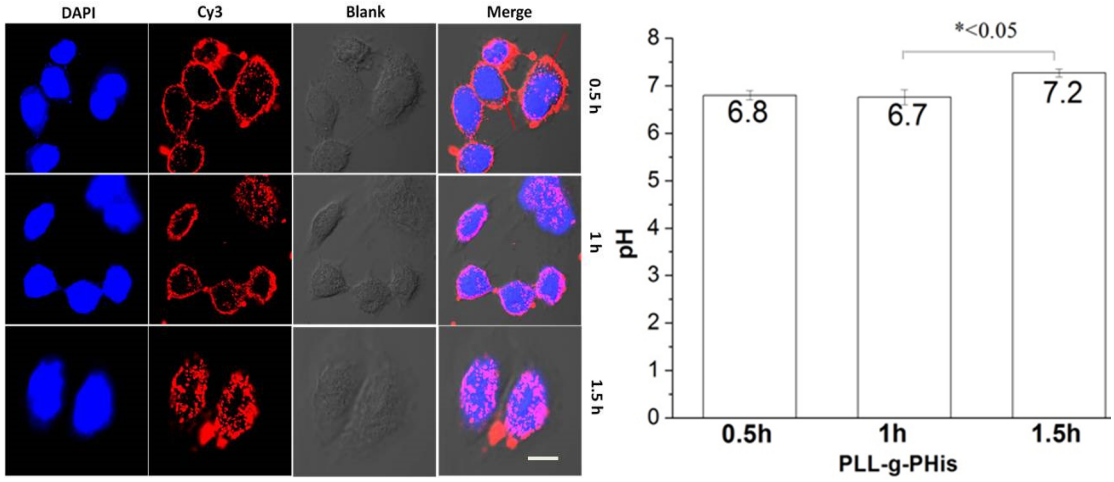

Figure 3.14. Confocal images and intracellular pHs of PLL-*g*-PHis (50 µg/mL) at different time points. Scale bar: 20 µm. (Data shown are the Mean ± SD; n = 3).

(a)

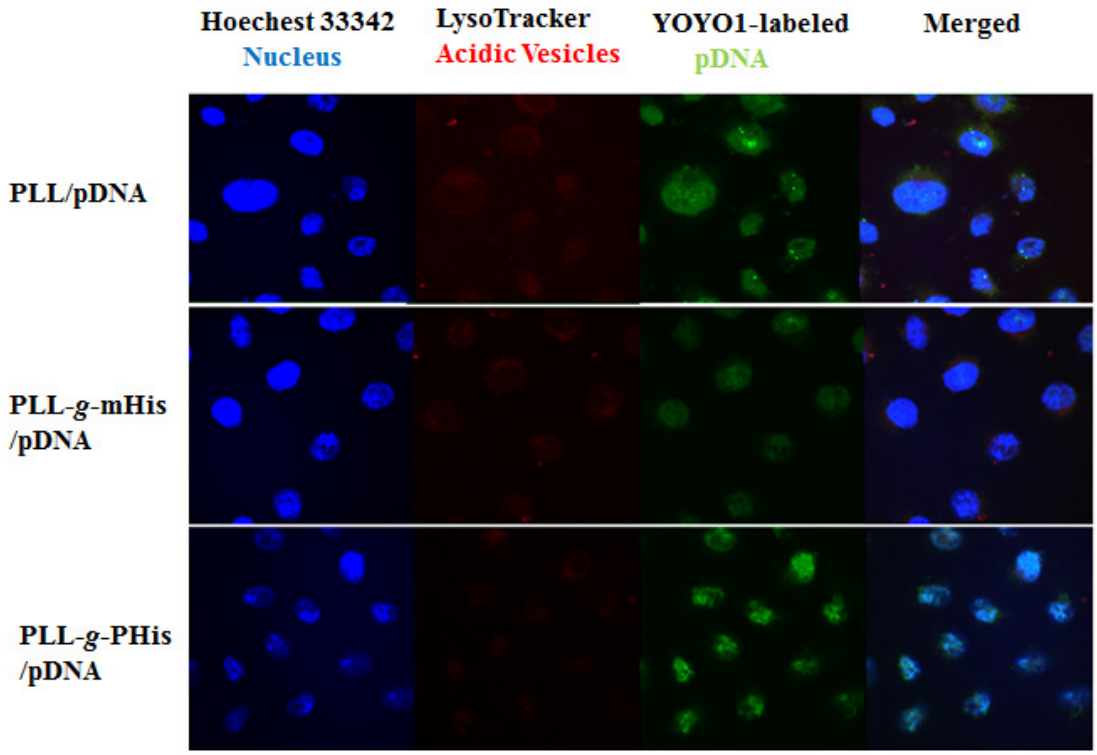

(b)

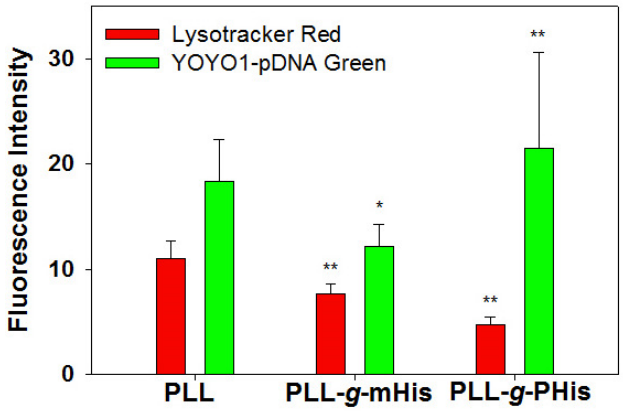

Figure 3.15. Cellular localization of polyplexes in Hela cells. (a) Confocal images of intracell distribution of YOYO1-pDNA delivered by polymers, Scale bar 10 μm. (b) Quantification of YOYO1-intercalated pDNA and red lysotracker in the inner-cytoplasm was generated from a z-stack of confocal images. Results indicate Mean ± SD; n = 7, where * $p<0.01$ and ** $p<0.001$ compared with PLL polyplexes.

intense in the cells treated with PLL/pDNA than in PLL-g-mHis/pDNA or PLL-g-PHis/pDNA. A large amount of green fluorescence was co-localized with red lysotracker, which implies that a significant fraction of PLL/pDNA complexes are trapped inside the acidic compartments. The lack of proton buffering and endosomal membrane rupturing ability prevented the release of polyplexes from the endosome, thus, the localized polyplexes in the endosomes are trafficked to the lysosomes and degraded, leading to low transfection efficiency.[50]

The intracellular intensity of YOYO1-pDNA (Figure 3.15(b)) delivered by PLL-g-mHis polyplexes was lower than other polyplexes at 4 hr post-transfection, probably because it has the lowest surface charge; however, YOYO1-pDNA was more localized in the nucleus than in the cytoplasm, and lower lysotracker intensity was observed in mHis grafted PLL than in PLL polyplexes due to the proton buffering capacity that lead to greater release of polyplexes from the endosomes.

The results support that the endosomolytic activity by mHis grafting plays a more important role than cellular uptake in transfection efficiency (Figure 3.16). The experiment with PLL-g-PHis polyplexes revealed that significant quantities of YOYO1-pDNA were translocated inside the nucleus and the polyplexes were barely detected in the acidic vesicles of the cell. The cluster of imidazole rings in PLL-g-PHis provided even higher endosomolytic activity than PLL-g-mHis which lead to stronger endosomal membrane destabilization and favored quick endosomal escape.

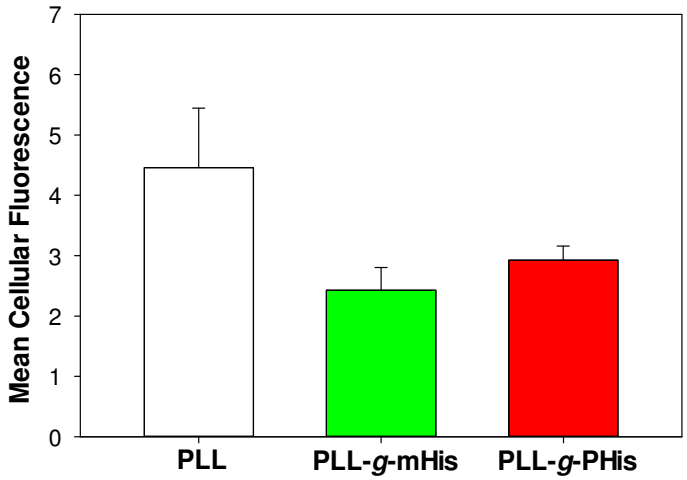

Figure 3.16. Cellular uptake of polyplexes in Hela cells. Polymers were complexed with YOYO1-intercalated pDNA at N/P 4 and mean value of the fluorescence intensity was observed after 4 hr incubation. (Data present the Mean ± SD; n = 3).

3.5. Conclusion

Both mHis and PHis grafting enhanced the buffering capacity of PLL, but despite having an equivalent number of imidazole groups, the two polymer architectures have different buffering capacity and gene transfection efficiency. More importantly, PLL-*g*-PHis containing imidazole rings in polymer form showed significantly stronger endosomolytic activity than that from PLL-*g*-mHis. This difference is due to higher local charge density at endosomal pH, which creates a stronger electrostatic stress force and interacts to a greater extent with the endosomal membrane (Figure 3.17). This dense ionic interactions result in greater local electrostatic stresses on the membrane as the endosome swells from the osmotic pressure build-up caused by the imidazole groups buffering capacity. The localized stress facilitates membrane destabilizing activity via a combination of increased osmotic potential due to the polymer buffering capacity and direct interactions with the membrane, as evidenced by improved hemolytic activity of PLL-*g*-PHis. This indicates that the ionization behavior of polymers depends on the architecture and may change the local stress intensity on the membrane and significantly contribute to endosomal disrupting activity. Thus, we conclude that the pH-sensitive polymeric endosomolytic agents (PLL-*g*-PHis) are more effective in gene transfer than monomeric and scattered counter parts (PLL-*g*-mHis), and results in enhanced transfection efficiency. In addition, grafting PHis to the PLL backbone lowered the cytotoxicity at the cost of a minimal reduction of free amines in PLL, resulting in slightly lowered gene condensation capability and a higher cellular uptake than mHis. Therefore, improved endosomal escape resulted in the highest intracellular localization in the nucleus as well as effective gene transfection.

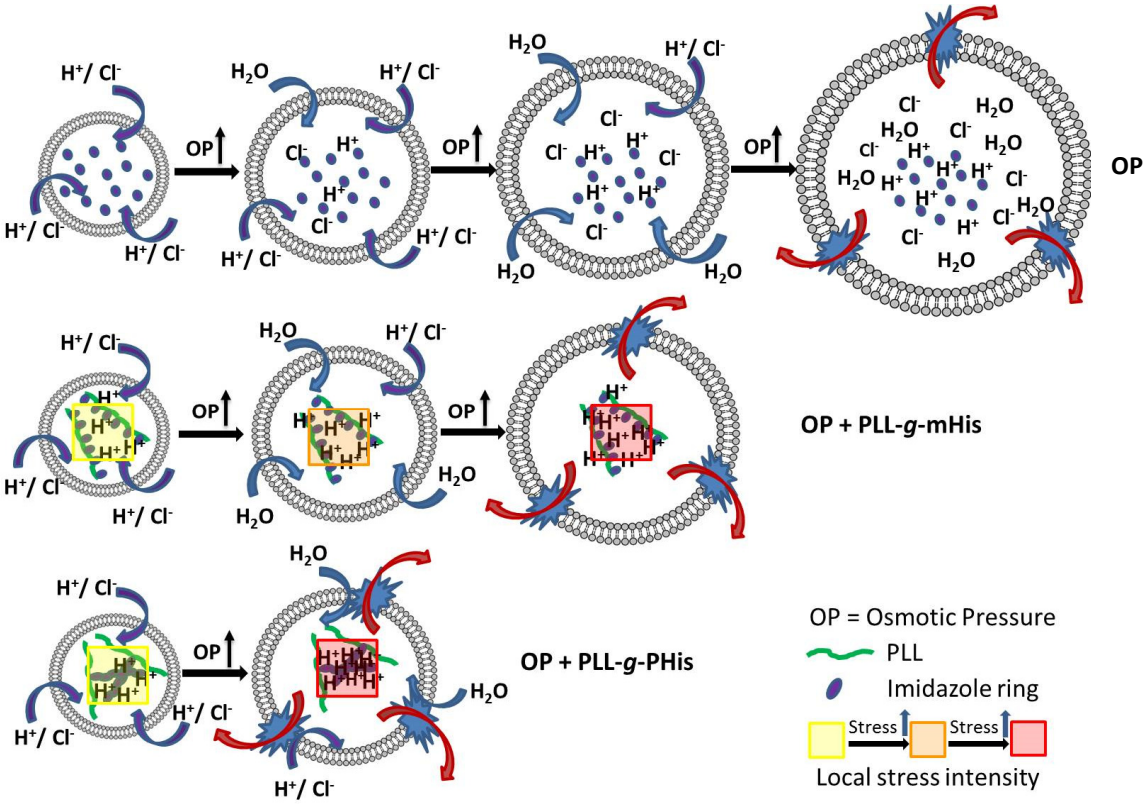

Figure 3.17. Schematic illustration of a local stress development by interactions between the PLL-*g*-mHis / PLL-*g*-PHis and the endosomal membrane.

3.6. References

1. Gruenberg J, van der Goot FG. Mechanisms of pathogen entry through the endosomal compartments. Nat. Rev. Mol. Cell Biol. 2006;7:495-504.

2. Lee Y, Miyata K, Oba M, Ishii T, Fukushima S, Han M, Koyama H, Nishiyama N, Kataoka K. Charge-conversion tternary polyplex with endosome disruption moiety: a technique for efficient and safe gene delivery. Angew. Chem. 2008;120(28):5241-5244.

3. Convertine A, Diab C, Prieve M, Paschal A, Hoffman A, Johnson P, Stayton P. pH-responsive polymeric micelle carriers for siRNA drugs. Biomacromolecules. 2010; 11(11):2904-2911.

4. Gu W, Jia Z, Truong NP, Prasadam I, Xiao Y, Monteiro MJ. Polymer nanocarrier system for endosome escape and timed release of siRNA with complete gene silencing and cell death in cancer cells. Biomacromolecules. 2013;14(10):3386-3389.

5. Rehman Zu, Hoekstra D, Zuhorn IS. Mechanism of Polyplex- and Lipoplex-mediated delivery of nucleic acids: real-time visualization of transient membrane Destabilization without Endosomal Lysis. ACS nano. 2013;7(5):3767-3777.

6. Kim TH, Ihm JE, Choi YJ, Nah JW, Cho CS. Efficient gene delivery by urocanic acid-modified chitosan. J. Controlled Release. 2003;93(3):389-402.

7. Yamagata M, Kawano T, Shiba K, Mori T, Katayama Y, Niidome T. Structural advantage of dendritic poly(L-lysine) for gene delivery into cells. Bioorg. Med. Chem. 2007;15(1):526-532.

8. Cho YW, Kim JD, Park K. Polycation gene delivery systems: Escape from endosomes to cytosol. J. Pharm. Pharmacol. 2003;55(6):721-734.

9. Putnam D, Gentry CA, Pack DW, Langer R. Polymer-based gene delivery with low cytotoxicity by a unique balance of side-chain termini. Proc. Natl. Acad. Sci. U.S.A. 2001;98(3):1200-1205.

10. Funhoff AM, van Nostrum CF, Koning GA, Schuurmans-Nieuwenbroek NM, Crommelin DJ, Hennink WE. Endosomal escape of polymeric gene delivery complexes is not always enhanced by polymers buffering at low pH. Biomacromolecules. 2004;5(1):32-39.

11. Leroueil PR, Berry SA, Duthie K, Han G, Rotello VM, McNerny DQ, Baker J R, Orr BG, Banaszak Holl MM. Wide varieties of cationic nanoparticles induce defects in supported lipid bilayers. Nano Lett. 2008;8(2):420-424.

12. Griffiths P, Paul A, Khayat Z, Wan KW, King S, Grillo I, Schweins R, Ferruti P, Franchini, J.; Duncan, R. Understanding the mechanism of action of polyamidoamines as

endosomolytic polymers: correlation of physicochemical and biological properties. Biomacromolecules. 2004;5(4):1422-1427.

13. Benjaminsen RV, Mattebjerg MA, Henriksen JR, Moghimi SM, Andresen TL. The possible "proton sponge " effect of polyethylenimine (PEI) does not include change in lysosomal pH. Mol. Ther. 2013;21(1):149-157.

14. Richard I, Thibault M, De Crescenzo G, Buschmann MD, Lavertu M. Ionization behavior of chitosan and chitosan–DNA polyplexes indicate that chitosan has a similar capability to induce a proton-sponge effect as PEI. Biomacromolecules. 2013; 14(6):1732-1740.

15. Midoux P, Monsigny M. Efficient gene transfer by histidylated polylysine/pDNA complexes. Bioconjugate Chem. 1999;10(3):406-411.

16. Pack DW, Putnam D, Langer R. Design of imidazole-containing endosomolytic biopolymers for gene delivery. Biotechnol. Bioeng. 2000;67(2):217-223.

17. Boeckle S, Fahrmeir J, Roedl W, Ogris M, Wagner E. Melittin analogs with high lytic activity at endosomal pH enhance transfection with purified targeted PEI polyplexes. J. Controlled Release. 2006;112(2):240-248.

18. Singh RS, Gonçalves C, Sandrin P, Pichon C, Midoux P, Chaudhuri A. On the gene delivery efficacies of pH-sensitive cationic lipids via endosomal protonation: a chemical biology investigation. Chem. Biol. 2004;11(5):713-723.

19. Fielden ML, Perrin C, Kremer A, Bergsma M, Stuart MC, Camilleri P, Engberts JB. Sugar-based tertiary amino gemini surfactants with a vesicle-to-micelle transition in the endosomal pH range mediate efficient transfection in vitro. Eur. J. Biochem. 2001;268(5):1269-1279.

20. Shi J, Schellinger JG, Johnson RN, Choi JL, Chou B, Anghel EL, Pun SH. Influence of histidine incorporation on buffer capacity and gene transfection efficiency of HPMA-co-oligolysine brush polymers. Biomacromolecules. 2013;14(6): 1961-1970.

21. Chang KL, Higuchi Y, Kawakami S, Yamashita F, Hashida M. Efficient gene transfection by histidine-modified chitosan through enhancement of endosomal escape. Bioconjug Chem. 2010;21(6):1087-1095.

22. Lee ES, Gao Z, Bae YH. Recent progress in tumor pH targeting nanotechnology. J. Controlled Release. 2008;132(3):164-170.

23. Lee ES, Na K, Bae YH. Super pH-sensitive multifunctional polymeric micelle. Nano Lett. 2005;5(2):325-329.

24. Lee ES, Na K, Bae YH. Doxorubicin loaded pH-sensitive polymeric micelles for

reversal of resistant MCF-7 tumor. J. Controlled Release. 2005;103(2):405-418.

25. Lee ES, Shin HJ, Na K, Bae YH. Poly (l-histidine)–PEG block copolymer micelles and pH-induced destabilization. J. Controlled Release. 2003;90(3):363-374.

26. Hu J, Miura S, Na K, Bae YH. pH-responsive and charge shielded cationic micelle of poly(l-histidine)-block-short branched PEI for acidic cancer treatment. J. Controlled Release. 2013;172(28):69-76.

27. Kim D, Lee ES, Park K, Kwon IC, Bae YH. Doxorubicin Loaded pH-sensitive micelle: antitumoral efficacy against ovarian A2780/DOXR Tumor. Pharm. Res. 2008; 25(9):2074-2082.

28. Oh KT, Yin H, Lee ES, Bae YH. Polymeric nanovehicles for anticancer drugs with triggering release mechanisms. J. Mater. Chem. 2007;17:3987-4001.

29. Lv H, Zhang S, Wang B, Cui S, Yan J. Toxicity of cationic lipids and cationic polymers in gene delivery. J. Controlled Release. 2006;114(1):100-109.

30. Hwang HS, Kang HC, Bae YH. Bioreducible polymers as a determining factor for polyplex decomplexation rate and transfection. Biomacromolecules. 2013;14(2):548-556.

31. Wiethoff CM, Middaugh CR. Barriers to nonviral gene delivery. J. Pharm. Sci. 2003;92(2):203-217.

32. Kang HC, Huh KM, Bae YH. Polymeric nucleic acid carriers: current issues and novel design approaches. J. Controlled Release. 2012;164(3):256-264.

33. Kang HC, Kang HJ, Bae YH. A reducible polycationic gene vector derived from thiolated low molecular weight branched polyethyleneimine linked by 2-iminothiolane. Biomaterials. 2011;32(4):1193-1203.

34. Lackey CA, Murthy N, Press OW, Tirrell DA, Hoffman AS, Stayton PS. Hemolytic activity of pH-responsive polymer-streptavidin bioconjugates. Bioconjugate Chem.1999;10(3):401-405.

35. Kang HC, Samsonova O, Bae YH. Trafficking microenvironmental pHs of polycationic gene vectors in drug-sensitive and multidrug-resistant MCF7 breast cancer cells. Biomaterials. 2010;31(11):3071-3078.

36. Fichter KM, Ingle NP, McLendon PM, Reineke TM. Polymeric nucleic acid vehicles exploit active interorganelle trafficking mechanisms. ACS nano. 2012;7(1): 347-364.

37. Sachs DH, Schechter AN, Cohen JS. Nuclear magnetic resonance titration curves of histidine ring protons. I. Influence of neighboring charged groups. J. Biol.

Chem. 1971;246(91):6576-6580.

38. Song Xj, McDermott AE. Proton transfer dynamics and N—H bond lengthening in N—H···N model systems: a solid-state NMR study. Magn. Reson. Chem. 2001;39(S1):S37-S43.

39. Kang HC, Lee M, Bae YH. Polymeric gene carriers. Crit. Rev. Eukaryotic Gene Expression. 2005;15(4):317-342.

40. Ferruti P, Manzoni S, Richardson SC, Duncan R, Pattrick NG, Mendichi R, Casolaro M. Amphoteric linear poly (amido-amine) s as endosomolytic polymers: correlation between physicochemical and biological properties. Macromolecules. 2000;33(21):7793-7800.

41. Chen R, Khormaee S, Eccleston ME, Slater NK. The role of hydrophobic amino acid grafts in the enhancement of membrane-disruptive activity of pH-responsive pseudo-peptides. Biomaterials. 2009;30(10):1954-1961.

42. Sovadinova I, Palermo EF, Huang R, Thoma LM, Kuroda K. Mechanism of polymer-induced hemolysis: nanosized pore formation and osmotic lysis. Biomacromolecules. 2010;12(1):260-268.

43. Jean-François F, Elezgaray J, Berson P, Vacher P, Dufourc EJ. Pore formation induced by an antimicrobial peptide: electrostatic effects. Biophys. J. 2008;95(12): 5748-5756.

44. Choudhury CK, Kumar A, Roy S. Characterization of conformation and interaction of gene delivery vector polyethylenimine with phospholipid bilayer at different protonation state. Biomacromolecules. 2013;14(10):3759-3768.

45. Bulmus V, Woodward M, Lin L, Murthy N, Stayton P, Hoffman A. A new pH-responsive and glutathione-reactive, endosomal membrane-disruptive polymeric carrier for intracellular delivery of biomolecular drugs. J. Controlled Release. 2003;93(2):105-120.

46. Boylan NJ, Kim AJ, Suk JS, Adstamongkonkul P, Simons BW, Lai SK, Cooper MJ, Hanes J. Enhancement of airway gene transfer by DNA nanoparticles using a pH-responsive block copolymer of polyethylene glycol and poly-l-lysine. Biomaterials. 2012; 33(7):2361-2371.

47. Zhou D, Li C, Hu Y, Zhou H, Chen J, Zhang Z, Guo T. PLL/pDNA/P(His-co-DMAEL) ternary complexes: assembly, stability and gene delivery. J. Mater. Chem. 2012;22:10743-10751.

48. Parelkar SS, Chan-Seng D, Emrick T. Reconfiguring polylysine architectures for controlling polyplex binding and non-viral transfection. Biomaterials. 2011;32(9): 2432-2444.

49. Akinc A, Thomas M, Klibanov AM, Langer R. Exploring polyethylenimine-mediated DNA transfection and the proton sponge hypothesis. J Gene Med. 2005;7(5):657-663.

50. Kang HC, Bae YH. pH-Tunable endosomolytic oligomers for enhanced nucleic acid delivery. Adv. Funct. Mater. 2007;17(8):1263-1272.

CHAPTER 4

RESULTS, CONCLUSIONS, AND FUTURE PROSPECTS

4.1. Results and Conclusions

Inefficient endosomal escaping and disassembly of polyplexes in the cytoplasm are the major intracellular barriers that hinder efficient gene transfer and expression.[1] The main focus of utilizing stimuli-sensitive polymers was to facilitate efficient gene delivery and achieve gene expression enhancement by taking advantages of biological environments inside the cells. The difference in pH and redox potential changes the complex status and controls the formation or dissociation of complexes by the stimuli-responsive system.[2] Therefore, gene will be released from polyplexes in a stimuli-responsive manner. Two different approaches of the stimuli-responsive system were applied to overcome intracellular barriers by designing polymers that response to specific stimuli. Thus, a disulfide-linked reducible polymer, and a pH-sensitive endosomolytic polymer were constructed. The first study investigated the effect of the decomplexation rate of pDNA on transfection efficiency using reducible PLL (RPLL) as a decomplexation controller. In this study, PLL and RPLL were mixed to balance the protection and release of genes from the carriers. As expected, RPLL showed negligible cytotoxicity in several cell lines compared with nondegradable PLL. Moreover, the

presence of RPLL in PLL100-x RPLLx/pDNA complexes (PRLx polyplexes) showed different release kinetics in reducing mimicking environments. As RPLL contents increase in PRL_x polymers, the release rate of gene was getting faster and more genes were released even in low concentration of heparin. We were able to observe the decomplexation rate varied by RPLL contents, and controlled release of gene from PRLx polyplexes was changed upon different amount of RPLL contents.

The transfection efficiency data showed that the maximum levels of luciferase expression obtained peak value at x=2.5 in MCF7 and x=10 in HEK 293 cells, respectively. Interestingly, neither PLL nor RPLL 100% resulted highest transfection efficiency. PLL 100% may induce strong interaction with pDNA and result slow release, whereas RPLL 100% may cause too fast release of gene before it reaches inside the nucleus. The highest transfection efficiency that was obtained at different RPLL contents in PRL_x polyplexes depends on the cell lines which explains that optimal decomplexation rate is different based on intracellular glutathione levels in each cell lines. From the GSH-Glo glutathione assay, intracellular glutathione levels in MCF7 tumor cells were 10 times higher than noncancerous HEK 293 cells. Thus, lower RPLL contents in MCF7 cells were able to induce the maximum transfection efficiency because low RPLL contents are enough to induce fast decomplexation of polyplexes.

From the intracellular localization observation, we were able to demonstrate that optimum decomplexation rate not only result high transfection efficiency but also induce high nuclear localization of pDNA in MCF7 cells. When an equal amount of Cy5-labeled pDNA was transfected via different contents of RPLL, $PRL_{2.5}$ and PRL_5 displayed the highest pDNA in the nucleus, whereas other PRL_x polyplexes were mostly localized in

the cytoplasm. Thus, the different distribution of pDNA localization in the nucleus resulted in different levels of transfection efficiency. This study showed that controlling the decomplexation rate of gene release from the carriers is an important event that determines the fate of gene, and it should happen at a right intracellular place and the right time. These observations may provide a better way to design stimuli-sensitive gene carriers targeting cancer which can balance the complexation and dissociation of polyplexes to efficiently deliver and express more gene upon redox sensitive mechanism in tumor cell lines.

The second study was focused on synthesis and evaluation of a pH-sensitive polymeric gene carrier which has a pH-dependent endosomolytic activity. Imidazole groups in histidine were introduced in PLL to favor endosomal escape via imidazole protonation in acidic endosomal environments. Two different types of histidylated PLLs were designed with equal number of imidazole rings, PLL-*g*- poly($_{L}$-histidine) (PLL-*g*-PHis) and PLL-*g*-mono-$_{L}$-histidine (PLL-*g*-mHis), to compare the differences in terms of endosomolytic activity, hemolytic activity, and transfection efficiency. Both PLL-*g*-PHis and PLL-*g*-mHis showed an enhanced buffering capacity compared with unmodified PLL, which explains the introduction of pH-sensitive ionizable groups that are protonated and endow the proton sponge effect within the endosomal pHs. Although both polymers have the same number of imidazole groups, the protonation behavior was different. Titration data showed that the imidazole rings' arrangement in PHis and mHis may change the pK_a values and ionization degree because of the different distance between imidazole groups. Thus, a shorter distance in PHis induces more rapid proton transfer through a hydrogen bridge and more protonated than that with mHis.

In the endosomal pH range, the hemolytic activity of both PLL-*g*-PHis and PLL-*g*-mHis was more advanced than PLL. Although PLL showed no differences in a hemolytic activity at pH 7.4 and pH 5.5, PLL-*g*-mHis displayed 18% and 42% at pH 7.4 and pH 5.5, respectively. In the case of PLL-*g*-PHis, the hemolytic activity significantly changed from 27% at pH 7.4 to 75% at pH 5.5. Hemolytic activity is produced by local electrostatic stress forces induced between polymer and the cell membrane. Thus, the density of protonated polymers per the membrane surface area decides the external stress forces to destabilize and disrupt the membrane. This hemolytic data demonstrated that PLL-*g*-PHis produced the strongest local stress due to the high charge density that induced at lower pH resulted stronger interactions between the membrane and protonated polymers. On the other hand, the dispersed imidazole rings in PLL-*g*-mHis are relatively less protonated at low pH which leads to weaker interactions with the membrane and induces weaker local stress forces. Thus, a local stress on the cell membrane induced by polymers can be a strong indicator of endosomal membrane disruption and endosomal escaping ability.

Histidylated PLLs also demonstrated enhancement of transfection efficiency which showed higher levels of luciferase activity than nonmodified PLL in two different cell lines. In MCF7 cells, PLL-*g*-mHis resulted ~2 times higher transfection efficiency at N/P 10 and PLL-*g*-PHis induced ~7 times higher gene expression even at N/P 4. In Hela cells, PLL-*g*-mHis resulted in a minor transfection efficiency enhancement, whereas PLL-*g*-PHis showed 10 times enhanced gene expression even at the lowest N/P ratio. Since mHis grafting used more Ɛ-amines than PHis, there will be fewer amines available for gene interactions; thus, higher N/P ratios of PLL-*g*-mHis will be required to further

enhance transfection efficiency. PLL-*g*-PHis showed a statistically significant enhancement of gene expression in both cell lines. This observation can be explained by previous experiments that PHis grafting induced a higher proton buffering and stronger endosomolytic activity which leads to enhanced gene expression.

The intracellular localization data showed that PLL resulted in pDNA localized in both the nucleus and the cytoplasm; the fluorescence from the lysotracker which stains inside the acidic compartments was the highest due to the absence of endosomal escaping ability. PLL-*g*-mHis resulted relatively less YOYO1-pDNA intensity inside the cell than that of PLL; however, more pDNA was localized in the nucleus and the lysotracker intensity was lower because of better endosomolytic activity that facilitate release of polyplexes from the endosomes. PLL-*g*-PHis induced the highest intracellular distribution of YOYO-1 labeled pDNA in the nucleus, whereas lysotracker was observed the lowest. The different data between PLL-*g*-mHis and PLL-*g*-PHis demonstrated that the arrangement of histidine in PHis provided a higher endosomolytic activity and rapid endosomal escaping of polyplexes which results in more genes available in the nucleus.

Therefore, PLL-*g*-PHis is a pH-sensitive endosomolytic polymer that changes its protonation and deprotonation state in a pH-dependent manner to avoid nonspecific membrane disruption. PHis conjugations compensate a less Ɛ-amines in PLL than mHis which result relatively stronger electrostatic interactions with pDNA and provides a stronger proton buffering and endosomolytic activity to promote rapid endosomal release.

4.2. Future Prospects

4.2.1. Potential Candidate Genes

Based on the previous observations, polymers that are sensitive to stimulus provided benefits in terms of efficient gene delivery and enhanced transfection efficiency. Therefore, it is necessary to investigate these stimuli-responsive polymer applications *in vivo* using therapeutic genes. There are several candidate genes that have been used in cancer gene therapy which belongs to tumor suppressor genes, stability genes, and oncogenes. Among these therapeutic genes, potential candidate genes are retinoblastoma (RB) gene and phosphatase and tensin homolog deleted on chromosome ten (PTEN) gene, which belong to tumor suppressor genes.

RB gene is known to be a potent negative regulator of cell cycle progression.[3] It plays an important role in controlling cell proliferation and inhibits the pro-apoptotic activity via blocking entry into the cell cycle.[4] It has been reported that the RB gene is disrupted in 25% of the breast tumor cell lines and loss of RB function is related to cell motility enhancement and invasion of breast cancer.[5] In addition, above 90% of small cell lung carcinoma cases are involved with RB inactivation, and loss of RB function is also associated with prostate cancer and liver cancer ~20% and 15~30%, respectively.[5]

RB directly binds to E2F transcription factor and block E2F transcription activity which results in inhibition of S-phase entry and cell cycle arrest.[3] When RB is phosphorylated by cyclin D/E, it allows RB/E2F complex to undergo a conformation change followed by E2F dissociation from Rb that makes E2F become active for transcription.[5] However, RB function is disrupted in tumor cells in a several ways. It has been reported that RB/E2F interaction is disturbed by papilloma virus E7, which is a

tumor virus oncoprotein that displace E2F and results in RB loss of function.[3] In addition, overexpression of cyclin D causes RB phosphorylation in an inappropriate way, thus deregulating E2F transcription function.[3] Therefore, maximized RB gene expression will interfere with cell cycle progression and contribute to proliferation rate and tumor aggressiveness.

PTEN is involved in various cellular progresses like cell proliferation, cell cycle progression, cell polarity apoptosis, DNA damage response, and angiogenesis.[6] It has been also known as a tumor suppressor, because PTEN is the one of the most commonly mutated or deleted tumor suppressors in human cancer.[6] Lack of PTEN has been reported in many cancers that include 66% of glioblastoma, 27% ovarian cancer, 20% prostate cancer, 41% colorectal cancer with microsatellite instability, and 17% colorectal cancer without microsatellite instability that are involved with reduced PTEN expression.[7]

The important role of PTEN signaling in cancer is that it plays as a major negative regulator in the phosphatidylinositol 3 kinase (PI3K) pathway which is involved in a tumor development.[6-8] When PTEN expression is reduced or inactivated by several causes such as reduced mRNA or altered chromatin located at the PTEN promoter, it results in inactivation of PTEN and stimulates the PI3K pathway.[7] Thus, the PI3K pathway drives many cancer-promoting events such as cell survival, and cell proliferation. The PTEN network also involves with other signaling pathways such as Ras, and p53; thus, they regulate each other in a direct or indirect way.[6,8] Therefore, therapeutic PTEN expression will regulate PI3K pathway signaling and other signaling pathways to suppress tumor cell growth, tumor cell invasion, and metastasis.

4.2.2. Potential Gene Carriers for *In Vivo*

The bioreducible polymer and the pH-sensitive endosomolytic polymer showed efficient gene delivery and enhanced transfection efficiency in *in vitro* studies. Disulfide bonds in the reducible polymer provided degradability, low toxicity, and controlled gene release. Imidazole groups in PHis generated endosomal buffering capacity and induced membrane disruption at endosomal pH due to pH sensitivity. Therefore, the potential gene carrier for *in vivo* applications will be designed by employing a combination approach from both strategies.

The first approach will be designing a polymer composed of PLL-g-PHis and RPLL to make PLL-g-PHis100-xRPLLx. It is similar to a prior approach, but PLL-g-PHis is mixed with RPLL instead of PLL since PLL has absence of proton buffering within endosomal pH range and lack of endosomal escape ability.

As shown in Figure 4.1, a disulfide-linked PHis in PLL (PHis-s-s-PLL) will be synthesized as an alternative strategy. In order to synthesize PHis-s-s-PLL, a synthesis will be conducted by the following method. First, PHis block will be prepared by a ring-opening polymerization using an initiator N-Boc-1, 4 butanediamine, which is an amine-containing small molecule.[9] The molecular weight will be controlled by the feed ratio of Boc group to imidazole ring, and the degree of polymerization will be calculated using ^{1}H NMR. Then 2-mercaptoethanol will be added to deprotect the amine end group, and it will react with 3-(2-pyridyldithio) propionic acid N-hydroxysuccinimide ester (SPDP) to produce a disulfide linkage. To synthesize PLL-SH, PLL will be reacted with 3-(acetylthio) propionic acid N-succinimidyl ester (SATP), then finally PHis-SH and PLL-SH will be mixed in DMSO for oxidative polymerization.

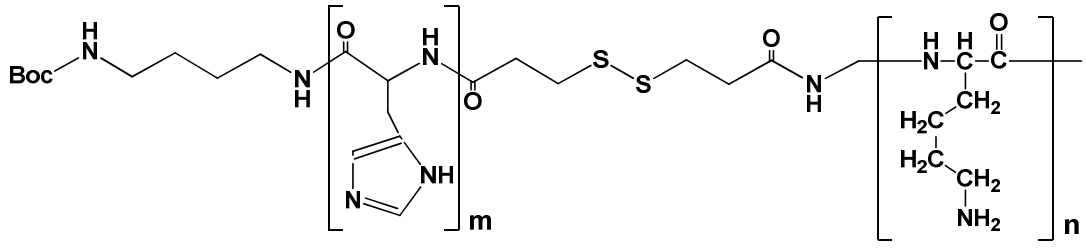

Fig. 4.1. The chemical structure of PHis-s-s-PLL

The PHis block will induce rapid release of polyplexes from the endosomal compartments, and the formation of disulfide bonds will facilitate pDNA release when polymer is exposed to reducing cytosolic environments. Therefore, this carrier system will maximize the level of transfection efficiency with minimal toxicity.

However, positively charged polyplexes may induce undesirable aggregation and toxicity which results in a reduced transfection efficiency. Thus, two approaches will be considered to overcome this drawback in *in vivo* applications. First, PEG incorporation can be applied to shield the positively charge surface of polyplexes. The potential benefits of PEGylation *in vivo* studies have been widely investigated and reported. PEG-modified nanoparticles have been shown to provide many benefits in gene delivery system that can reduce rapid renal clearance, escape reticulo-endothelial system (RES), provide prolonged circulating half-life in blood, and avoid immune cell recognition.[10] In addition, it further enhances tumor accumulation and inhibits nonspecific interactions.[10] Therefore, PEGylated polyplexes will not only solve cationic surface problem, but also show improved stability in the blood and induce higher *in vivo* distribution in tumor.

Recently, Bae's group reported the new approach of charge shielding and deshielding techniques using mPEG (2 kDa)-*block*-polysulfadimethoxine (4 kDa) (mPEG-b-PSDM) in a mouse xenograft model.[9] The electrostatic complexation between positively charged micelle and negatively charged mPEG-b-PSDM was used to shield a cationic surface charge. mPEG-b-PSDM displays a unique shielding and deshielding technique, since PSDM has a pH-sensitive property that is negatively charged at pH7.4, but becomes neutral at acidic pH. Thus, the reduction of pH results a dissociation of mPEG-b-PSDM from the cationic micelle. The system has been shown to be effective in

in vivo experiments. The shielding/deshielding technique showed successful anticancer therapeutic efficacy due to the rapid response in acidic tumor pH.[9] Therefore, several feeding ratios of mPEG-b-PSDM to cationic polyplexes will be tested to optimize the particle surface charge and gene expression should be monitored in a tumor bearing mouse model.

4.2.3. Sustained Gene Expression

Although many polymeric gene carriers have been synthesized to overcome intracellular barriers, the major limitation that hampers the successful nonviral gene therapy in clinical study is raised from a lack of sustained gene expression.[11] There are several reasons that cause a short-term gene expression. First, there is loss of the transfected cells during replication of the target population. Transgenes that are delivered inside the nucleus do not have an ability to replicate; thus, it will be diluted as the cancer cells continue to rapidly divide. Second, transgene can be lost by nuclease destruction, although genes are safely transfected inside the cells. Third, transgene can be functionally inactivated by partitioning to non-nuclear compartments which means genes delivered to non-nuclear compartments result in transcription inactivation. And last, inflammatory response can be induced by a bacterially derived pDNA transfection and cause reduction of gene expression.[12,13] Thus, to enhance the efficiency of gene therapy, we have to pay attention to not only to overcome delivery issues and but also to find the right gene expression cassette for therapeutic genes.

The level and duration of gene expression is important to obtain therapeutic levels, because short-term gene expression will cause failure for long-term clinical study due to

the limitation of reaching therapeutic protein levels for a certain time period. In addition, cancer gene therapies are not for one-time treatable diseases and generally require sustained expression of therapeutic gene until the treatments diminish the tumor and treat cancer.[14]

One strategy that will be considered in future work is designing a CpG free plasmid vector. CpGs are cytosine-guanine dinucleotides, and 'p' in CpG refers to the phosphodiester bond between the cytosine and the guanine. These CpG-rich regions occur in approximately 70% of the promoters of genes.[15] Plasmid vectors that are used in nonviral gene therapy are generally propagated in bacteria that contain unmethylated CpG dinucleotides within the pDNA, and the frequency of the CpGs in mammalian DNA is suppressed in four fold compared to bacterial DNA.[16] Due to the existence of differences, immunostimulatory unmethylated CpG sequences in pDNA regions are known to cause transient gene expression.

CpG motifs are reported as an immune-stimulating agent that have been used as an immune therapy. These motifs activate not only innate immunity by NK cells and macrophage activation, but also adaptive immune response by B and T cell activation. CpG motifs act as a 'pathogen-associated' molecular pattern (PAMPs) and are recognized by Toll-like receptor (TLR) 9 of dendritic cells (DCs).[17]

Initially, TLR9 is localized at the ER, but it migrates to the endosome upon the access of CpG-DNA to the endosomal compartment. Interactions between unmethylated CpG motifs within bacterial DNA and the cytosolic Toll/interleukin-1 receptor homology (TIR) domain of TLR9 induces dimerization and recruits the MyD 88 adaptor protein, which, upon T cell activation, leads to the activation of nuclear factor kB (NF-kB) and

activator protein 1 (AP-1).[18] Thus, high productions of proinflammatory cytokines towards CpG-DNA lead to transfected cells undergoing apoptosis and clearing the cells due to an inflammation response.[19,20] As a result, sequences in the bacterial backbone induce short duration of expression when it is transfected in mammalian cells.

In addition, hypermethylation of CpG islands is related to loss of target gene transcription. More specifically, within the promoter region, CpG motif is hypermethylated due to DNA methyltransferases (DNMTs) that add methyl groups to CpGs. Once promoter regions of genes are highly methylated, they will block transcriptional factors to bind and initiate transcription. Thus, CpG motifs within the bacterial DNA should be avoided before transfection, and elimination of CpG motifs will lead to low levels of inflammatory cytokines production and prolonged gene expression.

To obtain long-term therapeutic gene expression, therapeutic genes will be excised using restriction enzyme sites and inserted into CpG free-luciferase vectors. We will use a CpG free pDNA with a human EF1 α promoter which is widely expressed in mammalian cells to obtain more powerful DNA expression with reduced immune response.[21] The subcloned plasmid will be confirmed by gel electrophoresis and transformed into bacteria strain Escherichia coli DH5α. Then, each colony will be sequenced to obtain plasmids with the right direction. Although we use CpG free plasmid vectors, there will be CpG motifs within the therapeutic gene. Thus, after subcloning the therapeutic gene into pCpG free, cytosine residues in pDNA should be methylated to avoid TLR9 recognition. pCpG free-therapeutic gene will be treated with SssI methylase to methylate cytosine residues of CpG dinucleotides. Therefore, effective therapeutic gene expression will be obtained by replacing genes with the rational gene vector, and

will lead to clinically effective, long duration of expression.

4.3. References

1. Shim MS and Kwon YJ. Stimuli-responsive polymers and nanomaterials for gene delivery and imaging applications. Adv. Drug Deliv. Rev. 2012;64(11):1046-1059.

2. Yokoyama M. Gene delivery using temperature-responsive polymeric carriers. Drug Discov Today. 2002;7(7):426-432.

3. Giacinti C and Giordano A. RB and cell cycle progression. Oncogene. 2006;25(38):5220-5227.

4. Issa JPJ and Kantarjian HM. Targeting DNA methylation. Clin. Cancer Res. 2009;15(12):3938-3946.

5. Burke JR, Deshong AJ, et al. Phosphorylation-induced conformational changes in the retinoblastoma protein inhibit E2F transactivation domain binding. J. Biol. Chem. 2010;285(21):16286-16293.

6. Keniry M and Parsons R. The role of PTEN signaling perturbations in cancer and in targeted therapy. Oncogene. 2008;27(41): 5477-5485.

7. Parsons R. Human cancer, PTEN and the PI-3 kinase pathway. Semin. Cell Dev. Biol. 2014;15(2):171-176.

8. Cully M, You H, et al. Beyond PTEN mutations: the PI3K pathway as an integrator of multiple inputs during tumorigenesis. Nat. Rev. Cancer. 2006;6(3):184-192.

9. Hu J, Miura S, et al. pH-responsive and charge shielded cationic micelle of poly(l-histidine)-block-short branched PEI for acidic cancer treatment. J. Control. Release. 2013;172(1):69-76.

10. Molineux G. Pegylation: engineering improved pharmaceuticals for enhanced therapy. Cancer Treat. Rev. 2002;28(1):13-16.

11. Luten J, van Nostrum CF, et al. Biodegradable polymers as non-viral carriers for plasmid DNA delivery. J. Control. Release. 2008;126(2):97-110.

12. Cooper MJ, Lippa M, et al. Safety-modified episomal vectors for human gene therapy. Proc. Natl. Acad. Sci. U.S.A. 1997;94(12):6450-6455.

13. Yew NS, Zhao H, et al. CpG-depleted plasmid DNA vectors with enhanced safety and long-term gene expression in vivo. Mol. Ther. 2002;5(6):731-738.

14. De Wolf HK, Johansson N, et al. Plasmid CpG depletion improves degree and duration of tumor gene expression after intravenous administration of polyplexes. Pharm. Res. 2008;25(7):1654-1662.

15. Luczak MW and Jagodziński PP. The role of DNA methylation in cancer development. Folia Histochem Cytobiol. 2006;44(3):143-142.

16. Wagner H. Interactions between bacterial CpG-DNA and TLR9 bridge innate and adaptive immunity. Curr. Opin. Microbiol. 2002;5(1):62-69.

17. Takeshita F, Gursel I, et al. Signal transduction pathways mediated by the interaction of CpG DNA with Toll-like receptor 9. Sem Immunol. 2004;16(1):17-22.

18. Kumagai Y, Takeuchi O, et al. TLR9 as a key receptor for the recognition of DNA. Adv. Drug Deliv. Rev. 2008;60(7):795-804.

19. Krieg AM. The role of CpG motifs in innate immunity. Curr Opin Immunol. 2002;12(1):35-43.

20. Scheule RK. The role of CpG motifs in immunostimulation and gene therapy. Adv. Drug Deliv. Rev. 2000;44(2):119-134.

21. Gill D, Pringle I, et al. Progress and prospects: the design and production of plasmid vectors. Gene Ther. 2009;16(2):165-171.

APPENDIX

POLYSACHARRIDE-TAUROCHOLIC ACID CONJUGATES FOR DOXORUBICIN ORAL DELIVERY

A.1. Abstract

Doxorubicin (DOX) oral delivery has been challenged due to the poor intestinal permeability which results in low oral bioavailability. To enhance the Dox permeability, our strategy is to conjugate taurocholic acid (TCA) to the anionic polysaccharides and design Dox formulation for oral delivery. TCA-linked heparin (H-TCA) and TCA-linked chondroitin sulfate (CS-TCA) were constructed to enhance DOX absorption rate mainly targeting terminal ileum. Two DOX formulations, DOX/CS-TCA (1:2) and DDP/H-TCA (1:1:0.8:2.4) (w/w ratio), were prepared. DOX/CS-TCA and DDP/H-TCA showed a particle size of 205 nm and 230 nm, respectively, and were able to reconstitute in DI water after freeze-drying. DOX was encapsulated at high loading efficiency and content. Moreover, negatively charged DOX-loaded TCA nanoparticles (DOX-TCA-NPs) significantly reduced the cytotoxicity compared with free Dox. The *in vitro* DOX release study was investigated at pH 5 and 7.4. The release profile of DOX/CS-TCA showed that there was a faster release DOX than that of multiple coated DDP/H-TCA. We studied *in vivo* anticancer efficacy of the free DOX and DOX-TCA-NPs in HepG2 xenograft mouse

model. Free DOX delivered via both oral and IV administrations were used as a control group, and DOX-TCA-NPs were administered orally every 3 days at a dose of 4 mg Dox/kg. We observed a significant suppression of tumor growths without a marked reduction of body weight in TCA groups. In addition, the biodistribution study demonstrated that TCA groups showed more absorption of DOX from the ileum. The animal data confirmed TCA coating not only diminished DOX toxicity but also enhanced absorption in intestine, especially the ileum section. Therefore, these findings strongly provided that enterohepatic circulation of TCA elevated DOX systemic exposure and improved DOX plasma levels which lead to oral bioavailability enhancement and tumor growth reduction. This indicates promising DOX targeting delivery to cancer cells.

A.2. Introduction

Ideal oral formulation of anticancer drugs is determined by solubility, stability, dissolution rate, and permeability in the gastrointestinal (GI) tract that affects oral bioavailability.[1] Thus, the oral dosage form of these drugs should have a rapid dissolution rate and absorption rate that can lower half-life and metabolism in the GI tract to maximize oral bioavailability. However, oral delivery of anticancer drugs still has challenges that limit the use of drugs for cancer treatments. One of the major drawbacks that hamper the drug efficacy are barriers in the epithelial lining of gut walls.[2]

DOX is one of the anticancer drugs that have been widely used for lymphomas, sarcomas, breast, ovarian, and lung cancer.[3] DOX damages DNA by intercalating into the bases of DNA which inhibits topoisomerase II enzyme activity and interferes in DNA transcription.[4] DOX belongs to BCS classification III which has favorable solubility but

poor permeability which is responsible for the low oral bioavailability (about 5%) of DOX.[1, 5, 6] However, the major limitation in clinics is due to cardiotoxicity resulting from oxidative stress generation, and other side effects including nephrotoxicity, myelosuppresion, and developing multidrug resistance which leads to narrow therapeutic index.[7, 8] Thus, a new formulation strategy is required to improve its poor intestinal permeability and oral bioavailability since the limited intestinal absorption of DOX hampers the overall oral bioavailability.[9]

Bile acid transporters have been considered as an attractive therapeutic target for drug delivery, because bile acids secreted from the liver are reabsorbed from the terminal ileum throughout intestinal epithelial cells and transported back to the liver via the portal vein.[10] Thus, the high bile acid recycling ratios make the enterohepatic circulation of bile acids highly efficient process and benefit the bile acid transporters that are mainly expressed in the liver and the terminal ileum.[11, 12] Taurocholic acid (TCA) has been known to be one of the most abundant bile acids in human and it has been reported that TCA in human intestinal fluids is approximately 45%.[13, 14]

TCA has been used as a drug carrier by conjugating to anionic polymer and delivered via oral administration. Khatun *et al*. reported that TCA linked heparin-docetaxel conjugates enhanced the drug concentration in plasma 6 times.[15] They claimed the TCA exposed on the surface of nanoparticles interacted with the bile acid transporters in the small intestine and enhanced the intestinal permeability as well as drug bioavailability. In the case of DOX itself, the hydrophilic cationic properties of DOX lead to the crossing of intestinal epithelium cells mainly via the paracellular pathway.[9] However, the TCA coating of DOX surface will maximize the intestinal transcellular absorption via Na^+-

dependent apical sodium bile acid transporter (ASBT) mainly in the terminal ileum and facilitate DOX transport from terminal ileum to portal vein that enhance DOX into the systemic circulation.[16]

Heparin (H) and chondroitin sulfate (CS) were chosen as an anionic polymer backbone to conjugate TCA due to its outstanding biocompatibility, high water solubility, and biodegradability.[17, 18] These polysaccharides are natural polymers that have been used as carriers and provided clinical benefits.[19] Thus, H-TCA and CS-TCA will coat the surface of DOX to increase the stability of DOX in the gastrointestinal (GI) tract and protect the DOX-loaded nanoparticles from the GI environment. In addition, H-TCA and CS-TCA can form nanoparticles (NPs) with DOX. These NPs will lead to superior oral absorption since smaller NPs have shown elevated intestinal absorption compared to micron size particles.[20] This simple formulation strategy will avoid nonspecific adsorption and improve intestinal absorption which leads to DOX oral bioavailability improvement. The efficient TCA recycling via enterohepatic circulation could be beneficial to anticancer oral chemotherapy targeting liver carcinoma.

A.3. Materials and methods

A.3.1. Materials

Doxorubicin hydrochloride, sheared salmon sperm DNA (Trevigen, MD), Dimethyl sulfoxide (DMSO), 4-(2-hydroxy-ethyl)-1-piperazine (HEPES), 3-(4, 5-dimethylthiazol-2-yl)-2,5-diphenyltetrazolium bromide (MTT), D-glucose, sodium bicarbonate, recombinant human insulin, Hoechst 33342, RPMI 1640 medium, Dulbecco's phosphate buffered saline (DPBS), Dulbecco's modified eagle's medium (DMEM), carbodiimide (EDC), N-hydroxysuccinimide (NHS).

A.3.2. Preparation of H-TCA and CS-TCA

Heparin- taurocholic acid (H-TCA) was provided by Dr. Lee's lab and the preparation steps are reported in their previous report.[15] In brief, 1 mol of TCA sodium salt was dissolved in DMF at 0 °C followed by 6 mol of triehtylamine and 5 mol of 4-nitrophenyl chloroformate (NPC) addition. The reacted solution was then extracted three times with ethanol and DI water. A rotary evaporator was used to remove organic solvent and samples were freeze-dried to obtain TCA-NPC. 1 mol of TCA-NPC was dissolved in DMF with 2 mol of 4-methylomrpholine. Then 100 mol of ethylene diamine was added drop by drop and final product was dried to obtain TCA-NH_2. To synthesize the TCA conjugates to either heparin or chondroitin sulfate (CS), 1 mol of heparin/CS was dissolved in DI water first. Then EDC (5 mol) and NHS (5 mol) was added to the solution and stirred for 12 hr at RT. A same feed molar ratio of TCA-NH_2 was added to heparin and chondroitin sulfate to obtain the same coupling amount of TCA. Thus, the feed molar ratio of both heparin:TCA and chondroitin sulfate:TCA was 1:4. After 1 day of reaction, the solution was placed in MWCO 1000 dialysis membrane and dialyzed against water. The final product was lyophilized and confirmed by its ^{1}H-NMR spectrum.

A.3.3. Formation and reconstitution of DOX-loaded nanoparticles

DOX-loaded nanoparticles were formed via electrostatic interactions between DOX and TCA conjugates; CS-TCA and H-TCA. CS-TCA was directly mixed with DOX at 1:2 (w/w ratio). In the case of H-TCA, Dox was first mixed with sheared DNA (DD) to get negative surface charges and mixed with Ɛ-PLL (DDP) to get positively charged surfaces. Finally, the particles were mixed with H-TCA (DDP/H-TCA) to get negative surface

charges. For each preparation, the solutions were mixed using a vortex and sonicated 10 sec at 20 amplitude followed by incubation for 30 min at RT. Thus, the final formulation of DDP/H-TCA was prepared at 1:1:0.8:2.4 (w/w ratio).

The formed DOX nanoparticles were further evaluated. Particle sizes and surface charges of DOX nanoparticles were evaluated as previously reported.[21-23] After preparing DOX nanoparticles, they were diluted with HEPES buffer (20 mM, pH 7.4), then the hydrodynamic particle size and zeta potential of nanoparticles were monitored by dynamic light scattering (DLS) using a Zetasizer 3000 (Malvern Instrument, UK) with a wavelength of 677 nm and a constant angle of 90° at RT (25 ^{o}C).

After freeze-drying the samples, the freeze-dried formulations of nanoparticles were reconstituted in DI water and samples were sonicated about 10 sec at 20 amplitude before the DLS measurements. For *in vivo* samples, the lyophilized powder was stored at -20 °C until use.

A.3.4. Spectral measurement of DOX encapsulation

Ultraviolet–visible (UV-Vis) spectroscopy (SpectraMax, USA) was used to monitor the change of absorbance of DOX-loaded nanoparticles. 0.1 mL samples (25 µg of DOX per sample) were prepared and diluted in 0.9 mL DI water (total volume 1 mL) and loaded in a quartz cuvette for reading. UV–vis absorbance spectra of free DOX displayed peaks at 232 and 490 nm, and the spectral changes of Dox loaded nanoparticles is compared to peaks of control free DOX.

A.3.5. DOX loading and encapsulation efficiency

The drug loading content and loading efficiency was measured using UV-Vis absorption spectra at 490 nm and calculated based on a standard curve. The percent of drug loading and efficiency were calculated using the equation below.

$$\text{Drug loading } (\%) = \frac{\text{weight of DOX in nanoparticles}}{\text{weight of nanoparticles}} \text{ x } 100$$

$$\text{Drug Efficiency } (\%) = \frac{\text{weight of DOX present in nanoparticles}}{\text{weight of Dox used}} \text{ x } 100$$

A.3.6. *In vitro* DOX release study

The DOX release from nanoparticles was examined in pH 7.4 and pH 5 phosphate buffer using a dialysis method. 1mL of DOX nanoparticles (250 µg of DOX per sample) were prepared and loaded in a dialysis membrane (MWCO 3500 g/mol). The dialysis bag was placed in 20 mL of buffer and the buffer was stirred at 130 rpm at 37 ^{o}C. 1mL of external buffer was taken out at predetermined time points and the same volume of fresh buffer was added. The amount of released DOX was calculated by measuring absorbance at 490 nm based on a standard curve.

A.3.7. *In vitro* stability test of DOX NPs

The stability of DOX-loaded nanoparticles was tested in three different pHs (pH 1.5, 5, 7) in 0.1M Tris HCl buffer and the mean diameter of the nanoparticles was monitored by dynamic light scattering each day up to 7 days.

A.3.8. Cell Culture

HepG2 cells (a human hepatoma cell line) were cultured in DMEM supplemented with 10% FBS and D-glucose (4.5 g/L). Cells were grown and maintained under humidified air containing 5% CO_2 at 37 ^oC.

A.3.9. Cell Viability Test

The MTT assay was used to evaluate cell viability of polymers and DOX-loaded nanoparticles. HepG2 cells were seeded into a 96-well plate with a cell density 5 x 10^3 cells/well in 100 µL media. After 24 hr, different concentration ranges (0.01 - 100 µg/mL) of DOX and DOX-loaded nanoparticles were exposed to the cells for an additional 24 hr. MTT (10 µL; 5 mg/mL) solution was then added and incubated for 4 hr. All remaining media was aspirated, and DMSO (100 µL) was added to dissolve the formazan crystals produced from living cells with 10 min incubation at 37 °C. The absorbance of the cells was measured at 570 nm and their cell viability was calculated.

A.3.10. *In vivo* therapeutic efficacy test in tumor bearing model

HepG2 cells (5 x 10^6 cells/mL) in 100 µL PBS were injected subcutaneously on the back of the mice. When tumor size reached approximately 100-150 mm^3, mice received oral administrations of PBS, 4 mg/kg doxorubicin in free or TCA coated NPs form every three days. In addition, equal amount of doxorubicin was intravenously administered as a control group. Tumors were measured every 3 days with a digital calliper and calculated using an equation below.[24]

$$\text{Tumor volume} = \text{Length} \times \frac{\text{Width}^2}{2}$$

A.3.11. Biodistribution

The biodistribution study was performed in HepG2 tumor-bearing NOD/SCID mice. Liver, kidney, heart, stomach, small intestine including duodenum, jejunum, ileum, and tumor were collected and suspended in 70% ethanol with 0.3 N HCl. Then the samples were homogenized to extract doxorubicin. Then the samples were refrigerated for 24 hr and centrifuged to collect supernatant. 200 μL of the supernatant was loaded in a black opaque plate and DOX fluorescence was measured using a plate reader, where the wavelengths of excitation and emission were 470 and 590 nm, respectively.[25]

A.3.12. Statistical analysis

Sample size was estimated using one-way ANOVA with a significance level (α) of 0.05 and a power (1-β) of 0.9. Student's t-test was used to compare two groups and one-way ANOVA with the bonferroni post-hoc analysis was used to compare three or more groups. $p < 0.05$ was considered statistically significant.

A.4. Results and Discussion

A.4.1. Preparation and characterization of DOX-loaded nanoparticles

The synthesis of heparin- taurocholic acid (H-TCA) is prepared by the same method mentioned in the previous paper.[15] In brief, the carboxylic groups in heparin were coupled with the amine groups of TCA to form an amide bond in the presence of EDC and NHS, and chondroitin sulfate-TCA (CS-TCA) were constructed in a similar manner.

The feed molar ratio of TCA to heparin and chondroitin sulfate was set to about 4:1 and the conjugation of TCA in heparin and chondroitin sulfate was confirmed by ^{1}H (Ref [15] and Fig. A.1). DOX was coated with either CS-TCA or H-TCA via physical

(a)

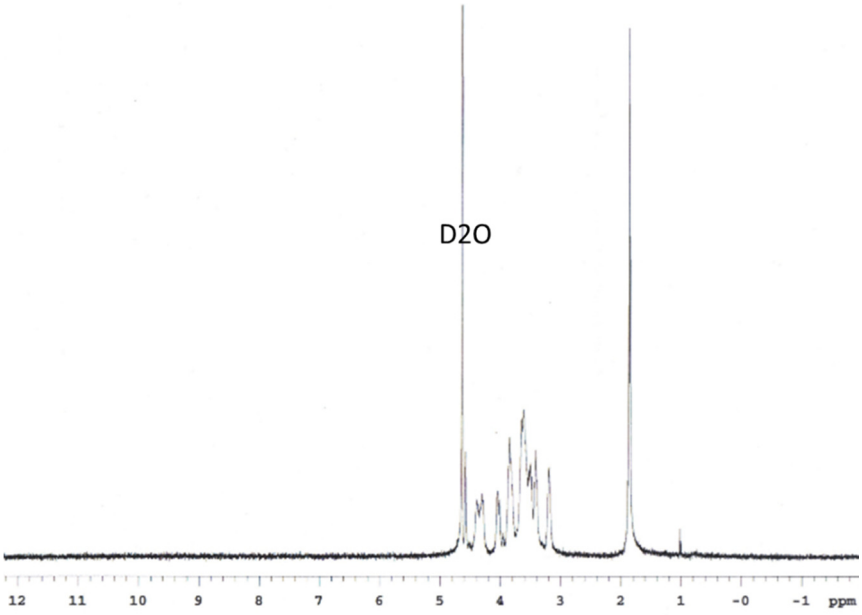

(b)

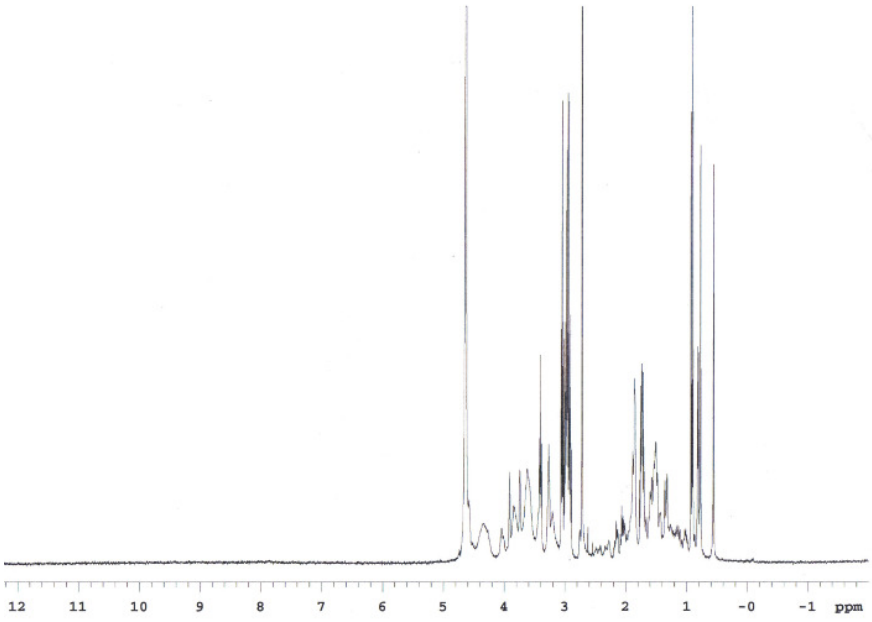

Figure A.1. Representative ^{1}H NMR spectra of (a) Chondroitin Sulfate (CS) and (b) CS-TCA in D2O.

complexation for oral administration. Although H-TCA showed an outstanding result in the previous report, CS-TCA was constructed because H-TCA coating to DOX produced a large particle size with a wide PDI. Thus, a single coating of CS-TCA was able to produce a smaller particle size with a narrow PDI at 1:2 (w/w ratio). In the case of H-TCA, it required multiple layer-by-layer assemblies to coat H-TCA at the end. Thus, sheared DNA was used primarily to coat DOX (DD) and Ɛ-PLL (DDP) was coated after to produce positively charged surfaces. Finally, H-TCA (DDP/H-TCA) was coated at 1:1:0.8:2.4 (w/w ratio).

The changes of UV-Vis absorption spectra of free DOX and DOX-loaded nanoparticles (DOX-loaded NPs) were monitored. As shown in Fig. A.2, DOX without any carriers displayed two main peaks at 232 nm and 490 nm, then DOX loading onto the H-TCA and CS-TCA was investigated. When DOX was loaded onto the TCA conjugated polysaccharides, there was a significant diminish of two peaks in DOX UV-VIS spectra. It is noted that both DDP/H-TCA and DOX/CS-TCA revealed a complete disappearance of the two peaks after single coating of CS-TCA or multiple coating for H-TCA which indicates the interactions between DOX and H-TCA/CS-TCA. The change of spectra also represented a successful loading of DOX in both formulations.

The electrostatic interactions between the cationic DOX and the anionic TCA conjugates formed DOX-TCA-NPs. Before the RT incubation, the particles were sonicated about 10 sec at 20 amplitude and a reduction of particle size with a narrow polydispersity index (PDI) was observed. Sonication induces acoustic cavitation which creates the shock waves with high forces in the solution. As a consequence, particles are colliding into each other and cause breakage of agglomerates that results in an overall

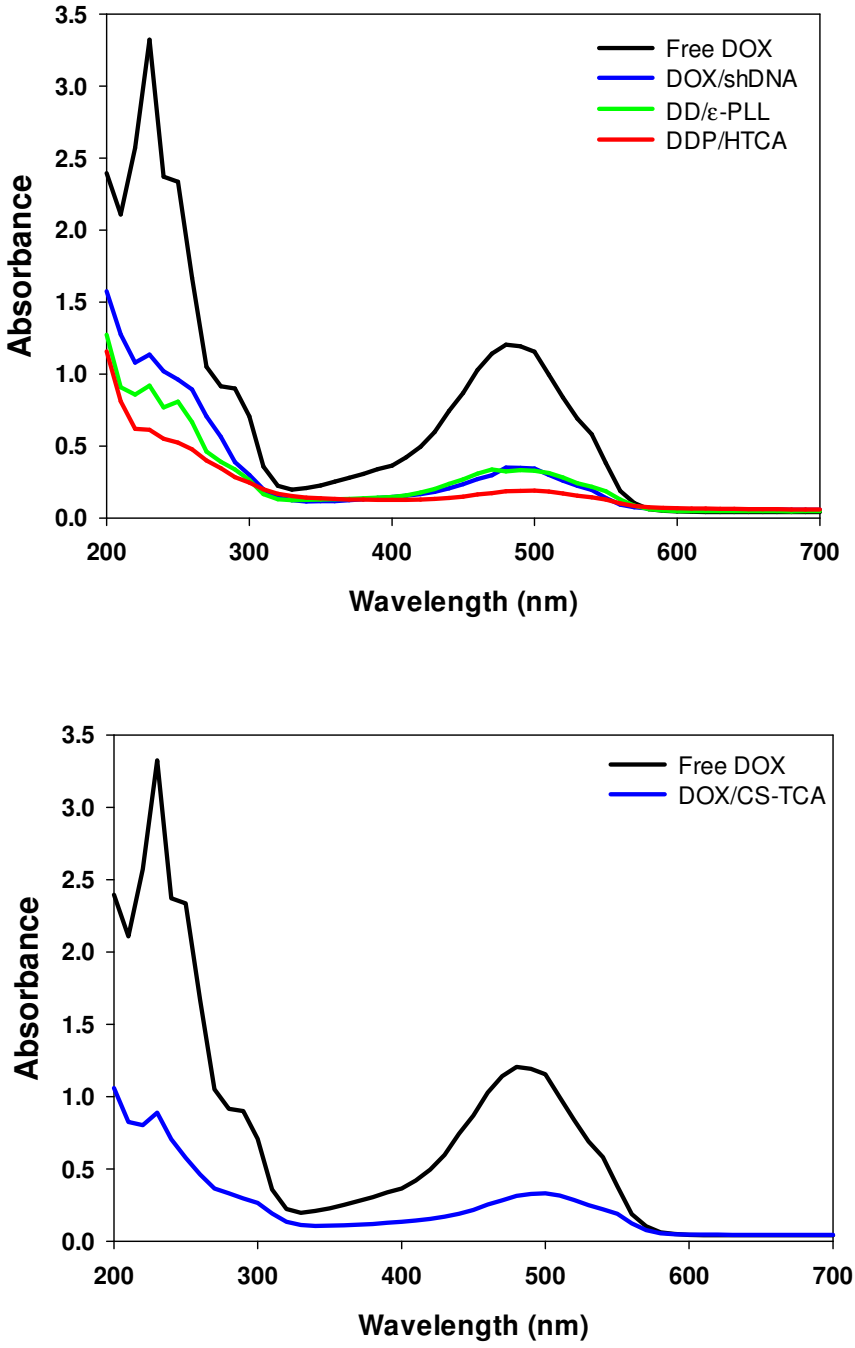

Figure A.2. UV-Vis absorption spectra of free DOX and DOX-loaded (25 µg of DOX per sample) nanoparticles.

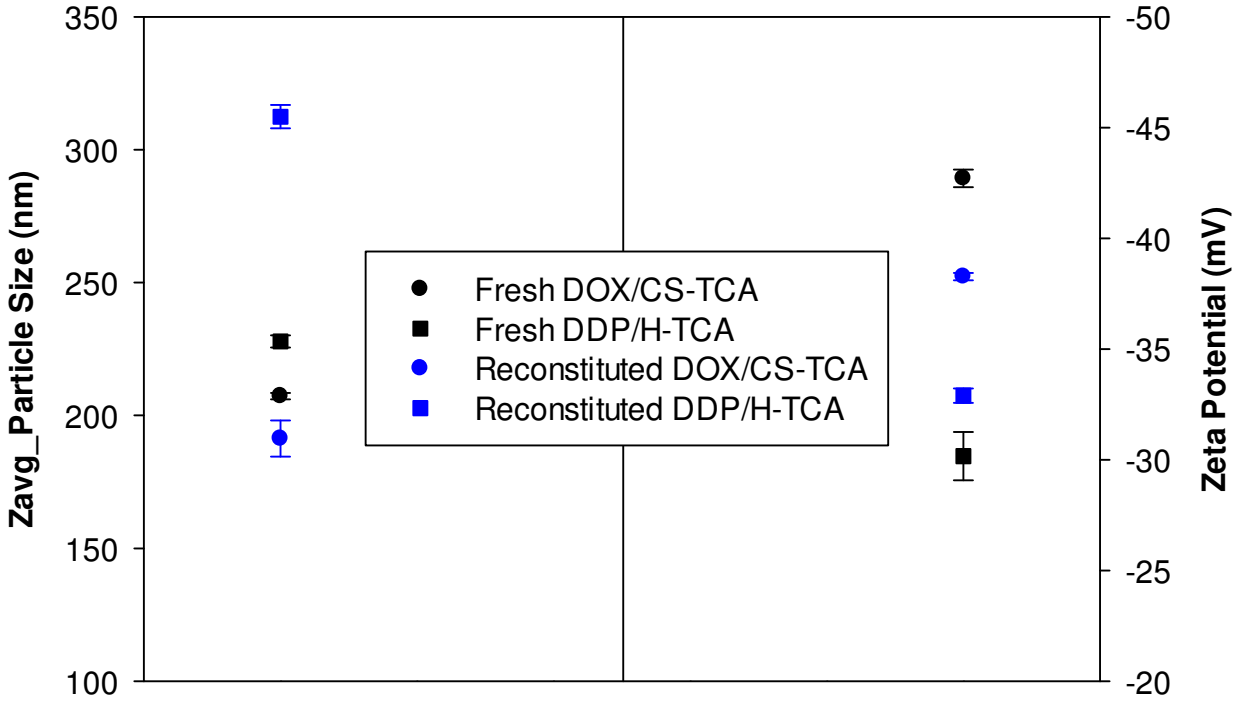

Figure A.3. Particle size and zeta potential before and after reconstitution (Data presented as Mean ± SD, n = 10)

decrease in particle size and PDI.[5, 26] The hydrodynamic diameter of DOX/CS-TCA at 1:2 and DDP/H-TCA at 1:1:0.8:2.4 (w/w ratio) were 200 nm and 230 nm, respectively (Fig. A.3). In the case of DDP/H-TCA, the subsequent assembly of the multiple layers increased the size. The zeta potential of DOX/CS-TCA was -42.7 mV and -30.2 mV for DDP/H-TCA. They were both negatively charged due to the presence of carboxylic groups in the polysaccharide backbones.

We further evaluated whether these nanoparticles have a possibility of reconstitution for long-term storage. After freeze-drying, a powder formulation was reconstituted and sonicated about 15 sec at 25 amplitude in DI water. The diameters of the DOX-loaded NPs were slightly increased after reconstitution compared to that of samples before freeze-drying. The DOX-loaded NPs displayed particle sizes around 201.3 nm for DOX/CS-TCA and 312.4 nm for DDP/H-TCA. However, there was no significant change in the zeta potentials of the DOX-loaded NPs.

A.4.2. *In vitro* stability study

In vitro stability of DOX-loaded NPs was tested to monitor whether the particles are stable in buffers against three different pHs; pH 1.5, pH 5, pH 7 (Fig. A.4(a)). In acidic pH 1.5, there was a decrease in particle sizes compared to the particles in higher pHs. DOX has a pKa of 7.2-8 which is partially ionized at pH 7.4 by protonation of the amino group.[27] Thus, DOX is more protonated at lower pHs, and as a consequence, the strong electrostatic interactions can be established between DOX and anionic CS-TCA or short DNA which contributes to decrease in particle size. The smaller particle size in low pH also demonstrated that the DOX-loaded NPs will be stable in stomach pH and protect

(a)

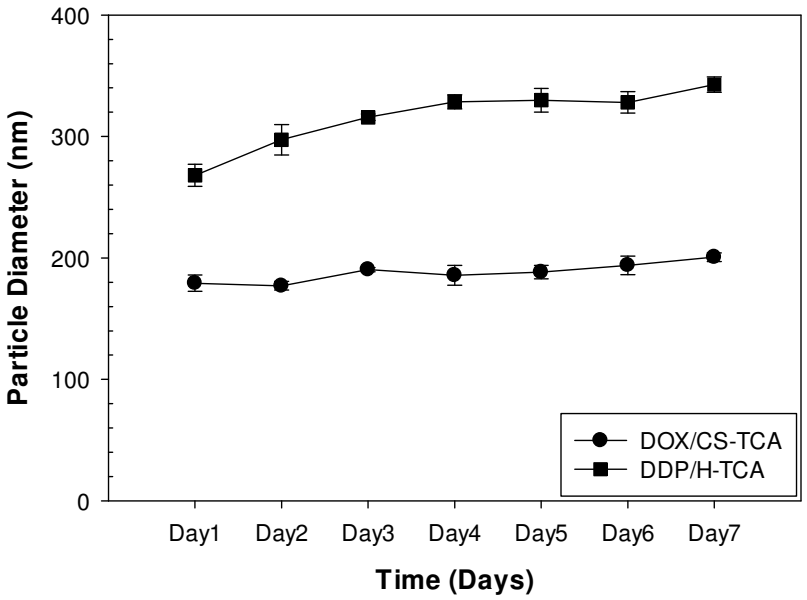

(b)

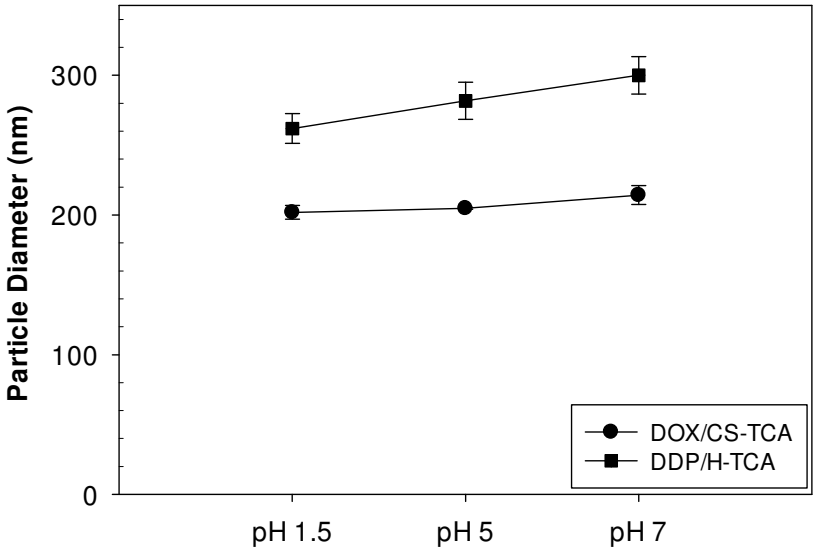

Figure A.4. The *in vitro* stability test of DOX-loaded NPs (a) at different pH values and (b) long-term storage (Mean ± SD, n = 3)

DOX from enzymatic degradation. The DOX/CS-TCA NPs showed that single coated nanoparticles were generally more stable and maintained similar sizes over the wide range of pH. However, DDP/H-TCA NPs were getting bigger as the pH increased.

In addition, the long-term stability of DOX-loaded NPs was evaluated by measurement of particle size over a long period of time (up to 7 days) (Fig. A.4(b)). After 7 days of storage, the DOX/CS-TCA formulation remained stable with a slight change of size. In the case of DDP/H-TCA, the particle size was increasing over time. This gradual increase in the particle size suggested that multiple coatings are physically instable compared to a single coating. Thus, the particle size measurement of DOX-loaded NPs showed that a single coating of CS-TCA provided better stability with regards to particle size.

A.4.3. DOX loading onto polysaccharide-TCA conjugates and *in vitro* DOX release

The loading efficiency and loading content of DOX were investigated by measuring the absorbance of DOX-loaded NPs and quantified based on a DOX standard calibration curve. The loading efficiency of DOX/CS-TCA and DDP/H-TCA was 61.6% and 77.8%, respectively. The multiple layers of DDP/H-TCA exhibited a much more drug loading ability and the loading efficiency. The loading content of DOX/CS-TCA and DDP/H-TCA was determined to be 30.8% and 18.5%, respectively. In both formulations, high loading content have been achieved and displayed efficient DOX loading.

The release of DOX from the polysaccharide-TCA conjugates was monitored upon pH changes and it was demonstrated at pH 7.4 and pH 5. As shown in Fig. A.5(a), a rapid

(a)

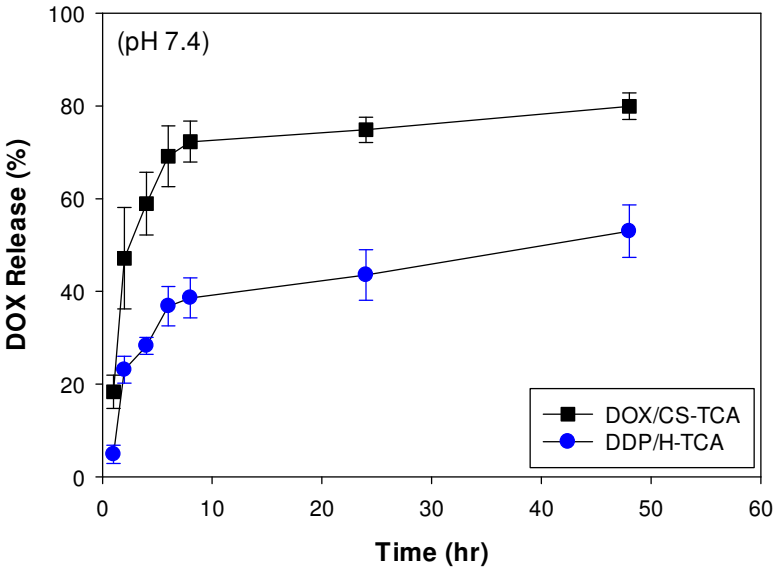

(b)

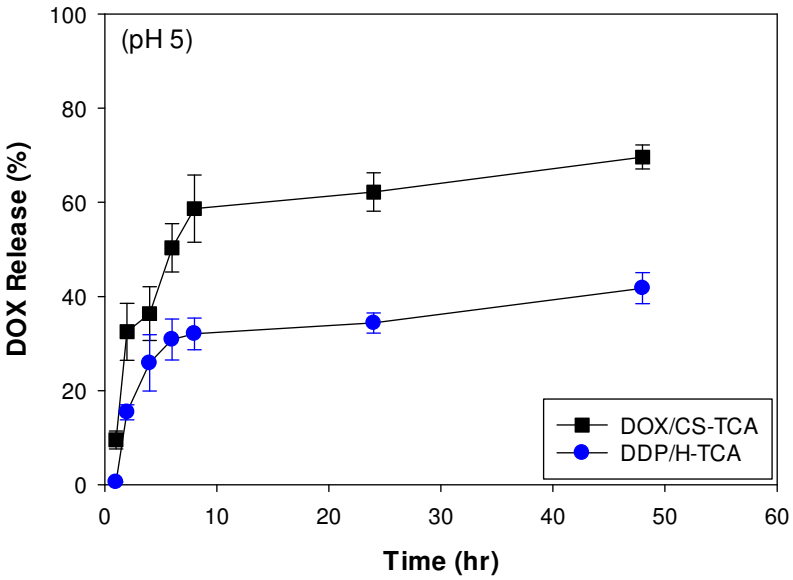

Figure A.5. *In vitro* DOX release profiles in PBS buffer at (a) pH 7.4 and (b) pH 5. Data are presented as Mean ± SD (n = 3)

release of DOX within 24 hr was monitored in DOX/CS-TCA NPs at pH 7.4. The release of DOX from DDP/H-TCA NPs was much slower and around 50% of DOX was released from NPs at 48 hr. In the aspect of released DOX, a single coating induced a much quicker release from the NPs. The multiple layer-by-layer assemblies may play as the diffusion barrier and delay the DOX release with a slower release rate compared to that of DOX with single coating.

At pH 5, the release rate of DOX from DOX-loaded NPs was significantly delayed (Fig. A.5(b)). DOX/CS-TCA showed around 65% of DOX release at 48 hr and DDP/H-TCA displayed about 40% Dox release at 48 hr. This observation could be due to the high degree of protonation of daunosamine groups in DOX at acidic environment. Therefore, DOX-loaded NPs may exhibit a slower release and a higher protonation of DOX at pH 5 which corresponds to endolysosomal pH, but accelerated DOX release rate at pH 7.4. Since the nucleus is the target site of DOX where pH is 7.4, more DOX will be released faster and available to intercalate DNA. This finding indicates that the pH-controlled DOX release from DOX-loaded NPs.

A.4.4. *In vitro* cytotoxicity of DOX-loaded NPs

To monitor the cytotoxicity of polymers and DOX-loaded NPs, samples were transfected in a dose-dependent manner and evaluated by an MTT-based cell viability assay using HepG2 cells. The MTT assay of polymers showed that incubations of TCA conjugated polymers, CS-TCA and H-TCA, exhibited about 90% and 60% of cell viability at 0.01 μg/mL and 100 μg/mL concentration, respectively (Fig. A.6). This indicated a negligible cytotoxicity from the polymers.

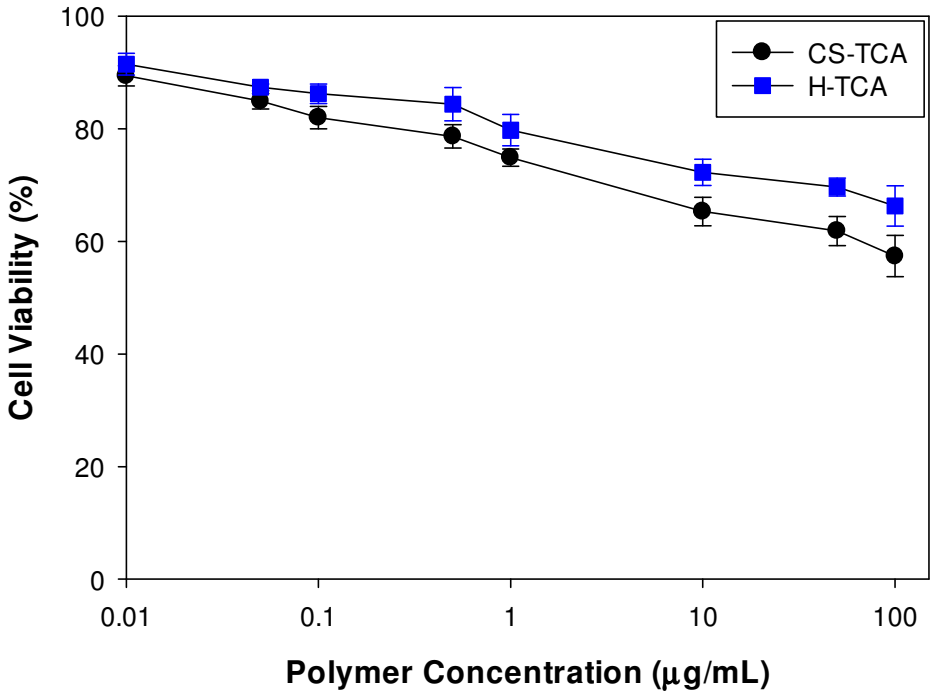

Figure A.6. Dose-dependent cytotoxicity of CS-TCA and H-TCA in HepG2 cells (Mean ± SD, n = 6)

Cell viability of the DOX-loaded NPs and free DOX was also investigated in HepG2 cells after 24, 48, and 72 hr incubation (Fig. A.7). As shown in Fig. A.7(a), free DOX showed the highest dose-dependent cytotoxicity due to the cationic properties of DOX which are more toxic to cells. In the case of D/CS-TCA (Fig. A.7(b)) and DDP/H-TCA (Fig. A.7(c)), the DOX-loaded NPs showed a relatively low toxicity compared to the one with free DOX and the DOX/CS-TCA NPs displayed slightly lower toxicity than the DDP/H-TCA. The CS-TCA or H-TCA anionic polymer coating improved DOX-induced cytotoxicity and resulted in negligible toxicity to the cell environments; thus, lower cell toxicity from DOX-loaded NPs were observed. However, multiple coated NPs showed a relatively higher toxicity than single coated NPs due to the three different concentration of polymers coated outside the free DOX.

A.4.5. Tumor growth suppression of DOX-TCA-NPs in tumor xenograft model

To reconstitute at high concentration, the lyophilized powder of DDP/H-TCA was reconstituted in DI water just prior to *in vivo* administration. First, the tumor growth inhibition efficacy of TCA conjugated DOX-loaded nanoparticles (DOX-TCA-NPs) was investigated in HepG2 xenograft model. 4 mg/kg Dox or an equivalent amount of DOX-TCA-NPs were prepared and delivered via IV or Oral administration every 3 days up to 18 days to monitor tumor progression. DOX-loaded NPs without TCA were also tested as a nontargeted formulation to evaluate the tumor inhibition efficacy of TCA. Since tumors in the PBS group were too aggressive and reached approximately over 10% of body weight around day 18, all treatments were terminated and mice were sacrificed at

(a)

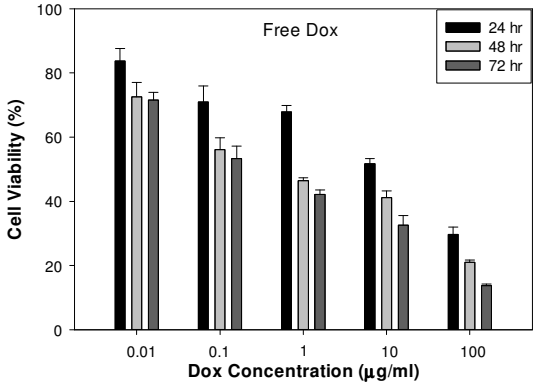

(b)

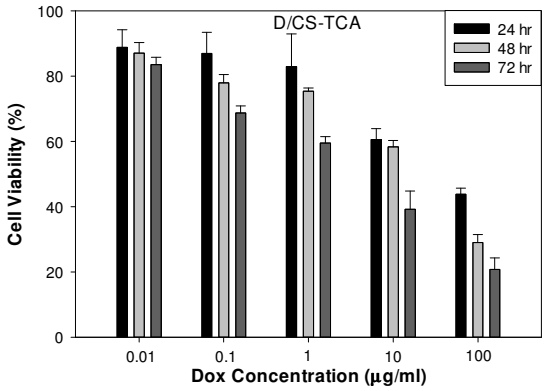

(c)

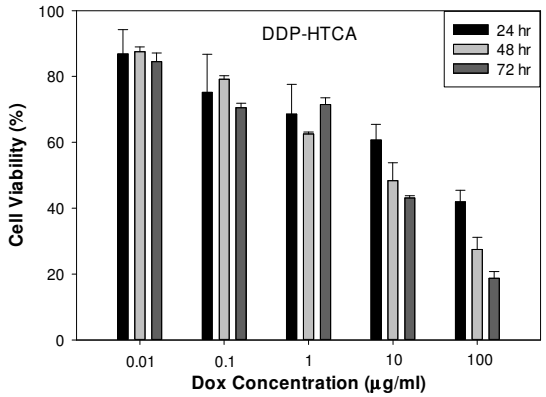

Figure A.7. Cytotoxicity of free DOX and DOX-loaded NPs after 24, 48, and 72 hr transfection in HepG2 cells (a) fee DOX, (b) DOX/CS-TCA, and (c) DDP/H-TCA (Mean ± SD, n = 6)

day 18.

All the treatment groups showed an increase of tumor volume over time. However, there was a significant difference in tumor growth rate and overall tumor volume change. As shown in Fig. A.8(a), the tumor volume in DOX IV group showed the most noticeable inhibition of tumor growth. However, a greater suppression of tumor growth was observed in mice treated with DOX-TCA-NPs compared to that of the other oral control groups. The tumor volumes in the DOX-TCA-NPs groups were significantly smaller ($p < 0.05$) than the tumor volumes of free oral DOX. The tumors in free oral DOX group increased almost 1400% change in volume, whereas the tumors in DDP/H-TCA and D/CS-TCA groups displayed only 400% and 600% change in volume, respectively. The tumors in D/CS-TCA showed higher tumor volume than the tumors in DDP/H-TCA and this result may be caused by the fast release of DOX from D/CS-TCA complexes compared to DDP/H-TCA. In contrast, tumors treated with non-TCA groups did not result in a significant inhibition of tumor growth and showed no marked change of tumor growth compared with the free oral DOX groups. There was no significant difference in tumor volume between the free DOX oral group and non-TCA group.

The TCA formulations contributed to more efficacious at tumor growth reduction compared with mice treated with non-TCA NPs. The effective tumor regression of TCA groups suggested strong anti-tumor efficacy of DOX-TCA-NPs against HepG2 xenograft models. The tumor burden on day 18 also represented considerable reductions in tumor burden in animal group that received the DOX-TCA-NPs as compared to tumor burden in free oral DOX (Fig. A.8(b)).

Second, mice body weight was also monitored and measured throughout the

(a)

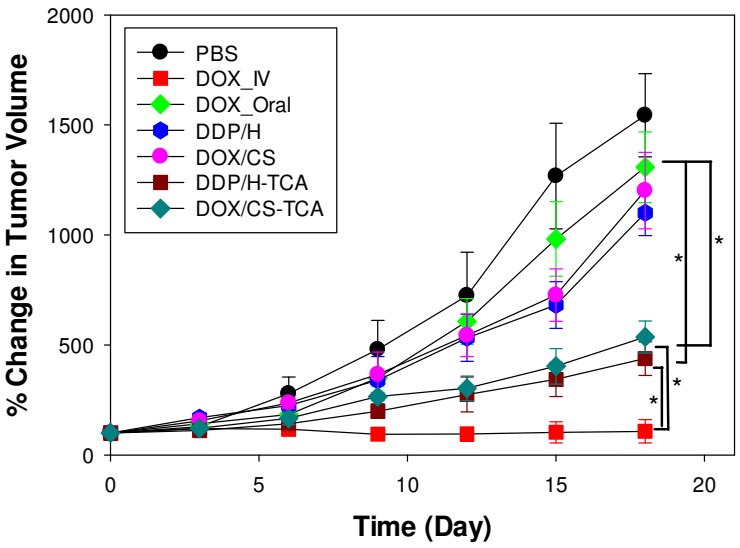

(b)

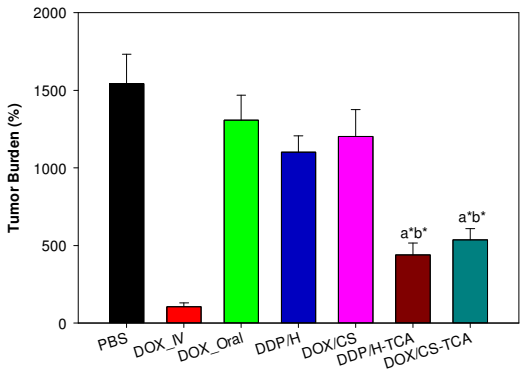

(c)

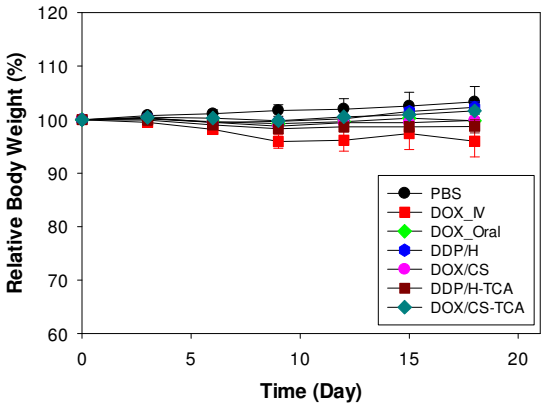

Figure A.8. Anti-tumor efficacy of free DOX and DOX-loaded NPs. (a) Relative tumor volume (%) (b) Tumor burden (%) (c) Relative body weight (%) of control, IV and orally administered free DOX and non-TCA conjugated and TCA conjugated NPs. (* $p<0.05$, (a) vs. DOX_IV, (b) vs. DOX_Oral, Mean ± SEM, n = 6)

treatments to assess the toxicity induced from the treatments (Fig. A.8(c)). Both control and non-TCA treated groups showed no significant weight loss in the beginning of the treatments and weight gain of the mice were observed over time which indicated no serious toxicity from the treatments. However, there was some weight loss in DDP/H-TCA group and the mice showed 5-7% weight loss throughout the course of the treatment, but slow weight gain was observed towards the end treatment.

A.4.6. Biodistribution study of DOX in tumor-bearing mice

For biodistribution studies, major organs and intestine were collected 4 hr after injection (Fig. A.9). We measured DOX concentration in major organs and intestine by measuring DOX fluorescence intensity and results are presented as μg DOX per gram of tissue. It is worthy to note that a higher concentration of DOX was presented in heart and liver tissues after IV injection of free DOX than orally administered groups.

The DOX distribution data showed that a highest DOX amount was observed in the ileum of samples treated with DOX-TCA-NPs. The DOX content for DOX-TCA-NPs in the ileum was around 3-4 fold higher than that for free DOX oral or non-TCA groups. DOX accumulation in the ileum is an indication of highly targeted absorption of DOX-TCA-NPs and demonstrates effective interactions of DOX-TCA-NPs with bile acid transporters in the ileum. TCA conjugated carriers have been enhancing drug absorption especially in terminal ileum where membrane transporters are existed and this result is consistent with previous reports.[15, 16]

Moreover, improved accumulation at tumor sites was also observed. These results suggest that bile acid-mediated DOX absorption leads to higher DOX concentration in

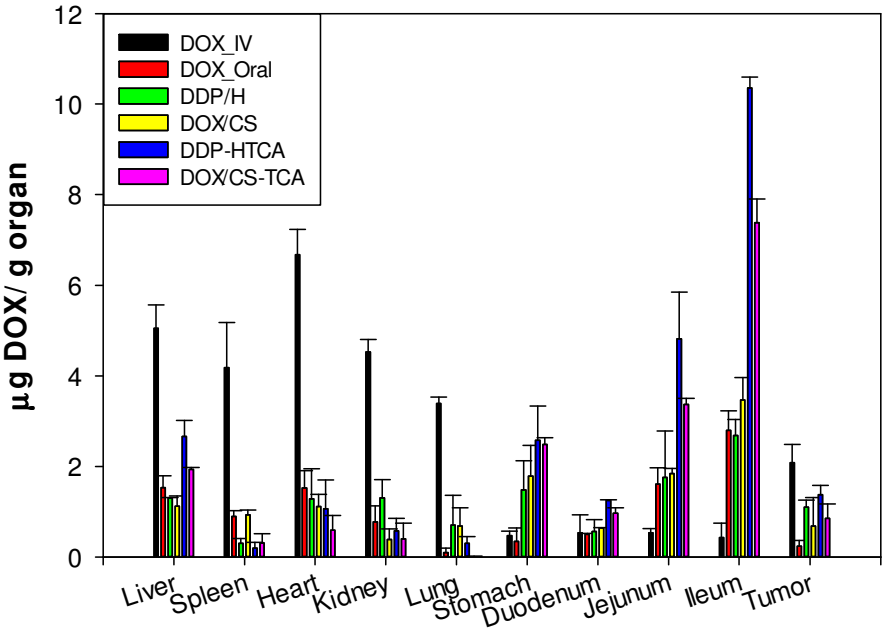

Figure A.9. Biodistribution of DOX in tumor-bearing mice (Mean ± SEM, n = 3). The results are presented as µg of DOX to the amount (g) of tissue.

the blood stream. As a consequence, high accumulation in the blood stream may contribute to slow tumor progression with superior DOX efficacy in comparison with free DOX oral administration.

A.5. Conclusion

To facilitate DOX oral delivery, we prepared DOX-loaded-TCA NPs via physical complexation. The DOX-TCA-NPs showed no change in nanoparticle stability upon freeze-drying which indicated the possibility of long-term storage. TCA coating also showed negligible toxicity compared with free DOX as well as high drug loading efficiency and pH-dependent DOX release. Most importantly, *in vivo* results showed that the DOX-TCA-NPs delayed tumor growth significantly. Biodistribution study also demonstrated improved DOX absorptions for the DOX-TCA-NPs in the ileum of the intestine. Overall, TCA formulation showed higher therapeutic efficacy in solid tumor than free DOX and non-TCA oral administered groups. This indicates bile acid-mediated targeting delivery enhanced therapeutic performance of DOX by utilizing TCA transporters and leads to oral absorption enhancement. Thus, the effect of TCA on oral administration of DOX has been proved to be an effective carrier for DOX oral delivery. In addition, this new formulation system showed a possibility of switching the intravenous to oral administration and implicated the promising oral chemotherapy.

A.6.References

1. Thanki K, Gangwal RP, Sangamwar AT, Jain S. Oral delivery of anticancer drugs: challenges and opportunities. J. Control. Release, 2013;170(1):15-40.

2. Mei L, Zhang Z, Zhao L, Huang L, Yang XL, Tang J, Feng SS. Pharmaceutical

nanotechnology for oral delivery of anticancer drugs. Adv. Drug Deliv. Rev. 2013;65(6):880-890.

3. Da Rocha AB, Lopes RM, Schwartsmann G. Natural products in anticancer therapy. Curr. Opin. Pharmacol. 2001;1(4):364-369.

4. Mohan P, Rapoport N. Doxorubicin as a molecular nanotheranostic agent: effect of doxorubicin encapsulation in micelles or nanoemulsions on the ultrasound-mediated intracellular delivery and nuclear trafficking. Mol. Pharm. 2010;7(6):1959-1973.

5. Swarnakar NK, Thanki K, Jain S. Bicontinuous cubic liquid crystalline nanoparticles for oral delivery of doxorubicin: implications on bioavailability, therapeutic efficacy, and cardiotoxicity. Pharm. Res. 2014;31(5):1219-1238.

6. Wang J, Li L, Du Y, Sun J, Han X, Luo C, Ai X, Zhang Q, Wang Y, Fu Q. Improved oral absorption of doxorubicin by amphiphilic copolymer of lysine-linked di-tocopherol polyethylene glycol 2000 succinate. Mol. Pharm. 2015;12(2):463-473.

7. Dayton A, Selvendiran K, Meduru S, Khan M, Kuppusamy ML, Naidu S, Kalai T, Hideg K, Kuppusamy P. Amelioration of doxorubicin-induced cardiotoxicity by an anticancer-antioxidant dual-function compound, HO-3867. J. Pharm. Exp. Ther. 2011;339(2):350-357.

8. Li Q, Lv S, Tang Z, Liu M, Zhang D, Yang Y, Chen X. A co-delivery system based on paclitaxel grafted mpeg-b-plg loaded with doxorubicin: preparation, in vitro and in vivo evaluation. Int. J. Pharm. 2014;471(1-2):412-420.

9. Kim JE, Cho HJ, Kim JS, Shim CK, Chung SJ, Oak MH, Yoon IS, Kim DD. The limited intestinal absorption via paracellular pathway is responsible for the low oral bioavailability of doxorubicin. Xenobiotica. 2012;43(7):579-591.

10. Thomas C, Pellicciari R, Pruzanski M, Auwerx J, Schoonjans K. Targeting bile-acid signalling for metabolic diseases. Nat. Rev. Drug Discov. 2008;7(8):678-693.

11. Alrefai WA, Gill RK. Bile acid transporters: structure, function, regulation and pathophysiological implications. Pharm. Res. 2007;24(10):1803-1823.

12. Dawson PA, Lan T, Rao A. Bile acid transporters. J. Lipid Res. 2009;50(12):2340-2357.

13. Yin Win K, Feng SS. Effects of particle size and surface coating on cellular uptake of polymeric nanoparticles for oral delivery of anticancer drugs. Biomaterials. 2005;26(15):2713-2722.

14. Holm R, Müllertz A, Mu H. Bile salts and their importance for drug absorption. Int. J. Pharm. 2013;453(1):44-55.

15. Khatun Z, Nurunnabi M, Reeck GR, Cho KJ, Lee Yk. Oral delivery of taurocholic acid linked heparin–docetaxel conjugates for cancer therapy. J. Control. Release. 2013;170(1):74-82.

16. Alam F, Al-Hilal TA, Chung SW, Seo D, Mahmud F, Kim HS, Kim SY, Byun Y. Oral delivery of a potent anti-angiogenic heparin conjugate by chemical conjugation and physical complexation using deoxycholic acid. Biomaterials. 2014;35(24):6543-6552.

17. Tran TH, Nguyen CT, Kim DP, Lee Yk, Huh KM. Microfluidic approach for highly efficient synthesis of heparin-based bioconjugates for drug delivery. Lab Chip. 2012;12(3):589-594.

18. Oprea AM, Profire L, Lupusoru CE, Ghiciuc CM, Ciolacu D, Vasile C. Synthesis and characterization of some cellulose/chondroitin sulphate hydrogels and their evaluation as carriers for drug delivery. Carbohydr Polym. 2012;87(1):721-729.

19. Zhang Y, Chan HF, Leong KW. Advanced materials and processing for drug delivery: the past and the future. Adv. Drug Deliv. Rev. 2013;65(1):104-120.

20. He C, Yin L, Tang C, Yin C. Size-dependent absorption mechanism of polymeric nanoparticles for oral delivery of protein drugs. Biomaterials. 2012;33(33): 8569-8578.

21. Kang HC, Bae YH. Co-delivery of small interfering RNA and plasmid DNA using a polymeric vector incorporating endosomolytic oligomeric sulfonamide. Biomaterials. 2011;32(21):4914-24.

22. Kang HC, Kang HJ, Bae YH. A reducible polycationic gene vector derived from thiolated low molecular weight branched polyethyleneimine linked by 2-iminothiolane. Biomaterials. 2011;32(4):1193-1203.

23. Kang HC, Samsonova O, Kang SW, Bae YH. The effect of environmental pH on polymeric transfection efficiency. Biomaterials. 2012;33(5):1651-62.

24. Hu J, Miura S, Na K, Bae YH. pH-responsive and charge shielded cationic micelle of poly (l-histidine)-block-short branched PEI for acidic cancer treatment. J. Control. Release. 2013;172(1):69-76.

25. Kim D, Gao ZG, Lee ES, Bae YH. In vivo evaluation of doxorubicin-loaded polymeric micelles targeting folate receptors and early endosomal pH in drug-resistant ovarian cancer. Mol. Pharm. 2009;6(5):1353-1362.

26. Jafari V, Allahverdi A, Vafaei M. Ultrasound-assisted synthesis of colloidal nanosilica from silica fume: Effect of sonication time on the properties of product. Adv Power Technol. 2014;25(5):1571-1577.

27. Talelli M, Iman M, Varkouhi AK, Rijcken CJ, Schiffelers RM, Etrych T, Ulbrich

K, van Nostrum CF, Lammers T, Storm G. Core-crosslinked polymeric micelles with controlled release of covalently entrapped doxorubicin. Biomaterials. 2010;31(30):7797-7804.